Title

The molecular basis of Htm1-mediated commitment of misfolded glycoproteins to endoplasmic reticulum-associated degradation

Author

Liu, Yi-Chang

Publication Date

2016

Peer reviewed|Thesis/dissertation

The molecular basis of Htm1-mediated commitment of misfolded glycoproteins to endoplasmic reticulum-associated degradation

by

Yi-Chang Liu

DISSERTATION

Submitted in partial satisfaction of the requirements for the degree of

DOCTOR OF PHILOSOPHY

in

Chemistry and Chemical Biology

in the

GRADUATE DIVISION

of the

UNIVERSITY OF CALIFORNIA, SAN FRANCISCO

Acknowledgements

First, I want to thank Jonathan and Danica for taking me in as a joint student. It is an invaluable experience to be able to witness the diverse researches in both labs. I also want to thank my thesis committee, David Agard and John Gross, for their sharp insights and thoughtfulness on my project and my career plan.

I want to thank all current and former members in both the Weissman and the Fujimori labs for all of the intriguing conversations and making both labs such fun places to be. It is my biggest privilege to be surrounded by so many great scientists. Specifically, I have to thank Jay Read, Edwin Rodriguez, Erin Quan Toyama, and especially Melanie Smith, for sharing reagents and insights on the ERAD project; Elizabeth Costa, Joshua Dunn, Calvin Jan, Manuel Leonetti, and Lindsey Pack, for being the common source of guidance.

I want to thank my classmates, Chris Novotny, David Paquette, Flora Rutaganira, Hai Tran, and Chris Williams, for making my first experience as an international student in the U.S. so welcome all these years. I also thank Melanie Smith, Calvin Jan, and Joshua Dunn, for being my coffee buddies; Clement Chu for introducing me to the world of coffee roasting; the Vibemme Double Domobar for being such a sturdy espresso machine and keeping me caffeinated.

I want to thank my parents, who have given me all the support and freedom to pursue my own career; my sister and my brother, and their extended families, for the support during my time here; my dogs for being my dogs.

Finally, there is no way to describe my thankfulness to my wife, Meng-Ying Lee. Her patience and love are the only reason I can make it through the failed experiments and the tough long-distance relationship. This dissertation is dedicated to her.

Abstract

In eukaryotes, nascent proteins that are destined for the secretory pathway enter the endoplasmic reticulum (ER) in unfolded states and generally leave only after they have reached their native conformation. Protein folding in the ER is challenging and often error-prone. To prevent accumulation of misfolded proteins, the ER uses the ER-associated protein degradation (ERAD) machinery to detect and commit these defective proteins for retrotranslocation to cytosol for degradation via the ubiquitin-proteasome system. Previously, our group and others discovered an ERAD pathway that requires the generation of a specific N-glycan structure on misfolded luminal N-glycoproteins to permit their degradation. This N-glycan degradation signal can potentially serve as a mark to flag the defective states of the attached protein, but whether the generation of this N-glycan degradation signal is directly connected to the folding state of the attached protein has remained unknown.

My thesis research is focused on characterization of Htm1p, the mannosidase that is responsible for generating this N-glycan signal in *Saccharomyces cerevisiae*. Utilizing an in vitro reconstitution system of Htm1p in complex with its interacting partner, Pdi1p, and glycoprotein substrates whose structures can be closely manipulated, I find that unlike other members of the same mannosidase family, Htm1p-Pdi1p is a glycoprotein-specific mannosidase that has little activity against free glycan. I find that Htm1p-Pdi1p targets intrinsically and artificially misfolded proteins but not their native counterparts. Most importantly, I find that Htm1p-Pdi1p differentiates detailed folding states of misfolded proteins and preferentially acts on partially folded proteins to

globally unfolded species. I further find that by forming a tight complex with Pdi1p, Htm1p blocks the intrinsic oxidoreductase function of Pdi1p but keeping the chaperone activity, suggesting a potential mechanism of how the Htm1p-Pdi1p complex recognizes misfolded proteins. In summary, this work demonstrates the tight correlation between the generation of the N-glycan degradation signal and the folding state of the attached protein, opening a future direction to investigate how the ER tells the bad from the good.

Contributions

At the time of completing this dissertation, the work described in Chapter 2 has been deposited as a preprint manuscript in BioRxiv (doi: http://dx.doi.org/10.1101/049825), and is accepted for publication in *Proceedings of the National Academy of Sciences of the United States of America* (doi: 10.1073/pnas.1608795113).

In Chapter 3, the original data in Figure 3 A, B, C, and D were obtained from Dr. Erin Quan Toyama. The CPY*noCys construct was originally designed by Dr. Melanie Smith. With the exception of the items in Chapter 3 listed above, Yi-Chang Liu performed the work presented in this dissertation under the supervision of Dr. Danica Galonić Fujimori and Dr. Jonathan S. Weissman.

Table of Contents

List of Figures

Chapter 1

Introduction:

Protein quality control in the ER and ER-associated protein degradation

To reach the functional states, proteins have to fold from their liner primary structures into specific three-dimensional structures after their biogenesis. While the primary sequence of a protein generally contains all the necessary information for it to fold into the most thermodynamically favored state (Anfinsen et al., 1961), folding energy landscape of most proteins is complicated and rugged, and intrinsic and extrinsic factors make the folding in the cell even more challenging (Brockwell and Radford, 2007; Eichner and Radford, 2011; Hartl et al., 2011). For most proteins, there exist multiple on-/off-pathway intermediate states, in which proteins may be trapped indefinitely and eventually form non-functional aggregates. Intracellular space is a extremely crowded environment, where macromolecules, proteins and nucleic acids, can occupy 10~40% of the total volume (Theillet et al., 2014). Macromolecular crowding has strong effect on folding kinetics and thermodynamics, which may lead to non-specific intermolecular association and thus aggregation (Mittal et al., 2015; Theillet et al., 2014). Structural dynamics of proteins are essential to achieve biological functions such as enzyme catalysis or protein-protein interaction, which inevitably increase the chance of misfolding and aggregation of proteins (Gershenson et al., 2014; Henzler-Wildman and Kern, 2007; Theillet et al., 2014). Cellular and environmental stresses often cause protein misfolding and thus detrimental physiological consequences (Chiti and Dobson, 2006; Labbadia and Morimoto, 2015).

All biological systems have sophisticated sets of machinery for protein quality control to promote folding and remove damaged proteins (Hartl et al., 2011; Labbadia and Morimoto, 2015). To promote folding, cells utilize a large and ever-expending set of

chaperones, the well-known examples to be the families of Hsp40, Hsp70, Hsp90, and chaperonin, which cover diverse client types and promote folding with different molecular mechanisms. When the proteins are severely damaged, cells utilize a diverse set of degradation machinery, such as the ubiquitin-proteasome system and the lysosome/autophagosome, to degrade defective proteins. Close communication between the folding machinery and the degradation machinery is critical to maintain proteostasis of the cell.

Being the major biogenesis site for secretory proteins in eukaryotes, not only does endoplasmic reticulum (ER) face all the general challenges for protein folding, but it also has to address challenges that are unique to the secretome (Braakman and Bulleid, 2011; Ellgaard and Helenius, 2003; Fewell et al., 2001). For example, transmembrane domains of membrane proteins have to be inserted into the lipid bilayer in correct membrane topology. Most proteins also acquire unique post-translational modifications, such as disulfide bonds and N-glycosylation, that directly influence the folding kinetics of the proteins (Hanson et al., 2009; Price et al., 2010; Shental-Bechor and Levy, 2008; Weissman and Kim, 1991, 1995). More importantly, ER is insulated from cytosol and requires its own chaperone system to maintain proteostasis (Braakman and Bulleid, 2011; Fewell et al., 2001). However, different from the cytosol, degradation does not directly happen in the ER. One major mechanism for degradation of damaged secretory and membrane proteins is through lysosome/autophagy, downstream along the secretory pathway (Araki and Nagata, 2011; Needham and Brodsky, 2013). Studies from the past three decades, in addition, have established that

the major quality control degradation in the ER is mediated through an ER-to-cytosol retrotranslocation process for proteasomal degradation, which has been generally referred to as ER-associated protein degradation (ERAD) (McCracken and Brodsky, 1996).

The idea of non-lysosomal protein degradation in the ER emerged during the 1980s. It was found that the ER-resident HMG-CoA reductase, the rate-limiting enzyme for cholesterol synthesis, was targeted for rapid degradation in a product-regulated manner (Gil et al., 1985). Studies on mammalian and viral membrane complexes also found that unassembled subunits of multisubunit membrane protein complexes were retained in the ER, and some of them were targeted for rapid degradation (Copeland et al., 1986; Gething et al., 1986; Lippincott-Schwartz et al., 1988). At a closer look, these unassembled subunits were sensitive to trypsin proteolysis, were different from their mature forms as detected by conformation-specific antibodies, and were often found to bind BiP, the ER-resident Hsp70 chaperone, which all suggested to that these proteins are in aberrant, dysfunctional states (Bole et al., 1986; Copeland et al., 1986; Gething et al., 1986; Haas and Wabl, 1983; Lippincott-Schwartz et al., 1988; Minami et al., 1987). It was quickly realized that there exists an ER quality control system to impose a conformational restrain to retain incompletely folded proteins or unassembled subunits of multisubunit complexes in the ER and to target them for degradation by a non-lysosomal pathway (Bonifacino and Lippincott-Schwartz, 1991; Hurtley and Helenius, 1989; Klausner and Sitia, 1990).

In 1988, Lippincott-Schwartz et al. made a key observation that unassembled T-cell receptor α chain was targeted for degradation through a pre-Golgi, non-lysosomal mechanism (Lippincott-Schwartz et al., 1988). With the newly available 26S proteasome inhibitors, it was then revealed that the turnover of the ER-retained, unstable mutants of CFTR are mediated by the 26S proteasome in mammals (Cheng et al., 1990; Jensen et al., 1995; Rock et al., 1994; Ward et al., 1995). Studies in budding yeast also showed that the proteasome and an ER-membrane-bound ubiquitination machinery mediate the degradation of defective ER proteins (Biederer et al., 1997; Hampton et al., 1996; Hiller et al., 1996; Sommer and Jentsch, 1993). Instead of being prevented from ER entry, these defective proteins first enter the ER and then undergo retrotranslocation from the ER to the cytosol before degradation, as shown by the accumulation of N-glycosylated forms of these proteins in the cytosol when the proteasome was inhibited (Hiller et al., 1996; Wiertz et al., 1996). Later, it was revealed that the ubiquitination is mediated by a transmembrane E3 ubiquitin ligase, Hrd1, the first E3 ligase to be found to be transmembrane (Bays et al., 2001a). The versatile p97 AAA-ATPase (Cdc48 in yeast) and its cofactors were also demonstrated to be required for the retrotranslocation (Bays et al., 2001b; Jarosch et al., 2002; Rabinovich et al., 2002; Ye et al., 2001). It became clear that this ER-to-cytosol degradation phenomenon, which had also started being called “ER-associated protein degradation” (ERAD) (McCracken and Brodsky, 1996), is responsible for degradation of a wide range of proteins for protein quality control in the ER.

In the past two decades, significant progress has been made for our understandings on ERAD, especially on the identities of factors participate in the ERAD process, which consists of diverse sets of pathways to target diverse sets of substrates. In our current knowledge, ERAD consists of three general steps (Araki and Nagata, 2011; Foresti et al., 2014; Smith et al., 2011): the first step is the identification of substrates by a diverse set of adapter proteins by different molecular principles to define specific sets of ERAD substrates; the second step is polyubiquitination and retrotranslocation of the identified substrates by a set of E3 ligase transmembrane complexes; the third step is the universally shared features of ER-to-cytoplasm retrotranslocation and degradation through the ubiquitin-proteasome system (UPS).

At the protein level, in addition to degrade defective proteins, ERAD is known to regulate key enzymes such as HMG-CoA reductase in response to metabolic cues (Hampton et al., 1996; Inoue et al., 1991). ERAD machinery is also hijacked by viruses to dismantle immune molecules (Hughes et al., 1997; Wiertz et al., 1996). In the systematic level, the regulatory roles of ERAD in multiple cellular processes have also been broadly described. In the cellular level, ERAD closely communicates with the ER stress response machinery, the unfolded protein response (UPR) machinery (Walter and Ron, 2011). Dysfunction of ERAD causes the accumulation of misfolded proteins in the ER and induces UPR, which in turn enhances the expression of ERAD genes to restore the ER proteostatsis (Jonikas et al., 2009; Shoulders et al., 2013; Travers et al., 2000). ERAD can directly communicate with the proteasome by constantly promote retrotranslocation of the ER form of NFE2L1 (also known as Nrf1), a key transcription

factor for 26S proteasome, to cytosol for proteasomal degradation. When the proteasome activity decreases, cytosolic NFE2L1 is stabilized and enter the nucleus to enhance expression of proteasome genes (Radhakrishnan et al., 2010; Steffen et al., 2010). ERAD machinery also regulates apoptosis by constantly targeting BOK, a mitochondrial surface membrane that belongs BCL-2 family apoptotic effector, for degradation. Upon inhibition of proteasome, BOK is stabilized and is able to activate apoptosis (Llambi et al., 2016). In the physiological level, increasing evidence has suggested the role of ERAD in various diseases. ERAD may inadvertently cause diseases by degradation of unstable but functional protein mutants, as seen in the cases of CFTR mutants that are the major genetic factors of cystic fibrosis (Cheng et al., 1990; Jensen et al., 1995; Ward et al., 1995); inability of ERAD to degrade aggregate-prone proteins may also cause diseases, such as the case of transthyretin mutants that escape from ER and eventually form toxic extracellular amyloids (Sekijima et al., 2005).

The key functionality of ERAD is to differentiate the myriad of proteins in the ER and accurately target the “right” proteins for degradation. The location of the folding defects/lesions is one of the molecular principles that have been systematically investigated. It was first found that luminal and transmembrane ERAD substrates have different dependence to different ERAD components (Swanson et al., 2001; Wilhovsky et al., 2000). Studies that systematically introduced lesions to different domains of luminal and membrane ER proteins have revealed that proteins are differently targeted through different ERAD pathways by the location of lesions (Carvalho et al., 2006; Christianson et al., 2011; Huyer et al., 2004; Vashist and Ng, 2004). In general, ERAD-L

targets proteins with folding lesions at ER luminal sides, ERAD-M targets proteins with lesions at their transmembrane domains, and ERAD-C targets lesions at cytosolic domains. It was also found that an E3 ligase complex mediates another ERAD pathway to target proteins that escape from the ER to inner nuclear membrane (Foresti et al., 2014).

It has been generally hypothesized that the essential molecular feature of the majority of ERAD substrates is an incompletely folded state with folding lesions (Hurtley and Helenius, 1989; Klausner and Sitia, 1990). How do ERAD adapters define lesions? Through systematically introducing structure-perturbing mutations, the Ng group has shown that it is possible to convert yeast procarboxypeptidase Y (CPY) and proteinase A (PrA), both normally well folded, into ERAD-L substrates (Xie et al., 2009). The Balch and Kelly groups have found that ERAD-L only targets the most kinetically and thermodynamically destabilized mutant variants of transthyretin (Sekijima et al., 2005; Wiseman et al., 2007). Particularly, the studies from the Balch and Kelly groups suggest that a folding-incompetent nature of a protein does not make it an obligatory substrate for ERAD. As the ER is also filled with nascent polypeptides and folding intermediates, it essential for ERAD to be able to differentiate true ERAD substrates from folding intermediates.

One unique molecular feature that ERAD-L uses to distinguish a subset of substrates of ERAD-L is their specific N-glycosylation states. It was first found that chemically inhibition of glucosidases accelerate ER degradation of model proteins, while inhibition of mannosidase inhibited degradation (Kearse et al., 1994; Moore and Spiro,

1993; Su et al., 1993; Yang et al., 1998). Around the same period of time, the role of the N-glycan structure for folding of nascent N-glycoprotein was just elucidated (Hammond et al., 1994; Hebert et al., 1995; Helenius, 1994; Ou et al., 1993; Peterson et al., 1995; Sousa and Parodi, 1995; Sousa et al., 1992). Briefly, nascent polypeptides acquire a tri-branched tetredecasaccharide ($Glc_3Man_9GlcNAc_2$) at specific asparagines when they enter ER (Figure 1.) (Helenius and Aebi, 2004). Two of the glucoses are then removed by glucosidase I and glucosidase II, leaving a monoglucosylated N-glycan that is recognized by lectins including calnexin/calreticulin, which also are chaperones that promote folding and prevent aggregation. Proteins are released from calnexin/calreticulin when the last glucose is removed by glucosidase II. However, if the released N-glycoproteins are not fully folded by the time when the last glucose is removed, UDP-glucose glucosyltransferase (UGGT) recognizes this partially structured state and reglucosylated these proteins to promote re-binding with calnexin/calreitculin, conferring an N-glycan-dependent folding cycle. The system is simplified in Saccharomyces cerevisiae, in which there is not detectable UGGT activity (Fernández et al., 1994).

The connection between ERAD-L and the N-glycan structure was further established when it was found that removal of the N-glycosylation site from the defective yeast procarboxypeptidase Y G255R mutant (CPY*), a prototypic ERAD substrate, retards its degradation via ERAD (Knop et al., 1996). By genetically manipulating the N-glycan structures in yeast, Jakob et al. then made a critical observation that ERAD-L of CPY* is dependent on specific N-glycan structures (Jakob et al., 1998). Specifically,

they found that the action of Mns1p, the exomannosidase that is downstream from glucosidase II to remove the terminal α1,2-linked mannose from its B branch and generate a $Man_8GlcNAc_2$ as the last step of N-glycan maturation in the ER (Herscovics, 2001), is essential for ERAD-L of CPY*.

It was then found that Yos9p, and its mammalian homologs, plays this role as a folding sensing lectin (Bhamidipati et al., 2005; Christianson et al., 2008; Kim et al., 2005; Szathmary et al., 2005). The glycan-binding MRH domain of Yos9p is critical for its ERAD function, and both Yos9p and its interacting partner Hrd3, a transmembrane protein that is important to anchor the Hrd1p transmembrane complex, are capable of binding to misfolded protein mutants but not native ones (Bhamidipati et al., 2005; Carvalho et al., 2006; Denic et al., 2006; Gauss et al., 2006; Kim et al., 2005; Szathmary et al., 2005). Vladimir Denic and Erin Quan, former members in our group, made key findings that Yos9p and Hrd3p play the role as an ERAD gatekeeper: only in the presence of both N-glycans and protein lesions does Yos9p-Hrd3p allow the action of Hrd1p (Denic et al., 2006). A severe growth phenotype was observed when this gatekeeping step is bypassed in a *HRD1* overexpression yeast background.

How does the ERAD-L machinery use the N-glycan structure to faithfully target the “right” proteins for degradation if all proteins have the same N-glycan generated by Mns1p? In collaboration with the group of Koichi Kato in Nagoya City University, Erin performed a detailed biochemical investigation in the lectin specificity of Yos9p (Quan et al., 2008). Interestingly, Yos9p only binds to glycans with a terminally exposed α1,6-linked mannose, a structure most likely to be found by the removal of α1,2-linked

mannose from the C branch, suggesting there may be one more mannosidase to mediate N-glycan-dependent ERAD-L. The last piece of the picture for this N-glycan-dependent ERAD-L pathway was filled when the Aebi group made critical *in vivo* and *in vitro* observations to establish that an additional exomannosidase, Htm1p, is responsible for the removal of α1,2-linked mannose from the C branch (Clerc et al., 2009; Gauss et al., 2011). Both the lectin specificity of Yos9p and the mannosidase activity of Htm1p have also been observed for their orthologs in mammalian cells (Christianson et al., 2008; Molinari, 2003; Ninagawa et al., 2014; Oda, 2003; Olivari et al., 2006; Satoh et al., 2010).

In sum, two steps of demannosylation by Mns1p and Htm1p are required to generate a degradation signal. The step-wise N-glycan remodeling suggests a timer model of this N-glycan-dependent ERAD-L pathway, in which all nascent N-glycoproteins are given a window of time to fold that is immune from ERAD till Htm1p remove the mannose, presumably only after the action of Mns1p (Clerc et al., 2009; Gauss et al., 2011; Helenius and Aebi, 2004; Jakob et al., 1998). After the timer ends, $Man_8GlcNac_2$-carrying proteins that are not folded are then demannosylated by Htm1p to expose the terminal α1,6-linked mannose as a glycan degradation signal. Only in the presence of both the glycan degradation signal and the lesion will Yos9p-Hrd3p then allow the defective N-glycoprotein to be targeted for Hrd1p-mediated retrotranslocation, polyubiquitination, and thus cytosolic degradation via the proteasome (Denic et al., 2006; Stein et al., 2014). However, this model cannot explain the observations that turnover rates of proteins are not accelerated in yeast strains that directly produce N-

glycans with terminally exposed α1,6-linked mannose (Clerc et al., 2009; Quan et al., 2008; Xie et al., 2009). Thus, the rate-limiting step in ERAD-L is still the recognition of specific folding lesions. Indeed, all the key adapters but Mns1p have been revealed to have general biochemical preference to canonical misfolded proteins than their native counterparts (Bhamidipati et al., 2005; Carvalho et al., 2010; Denic et al., 2006; Gauss et al., 2011; Lipari and Herscovics, 1994; Smith et al., 2014; Stein et al., 2014).

The unique requirement of a specific N-glycan structure to permit degradation has arguably made the N-glycan-dependent ERAD-L pathway the most well characterized ERAD pathway (Foresti et al., 2014; Smith et al., 2011). Despite so, what the chemical and physical properties of a misfolded protein are has been one critical question that has not been answered. A major limiting factor behind is our ability to monitor and correlate protein folding states to degradation in the cell, whose resolution has not improved significantly since the idea of ERAD emerged thirty years ago. Using this N-glycan degradation signal as a handle, we may be able to obtain a systematic view of how the ER defines defective proteins. To achieve this ultimate goal, my thesis work is focused on investigating the correlation between the conformation of an ERAD-L substrate with the generation of the N-glycan degradation signal by Htm1. Chapter two describes the experimental evidence to support the model that Htm1 impose a conformational standard to target misfolded N-glycoproteins for ERAD-L. Chapter three covers the investigation of how the interacting partner of Htm1 may contribute to this process.

Figure

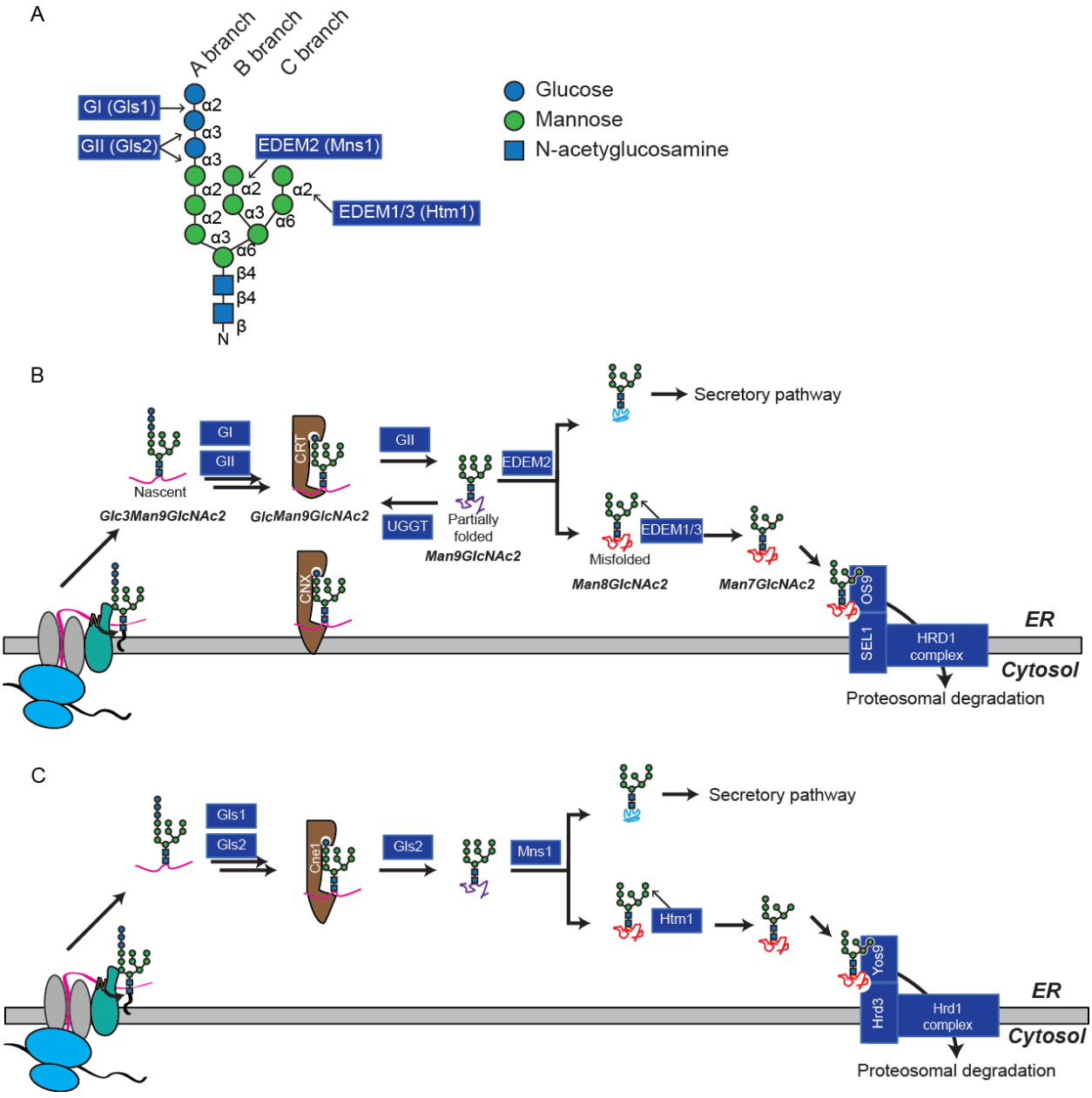

Figure 1. Models of N-glycan-mediated protein folding and ERAD-L in mammalian cells and yeast.

(A) Schematic representation of the tetradecasaccharide that is installed onto specific asparagines on polypeptides co-/post-translocationally. The anomeric isoform and the position of the acceptor hydroxyl group of each glycosidic bond are indicated. The

mammalian glycosidases that are responsible for removal of each specific monosaccharide after the N-glycosylation, as well as the yeast orthologs in parenthesis, are indicated.

(B) N-glycan-mediated folding and ERAD in the ER in mammalian cells. See the main text for the full description of the process.

(C) N-glycoprotein folding and ERAD in the ER in yeast.

Chapter 2

Htm1p-Pdi1p is a folding sensitive mannosidase that marks N-glycoproteins for ER-associated protein degradation

Abstract

Our understanding of how the endoplasmic reticulum-associated protein degradation (ERAD) machinery efficiently targets terminally misfolded proteins while avoiding the misidentification of nascent polypeptides and correctly folded proteins is limited. For luminal N-glycoproteins, demannosylation of their N-glycan to expose a terminal α1,6-linked mannose is necessary for their degradation via ERAD, but whether this modification is specific to misfolded proteins is unknown. Here we report that the Htm1p-Pdi1p complex acts as a folding-sensitive mannosidase for catalyzing this first committed step. We reconstitute this step *in vitro* with Htm1p-Pdi1p and model glycoprotein substrates whose structural states we can manipulate. We find that Htm1p-Pdi1p is a glycoprotein-specific mannosidase, which preferentially targets nonnative glycoproteins trapped in partially structured states. As such, Htm1p-Pdi1p is suited to act as a licensing factor that monitors folding in the ER lumen and preferentially commits glycoproteins trapped in partially structured states for degradation.

Introduction

Proteins destined for the secretory pathway enter the endoplasmic reticulum (ER) in unfolded states and generally leave only after they have reached their native conformation. Protein folding in the ER is challenging and often error-prone (Ellgaard and Helenius, 2003; Fewell et al., 2001). Thus the ER must continuously monitor the pool of folding proteins and remove terminally misfolded forms before they induce toxicity. This is accomplished through a series of pathways collectively referred to as the ER-associated protein degradation (ERAD) machinery (Smith et al., 2011). Generally, the process of ERAD involves three steps: 1) identification of the misfolded protein, 2) retrotranslocation and polyubiquitination of the misfolded protein through individual E3 ubiquitin ligase complexes, and 3) degradation of the misfolded protein by the ubiquitin-proteasome system in the cytosol.

Each ERAD pathway needs to accurately identify substrates to avoid overly promiscuous destruction of functional proteins while preventing the accumulation of toxic forms (Ellgaard and Helenius, 2003). For the ERAD pathway responsible for the destruction of proteins with misfolded luminal domains (ERAD-L) (Carvalho et al., 2006; Vashist and Ng, 2004), this process of discrimination depends not only on the folding status of a polypeptide but also on its N-glycosylation state (Bhamidipati et al., 2005; Denic et al., 2006; Jakob et al., 1998; Kim et al., 2005; Quan et al., 2008; Szathmary et al., 2005). Upon entering the ER lumen, nascent proteins acquire *en bloc* a high-mannose oligosaccharide, $Glc_3Man_9GlcNAc_2$, appended to a specific subset of asparagine residues (Fig. 1*A*). The N-glycan is then deconstructed monosaccharide-by-

monosaccharide to $Man_8GlcNAc_2$ (Man8) in the ER by a series of glycosidases concurrently with the protein folding process (Aebi et al., 2010; Helenius and Aebi, 2004). The action of the mannosidase Mns1p, which is responsible for generating Man8, has been proposed to yield a "timer" that universally gives all N-glycoproteins a defined period of time to fold during which they are immune from ERAD-L (Helenius and Aebi, 2004; Jakob et al., 1998). Misfolded proteins that are destined for degradation via ERAD-L are further demannosylated by Htm1p (also known as Mnl1p), an enzyme that removes the α1,2-linked mannose from the C branch of Man8, generating a $Man_7GlcNAc_2$ (Man7) glycan structure with a terminally exposed α1,6-linked mannose that serves as a signal for ERAD-L commitment (Clerc et al., 2009; Gauss et al., 2011). The Yos9p lectin subsequently binds this terminally exposed α1,6-linked mannose and, in coordination with Hrd3p, queries the misfolded regions on potential substrates (Bhamidipati et al., 2005; Denic et al., 2006; Gauss et al., 2006; Kim et al., 2005; Quan et al., 2008; Szathmary et al., 2005). Only the presence of both the Htm1p-generated N-glycan signal and the misfolded regions on the substrate enables Yos9p-Hrd3p to trigger the downstream retrotranslocation, polyubiquitination, and proteasomal degradation of target proteins (Clerc et al., 2009; Quan et al., 2008; Xie et al., 2009). The physiological importance of these checkpoints is exemplified by the severe growth defect acquired when the requirement for Hrd3p and Yos9p was bypassed by overexpression of *HRD1*, which encodes the downstream E3 ubiquitin ligase for this pathway (Denic et al., 2006).

As the first committed step, the generation of the terminally exposed α1,6-linked mannose by Htm1p has the potential to determine which proteins, and at what stage during their folding process, are shunted down the ERAD-L pathway. This potential "licensing" role has been supported by *in vivo* observations that genetic deletion of *HTM1*, as well as point mutations in its putative active sites, not only retards the degradation of misfolded N-glycoproteins, but also decreases substrate-binding by Yos9p (Clerc et al., 2009; Jakob et al., 2001; Nakatsukasa et al., 2001; Szathmary et al., 2005; Xie et al., 2009). This retardation of ERAD by deletion of *HTM1* can be circumvented in a genetic background that generates the terminally exposed α1,6-linked mannose (Quan et al., 2008). The importance of the mannosidase function of Htm1p is further evidenced by the conserved role of HTM1 homologs for the N-glycan-dependent ERAD pathway (Molinari, 2003; Ninagawa et al., 2014; Oda, 2003). Finally, both *in vivo* and *in vitro* studies have provided evidence for the mannosidase activity of Htm1p in generating Man7 (Clerc et al., 2009; Gauss et al., 2011; Pfeiffer et al., 2016). However, despite the well-documented role of Htm1p in the N-glycan processing for ERAD-L commitment, it is still unclear how specifically and accurately Htm1p targets misfolded proteins. This uncertainty is mainly due to the challenges in simultaneously monitoring protein conformations and their N-glycosylation states in the highly heterogeneous pool of glycoproteins in the ER. Additionally, only minimal mannosidase activities of Htm1p were observed in previous *in vitro* studies (Gauss et al., 2011; Pfeiffer et al., 2016). To advance our understanding of this commitment step, it is critical to develop a

reconstituted system for direct investigation of enzymatic activities of Htm1p against glycoproteins with defined glycosylation and folding states (Denic, 2011).

Here, we reconstituted this ERAD-L commitment step, which consists of a recombinantly expressed Htm1p-Pdi1p complex and glycoprotein substrates with various native and nonnative conformations. Our results reveal that Htm1p-Pdi1p is a glycoprotein-specific mannosidase complex that preferentially demannosylates intrinsically or artificially misfolded proteins compared to their native counterparts. Furthermore, among the various nonnative conformations, Htm1p-Pdi1p prefers partially structured proteins over globally unfolded ones. Our findings suggest that Htm1p-Pdi1p monitors the protein folding states in the ER lumen and preferentially licenses glycoproteins trapped in partially structured states for ERAD-L.

Results

Generation of Man7 *in vivo* is folding- and *HTM1*-dependent

It has been reported that the prototypic ERAD-L substrate, CPY*, contains higher levels of Man7 than its folding-competent counterpart, pro-carboxypeptidase Y (CPY) in a wild-type yeast background (Szathmary et al., 2005). We first explored whether the higher level of Man7 of CPY* reflects the differences in intrinsic folding competence between CPY* and CPY, or rather results passively from the prolonged ER retention of CPY*. Utilizing a previously described overexpression construct (Stein et al., 2014), we expressed and purified native CPY and CPY* that are retained in the ER by a C-terminal HDEL tag. We used MALDI-TOF mass spectrometry to determine the glycan

profile of CPY and CPY*. This approach provides higher throughput capacity than HPLC-based measurement while still allowing quantitative analysis of neutral glycans (Thaysen-Andersen et al., 2009). As such, it is also amenable to the analysis of mannosidase activities described below. Both CPY and CPY* purified from wild-type (BY4741) yeast strain carried predominantly Man8 and minor populations of Man7, Man9 and $Hex_{10}GlcNAc_2$ (Hex10), which is likely $GlcMan_9GlcNAc_2$ (Fig. S1 *A* and *B*). The majority of the signal of Man7 disappeared when CPY and CPY* were purified from the *htm1Δ* strain background (Fig. 1 *B* and *C*). When CPY and CPY* were purified from a *mns1Δhtm1Δ* background, the dominant glycan species shifted from Man8 to Man9, further verifying that the majority of Man8 from the WT strain is the product of Mns1p, the putative substrate of Htm1p (Fig. S1 *A* and *B*). Importantly, CPY* carried a significantly higher level of Man7 than CPY (Fig. 1 *B* and *C*). Taken together, these observations suggests that despite both being retained in the ER, CPY* and CPY are differentially demannosylated to Man7 in an *HTM1*-dependent manner. Given that CPY and CPY* purified through this HDEL-tagged system are only different at the G255R point mutation on CPY* that disrupts the hydrophobic core on the native structure (Endrizzi et al., 1994), we conclude that the generation of Man7 in the ER is correlated with the intrinsic folding competence of the underlying protein.

Reconstitution of an Htm1p-Pdi1p complex

In order to explore the activity of Htm1p *in vitro*, we tested the feasibility of producing Htm1p from the native host *Saccharomyces cerevisiae*. We introduced a 3xFLAG tag,

followed by a HDEL tail before the stop codon, to the C-terminus of Htm1p for affinity purification. The result of cycloheximide degradation assay on CPY* suggests that the chromosomally tagged version is similarly functional as the wild-type Htm1p (Fig. 2*A*). Since the endogenous level of Htm1p is low, we enhanced the expression of Htm1p by chromosomally substituting its endogenous promoter with a *TDH3* promoter (Fig. 2*B*). Consistent with a previous study (Sakoh-Nakatogawa et al., 2009a), Htm1p readily formed a disulfide complex with endogenous Pdi1p as resolved by non-reducing SDS-PAGE (Fig. 2*B*). Large-scale immunoprecipitation yielded an Htm1p-Pdi1p complex with near 1:1 stoichiometry (Fig. 2*C*), with a yield of 200 μg of the complex from three liters of yeast culture. Endoglycosidase H treatment of the complex confirmed that both Htm1p and Pdi1p were N-glycosylated, indicating that they are correctly targeted to the secretory pathway (Fig. 2*D*). The complex behaved as a monodisperse species in size-exclusion column chromatography (Fig. 2*E*), which contained a mixture of both disulfide-linked and non-covalent complexes of Htm1p and Pdi1p (Fig. 2*F*). We did not detect any monomeric Htm1p or Pdi1p corresponding to their predicted mass (90.2 kDa for Htm1p, and 56.0 kDa for Pdi1p). Finally, we observed the mannosidase activity against the most preferred glycoprotein substrate, RBsp, only in the fractions containing the Htm1-Pdi1p complex (Fig. 2*G*), *vide infra*.

Htm1p-Pdi1p preferentially demannosylates CPY* and misfolded CPY variants

We first explored the mannosidase activity of reconstituted Htm1p-Pdi1p on CPY and CPY* that we purified from wild-type yeast. After a 20-hour reaction, Htm1p-Pdi1p

converted a portion of Man8 on CPY and CPY* to Man7 (Fig. 3 *A* and *B*). Consistent with our *in vivo* observation, the increase in Man7 on CPY* is significantly higher than that on CPY after incubation with Htm1p-Pdi1p (Fig. 3*C*). To further validate that Htm1p-Pdi1p preferentially targets nonnative proteins, we reductively denatured CPY to remove its structurally essential disulfide bonds (Winther and Sørensen, 1991). Reduced CPY was then either oxidized under denaturing condition into "scrambled" species with randomly distributed nonnative disulfide bonds (Scr-CPY), or carbamidomethylated to block reformation of disulfide bonds (Carb-CPY). Htm1p-Pdi1p also demannosylated both Scr-CPY and Carb-CPY more efficiently than the native form, and the yield of Man7 was higher on Scr-CPY than Carb-CPY (Fig. 3*D*). Taken together, these results suggest that our reconstituted Htm1p-Pdi1p is an active mannosidase and preferentially acts on intrinsically folding-incompetent CPY*, as well as artificially misfolded CPY variants, in comparison to the native CPY.

We then wanted to verify whether demannosylation is catalyzed through the predicted mannosidase domain of Htm1p, and whether Pdi1p is required for this process. We carried out the reaction in the presence of EDTA, which sequesters the structurally essential Ca^{2+}, as well as 1-deoxymannojirimycin (DMJ), which inhibits the GH47 mannosidase family that Htm1p is predicted to belong to (Vallee et al., 2000). Both chemicals inhibited the generation of Man7 on CPY*(Fig. 3*E*). We further verified the predicted mannosidase function of Htm1p with an Htm1 mutant that has one of the putative active site residues Glu_{222} mutated to Gln (E222Q) (Clerc et al., 2009; Hosomi et al., 2010), which was indeed incapable of generating Man7 on CPY* (Fig. 3*E*).

Finally, we made a second Htm1 mutant that has a truncation of the amino acyl region from 572 to 657 (Δ572-657), which covers the region necessary for interaction with Pdi1p (Fig S2*A*) (Clerc et al., 2009; Pfeiffer et al., 2016; Sakoh-Nakatogawa et al., 2009a). Immunoprecipitation confirmed that Δ572-657 showed little detectable interaction with Pdi1p (Fig S2*B*). Similar to the catalytically dead E222Q, Δ572-657 was incapable of generating Man7 on CPY* (Fig. 3*E*). Collectively, our results support that the predicted mannosidase domain of Htm1p mediates the demannosylation reaction, and that the interaction with Pdi1p is required for this activity.

The conversion of Man8 to Man7 on CPY* continued during prolonged incubation with Htm1p-Pdi1p (Fig. S3*A*), but this rate of demannosylation is nonetheless much slower than what would be expected from the *in vivo* half-life of CPY*, which is about 60 minutes (Fig. 2*A*). This slow rate in principle could be a consequence of the fact that CPY has four N-glycans, and thus Htm1p-Pdi1p may only act on a subset of glycans on CPY*. Indeed, the C-terminal most N-glycan of CPY* is known to be necessary and sufficient to support its ERAD *in vivo* (Kostova, 2005; Spear and Ng, 2005; Xie et al., 2009). However, we found that *in vitro,* Htm1p-Pdi1p demannosylated a CPY* mutant, in which this ERAD-competent glycosylation site, Asn_{479}, was mutated to Gln (CPY*1110), to a level similar to CPY* with all four glycosylation sites (Fig. S3*B*). A similar level of demannosylation was observed on another CPY* mutant in which the other three glycosylation sites (Asn_{124}, Asn_{198}, and Asn_{279}) were all mutated to Gln (CPY*0001). The glycosylation site is thus not likely the key factor limiting the catalytic activity. Increasing the amount of Htm1p-Pdi1p by four folds did not proportionally

increase the yield, suggesting that the enzyme concentration is not the limiting factor either (Fig. S3*E*).

The incomplete reaction may also reflect conformational heterogeneity or the aggregation-prone nature of CPY*. Indeed, in our hand, the majority of purified CPY* is in oligomeric forms (Fig. S4), and we observed formation of visible aggregates from both CPY* and artificially misfolded CPY variants after incubation with Htm1p-Pdi1p for twenty hours. A potential consequence of aggregation is that the glycans become inaccessible to the deep active pocket of Htm1p as predicted by the GH47 family mannosidase domain (Vallée et al., 2000). We first explored whether Htm1p-Pdi1p has higher activity against free Man8 glycan. Htm1p-Pdi1p only generated limited amount of Man7 after 24 hours of reaction (Fig. S5*A*). In contrast, Mns1p, which similarly contains a GH47 family mannosidase domain, was able to completely demannosylate Man9 into Man8 (Fig. S5*B*). Then, to assess the accessibility to glycans on CPY, we tested the activity of Mns1p against Man9-carrying CPY (CPYm9) and its scrambled form (Scr-CPYm9) purified from the *mns1Δhtm1Δ* strain background. Mns1p converted most of Man9 on both CPYm9 and Scr-CPYm9 into Man8, suggesting that the glycans are accessible on both native and nonnative forms of CPY (Fig. 4). Mns1p alone did not produce any detectable Man7. Only co-treatment of Mns1p and Htm1p-Pdi1p yielded Man7 to a level similar to what we observed in Figure 3. We found that Htm1p-Pdi1p alone, without Mns1p, was also capable of demannosylating Man9 on CPYm9 and Scr-CPYm9 into Man8, albeit to a lower extent. Similar to the results in Figure 3*D*, the level of Man8 generated by Htm1p-Pdi1p treatment was higher on Scr-CPYm9 than CPYm9.

Collectively, these observations suggest intrinsic differences in substrate specificity between Mns1p and Htm1p-Pdi1p: while Mns1p is capable of targeting both free glycans and glycoproteins independently of the attached protein conformations, Htm1p-Pdi1p preferentially targets glycans installed on nonnative proteins. In addition, consistent with previous *in vivo* studies (Bhamidipati et al., 2005; Chantret et al., 2011; Hosomi et al., 2010), our findings suggest that Htm1p-Pdi1p is capable of bypassing the action of Mns1p to directly demannosylate Man9.

Htm1p-Pdi1p preferentially demannosylates partially structured RNase B variants

To this point, our findings support two potential models of how Htm1p-Pdi1p generates the α1,6-lniked mannose signal for ERAD-L commitment. In one model, the catalysis by Htm1p-Pdi1p may be intrinsically slow and stochastic as previously suggested (Gauss et al., 2011; Pfeiffer et al., 2016), and unfolding facilitates demannosylation by increasing access to the glycan. Alternatively, Htm1p-Pdi1p may preferentially target specific folding states of nonnative proteins, and the absence of ER factors, such ER chaperones (Nishikawa et al., 2001), prevents CPY* from populating in these specific states. To test these two potential models, we introduced bovine pancreatic ribonuclease B (RNase B) as an alternative substrate. RNase B is identical to the well-characterized classic protein folding substrate RNase A protein with the exception that it contains a single N-glycosylation site (Raines, 1998). The folding of RNase B has been extensively studied, and the proteins can be manipulated to form well-defined, homogeneous states of native, misfolded or unfolded conformations (Ritter and

Helenius, 2000; Ritter et al., 2005; Trombetta and Helenius, 2000). Using a concanavalin A lectin-based enrichment approach (González et al., 2000), we can enrich for Man8-abundant RNase B from commercial sources in biochemical quantities (Fig. S6). To generate a nonnative variant of RNase B, we proteolytically removed the N-terminal S peptide from native RNase B to produce RNase BS protein (RBsp) (Fig. 5*A*). RBsp is trapped in a compact, disordered but nonetheless well-behaved state, and it can be readily reconstituted into a native-like RNase BS form by addition of the S peptide (Trombetta and Helenius, 2000).

Remarkably, Htm1p-Pdi1p differentiated between native RNase B and RBsp, and only efficiently demannosylated RBsp (Fig. 5*B*). Demannosylation of Man8 on RBsp into Man7 nearly reached the plateau after one hour of incubation with Htm1p-Pdi1p (Fig. S7*A*). We further investigated whether Htm1p-Pdi1p can be *trans*-activated by RBsp, or *trans*-inhibited by CPY*. We tested this possibility by incubating Htm1p-Pdi1p with CPY* for two hours, and then adding RBsp. Mass differences between CPY* (76.7 kDa) and RBsp (13.2 kDa) allow them to be readily separated by SDS-PAGE for subsequent glycan profiling. No obvious differences was observed on demannosylation of RBsp in the presence of absence of CPY*, and *vice versa* (Fig. S8 *A* and *B*). We further extended this experiment with a mixture of native RNase B and RBsp, which can be similarly separated by SDS-PAGE by the mass of the S-peptide (Fig. 5*C*). The presence of RBsp did not induce the demannosylation of native RNase B by Htm1p-Pdi1p (Fig. 5*D*). Collectively, these data establish that Htm1p-Pdi1p is capable of efficiently

demannosylating specific types of nonnative proteins that RBsp belongs to, and the activity is not *trans* regulated in a mixture of different glycoproteins.

Consistent with the results in Figure 4, we observed the disappearance of Man9 on RBsp during the reaction with Htm1p-Pdi1p (Fig. S7 *A* and *B*). The residual Man8 can be attributed to the other two less abundant Man8 isoforms on RNase B that already have the C branch α1,2-mannose removed (Fu et al., 1994). Indeed, all of the Man9 and Man8 on RBsp were removed after co-treatment with Mns1p and Htm1p-Pdi1p (Fig. S7*B*), which also verified that Mns1p and Htm1p-Pdi1p target different mannoses on Man9. We further explored whether Htm1p-Pdi1p targets the α1,2-linked mannose on the C branch or the A branch, a question that has never been thoroughly investigated. To obtain a structural view of which mannose is removed by Htm1p-Pdi1p, we performed ^{1}H-NMR analysis on the glycans released from denatured RNase B before and after an overnight reaction with Htm1p-Pdi1p. Indeed, we found only the α1,2-linked mannose on the C branch was removed after an overnight incubation with Htm1p-Pdi1p (Fig 6), providing structural evidence to support the existing model that Htm1p-Pdi1p specifically removes the α1,2-mannose on the C branch.

To further characterize how accurately Htm1p-Pdi1p differentiates proteins with different nonnative conformations, we generated three additional variants of RNase B: 1) subtilisin-nicked non-covalent complex of RBsp and S-peptide (RNase BS), 2) disulfide-scrambled RNase B (Scr-RB), and 3) cysteine-carbamidomethylated RNase B (Carb-RB) (Fig. 7*A*). Consistent with the known properties of these variants (Ritter and Helenius, 2000; Trombetta and Helenius, 2000), our far-UV circular dichroism analysis

verified that these RNase B variants cover a range of different conformations (Fig. 7*B*): RNase BS behaves essentially identically to native RNase B; RBsp is a compact folding intermediate with relatively abundant secondary structure features; Scr-RB consists of random, less compact structures with residual signals from secondary structures; Carb-RB consists of globally unfolded species with the majority of the signals from random coils. We further confirmed this increasing trend of unfolding from native RNase B to Carb-RB by monitoring the differences in peptide backbone flexibility and glycan accessibility of different RNase B variants through trypsin and PNGase F treatment (Fig. S9 *A* and *B*). Of a particular note, unlike CPY* and nonnative CPY variants, both Scr-RB and Carb-RB did not oligomerize or aggregate even after overnight incubation with Htm1p-Pdi1p at 30°C (Fig. S9 *C* and *D*).

Analysis of the demannosylation of RNase B variants by Htm1p-Pdi1p revealed that Htm1p-Pd1ip was able to distinguish differences in conformations of these variants (Fig. 7*C*). Htm1p-Pdi1p showed minimal mannosidase activities on the native-like RNase BS, suggesting that Htm1p-Pdi1p is insensitive to the mild increase in peptide flexibility around the N-glycosylation site of RNase BS (Blanchard et al., 2008). For nonnative variants, we observed a clear trend of increasing demannosylation efficiency as one goes from the globally unfolded Carb-RB, to the more compact but heterogeneous Scr-RB, and finally to the most compact and homogenous form RBsp. Demannosylation of Carb-RB continued during prolonged incubation (Fig. S10*A*), suggesting that the lower levels of demannosylation of Carb-RB at earlier time points resulted from slower kinetics. Scr-RBsp and Carb-RBsp were similarly susceptible to

Htm1p-Pdi1p as their full-length counterparts, suggesting that the difference in the kinetics was not due to the absence of the S peptide *per se* (Fig. S10*B*). The slower kinetics against Carb-RB was not due to alkylation of cysteines, as a fully reduced RNase B (Red-RB) was demannosylated at a rate similar to Carb-RB (Fig. S10*C*). In addition, Htm1p-Pdi1p was not inhibited when its cysteines were first blocked with iodoacetamide before reaction with RBsp, ruling out the possibility of a cysteine-mediated demannosylation mechanism (Fig. S10*D*). To conclude, our findings demonstrate that not only does Htm1p-Pdi1p differentiate nonnative proteins from native ones, but it also prefers nonnative proteins with compact, partially structured conformations over globally unfolded. Our findings support our second model that Htm1p-Pdi1p is a folding-sensitive mannosidase that preferentially targets nonnative proteins trapped at partially structured states.

Discussion

A fundamental question of ERAD is what are the biochemical properties that differentiate an ERAD substrate from a normal protein in the ER (Ruggiano et al., 2014; Smith et al., 2011). The unique requirement of a N-glycan remodeling step for ERAD-L commitment potentially provides a chemical handle to investigate the biochemical basis that determines an ERAD-L substrate. Here, our study provides biochemical evidence to support a model that this commitment step by Htm1p-Pdi1p is closely coordinated with the conformations of potential ERAD-L substrates. As such, the resulting terminally

exposed α1,6-linked mannose is suitable to be a folding-state mark that flags folding defects in the attached proteins.

Several lines of biochemical evidence support our conclusion that Htm1p-Pdi1p is a folding-sensitive mannosidase. First, we see the mannosidase activity of Hm1p-Pdi1p against misfolded forms of CPY and RNase B variants but not against free Man8, suggesting that unlike Mns1p, Htm1p-Pdi1p is a glycoprotein-specific mannosidase. Second, we see a marked enhancement of demannosylation activity of Htm1p-Pdi1p when native CPY and native RNase B were artificially converted to misfolded forms, suggesting Htm1p-Pdi1p prefers proteins of nonnative folding states to their native forms. Third, we see significantly higher rate of activity of Htm1p-Pdi1p against partially structured RNase B variants compared to their globally unfolded forms, indicating that Htm1p-Pdi1p can distinguish different nonnative states. Our biochemical analysis of the conformational sensitivity of Hmt1p-Pdi1p is supported by our *in vivo* findings that reveal a higher abundance of steady-state Man7 on ER-retained CPY* than CPY in wild-type yeast; this suggests that generation of Man7 is not a passive, universal event of prolonged ER retention.

The observed preference for partially folded forms can explain why Htm1p-Pdi1p has higher mannosidase activity against Scr-CPY than Carb-CPY. On the other hand, the absence of ER chaperones to keep CPY* in partially structured states may explain why Htm1p-Pdi1p is unable to exert its full activity on CPY* in our *in vitro* system (Nishikawa et al., 2001). As proteins populated at partially structured states have the propensity to form aggregates and amyloids (Eichner and Radford, 2011; Fink, 1995),

this conformational preference of Htm1p-Pdi1p may ensure that proteins on the verge of aggregating are promptly committed for degradation. Additionally, this folding-sensitivity of Htm1p-Pdi1p can ensure that nascent, globally unfolded polypeptides are allowed sufficient time for folding.

Interestingly, this conformational preference is reminiscent of that of UDP-glucose glucosyltransferase (UGGT), which reglucosylates partially structured proteins to help their retention in the ER folding cycle (D'Alessio et al., 2010a). The presence of multiple N-glycan-remodeling enzymes with a similar preference for compact intermediates further argues for the broad biological importance of detection of partially structured proteins in the ER. The essential interaction of Htm1p with Pdi1p is also reminiscent of the predicted structure of UGGT, which contains three thioredoxin-liked domains that may contribute to peptide binding (Zhu et al., 2014). The reconstitution system that we have established here provides a roadmap for future structural investigation of whether and how the thioredoxin domains of Pdi1p contribute to the recognition of partially structured proteins. Furthermore, our discovery that Htm1p-Pdi1p can remove the α1,2-linked mannose from Branch C on Man9 without the prior action of Mns1p suggests a future direction to apply synthetic Man9-glycoconjugates that were developed for the investigation of UGGT (Ito et al., 2015) for more detailed analysis on how the N-glycan is used as a potential time indicator by Htm1p-Pdi1p for glycoprotein quality control in the ER.

To conclude, in addition to the previous characterized ERAD-L surveillance step mediated by the Yos9p-Hrd3p complex (Denic et al., 2006; Gauss et al., 2006; Quan et

al., 2008; Smith et al., 2014), here we provide evidence for an upstream folding surveillance step that is mediated by Htm1p-Pdi1p. The presence of multiple folding surveillance steps, each with its own unique N-glycan processing or recognition functions, supports a model that ERAD-L follows a kinetic proofreading mechanism to achieve high fidelity in targeting the “right” proteins for degradation (Denic et al., 2006; Hopfield, 1974; Quan et al., 2008).

Materials and Methods

Yeast strains

All yeast transformations were conducted according to standard procedures. For chromosomal overexpression of *HTM1* (yJW1819 and yJW1820), the chromosomal *HTM1* locus was deleted from BY4741 by a *URA3* selection marker. Double-stranded DNA starting either with the endogenous 5'UTR promoter or a *TDH3* promoter for overexpression, followed by the full coding-region of wild-type or mutant *HTM1,* with a C-terminal 3xFLAG-HDEL tag, 3'-UTR of *HTM1* and finally a KANMX selection marker was then introduced into the *htm1Δ::URA3* strain. A pGAL1-MNS1-3xFLAG::KANMX strain (yJW1832) was generated by the same procedure for the preparation of 3xFLAG-tagged Mns1p that is controlled by a *GAL1* promoter.

Plasmids

The plasmid for *GAL1* promoter-driven CPY* expression (pJW1528) was kindly provided by Tom Rapoport (Harvard Medical School). To generate a native CPY expression plasmid (pJW1529), PCR primers carrying the native G255 codon were used to amplified the G255R region from the CPY* expression plasmid, and then assembled into the same vector backbone by the Gibson method. To generate the CPY*0001 expression plasmid (pJW1530), PCR primers carrying asparagine to glutamine mutations of the first three N-glycosylation sites were used to make mutant fragments on CPY* by PCR amplification, which were then assembled into the same 2-μm vector backbone by the Gibson method (Gibson et al., 2009). The same procedure

was used to generate the CPY*1110 plasmid (pJW1609).

Antibodies

Anti-FLAG M2 mouse monoclonal antibody and the antibody-conjugated agarose beads were purchased from Sigma-Aldrich (St. Louis, MO). Anti-yeast Pdi1p rabbit antisera was a gift from Peter Walter (University of California, San Francisco), which was confirmed by recombinantly expressed Pdi1p. IR fluorescence-conjugated secondary antibodies were purchased from LI-COR (Lincoln, NE).

Recombinant preparation of Htm1p-Pdi1p and Mns1p

The yJW1820 yeast was grown in three liters of YEPD 30°C to reach the stationary phase. Cells were harvest by centrifuging at 4,000 x *g* for 5 minutes, washed with cold deionized water, and stored at -80°C. All of the following purification steps were carried out at 4°C. Approximately 15 g of cell pellet was mixed with 5 g of dry ice, and then was ground by a Proctor Silex E160BY grinder (Southern Pine, NC) for a 30-second On/Of cycle for 5 times. The cell ground was vacuum-degassed for 5 minutes to remove residual dry ice, and thawed and resuspended in 25 ml Lysis Buffer (20 mM HEPES pH 7.0, 150 mM NaCl, 2 mM $CaCl_2$, 0.5% (v/v) NP-40, 15% (v/v) glycerol, 1x *cOmplete* EDTA-free protease inhibitor cocktail (Roche Diagnostics)). The slurry was centrifuged at 6,000 x *g* twice to remove cell debris, nutated for 30 minutes to solubilize the lipid membrane, and then ultracentrifugation at 60,000 x *g* for 30 minutes. The supernatant was collected and transferred into a new tube containing approximately 300 µl bed-

volume of anti-FLAG M2 affinity agarose beads (Sigma-Aldrich) that has been equilibrated with the Lysis Buffer. The mixture was nutated for 3 hours and then transferred into an open column. The column was washed with 3 ml Wash Buffer 1 (20 mM HEPES pH 7.0, 150 mM NaCl, 2 mM $CaCl_2$, 1x *cOmplete* EDTA-free protease inhibitor cocktail, 15% (v/v) glycerol), 1 ml Wash Buffer 2 (20 mM HEPES pH 7.0, 300 mM NaCl, 2mM $CaCl_2$, 15% (v/v) glycerol), and 1 ml Wash Buffer 3 (20 mM HEPES pH 7.0, 150 mM NaCl, 2 mM $CaCl_2$, 20 mM imidazole, 15% (v/v) glycerol). To release Htm1p-Pdi1p from the affinity beads, the column was closed by an end-cap, and 10 µg TEV protease and 300 µl Wash Buffer 3 were added. After overnight incubation without agitation, the cleaved products were eluted with 400 µl more Wash Buffer 3. All eluent was collected into a bottom-sealed Micro Bio-Spin column (Bio-Rad, Hercules, CA) containing 100 µl bed volume of Ni-NTA agarose beads (Qiagen, Valencia, CA) that had been equilibrated with Wash Buffer 3. After 30 minutes of incubation, the spin column was centrifuged at 50 x *g* for 10 seconds. The eluent was collected, and the Ni-NTA beads were further eluted with 100 µl Wash Buffer 3 twice more for full elution. The eluent was buffer-exchanged into HSCG Buffer (20 mM HEPES pH 7.0, 150 mM NaCl, 2 mM $CaCl_2$, 15% (v/v) glycerol) on a PD MiniTrap G-25 column (GE Healthcare Life Sciences, Pittsburgh, PA). Purified Htm1p-Pdi1p was stored in aliquots at –80°C. Endoglycosidase H (New England Biolabs, Ipswich, MA) treatment was carried out according to the manufacturer's protocol. For size-exclusion column chromatography, Htm1p-Pdi1p was eluted with 500 *µ*l of 1mg/ml 3xFLAG peptide (Sigma-Aldrich) in Wash Buffer 3, instead of TEV protease. The eluent was then loaded and separated in a

Superdex 200 10/300 GL column (GE Healthcare Life Sciences) for subsequent western blot and mannosidase assay. Protein concentration was determined by Pierce BCA protein assay (Thermo Fisher Scientific, Waltham, MA).

For Mns1p preparation, yJW1832 was grown in 3-liter dextrose-free YP with 2% (w/v) raffinose at 30ºC to early stationary phase. Galactose was then added to a final concentration of 2% (w/v) to induce expression for 12 hours. Cells were then harvested. Cell lysis and affinity purification were carried with the same procedure as Htm1p-Pdi1p.

Recombinant preparation of CPY and CPY*

CPY plasmids were introduced into the desired yeast strain, and the transformed cell was grown in 3-liter SC-LEU with 2% (w/v) raffinose till OD_{600} reached 1.0~1.2. Galactose was then added to a final concentration of 2% (w/v) to induce expression at 30°C for another 12 hours. Cells were then harvested and stored at -80°C. All of the purification steps were carried out at 4°C. For CPY*, 15 g of cells were ground and then resuspended in 25 ml C-Lysis Buffer (20 mM HEPES pH 7.0, 500 mM NaCl, 10 mM imidazole, 10 mM TCEP-HCl, 6 M guanidine hydrochloride, 1% (v/v) NP-40, 1x *cOmplete* protease inhibitor cocktail). The slurry was nutated for 30 minutes to solubilize the inclusion body, centrifuged at 6,000 x *g* for 10 minutes, and then ultracentrifuged at 60,000 x *g* for 30 minutes. Supernatant was collected and loaded on a Ni-NTA column containing 1 ml bed-volume of resins that had been equilibrated with C-Lysis Buffer. The column was washed with 10 ml C-Wash Buffer (20 mM HEPES pH 7.0, 500 mM NaCl, 10 mM imidazole, 10 mM TCEP-HCl, 6 M guanidine hydrochloride), and then eluted with

C-Elution Buffer (20 mM HEPES pH 7.0, 500 mM NaCl, 500 mM imidazole, 6 M guanidine hydrochloride). The eluent was buffer-exchanged into HSGG Buffer (20 mM HEPES pH 7.0, 150 mM NaCl, 15% (v/v) glycerol, 0.1% (w/v) octyl-α-glucopyranoside) and stored at -80°C in aliquots.

The purification of native CPY was performed in the same way as CPY* except that guanidine hydrochloride and TCEP-HCl were omitted from C-Lysis and C-W Buffer, respectively. To make Scr-CPY, CPY was first reduced with 6 M guanidine hydrochloride and 5 mM dithiothreitol (DTT) at 42°C for one hour. N,N,N',N'-tetramethylazodicarboxamide (diamide) (Santa Cruz Biotechnology, Dallas, TX) was then added to a final concentration of 25 mM. The solution was kept at room temperature for one hour and then buffer-exchanged into HSGG buffer. To make Carb-CPY, CPY was first reduced with 6 M guanidine hydrochloride and 5 mM DTT at 42°C for one hour. Iodoacetamide was then added to 25 mM. The solution was kept dark at room temperature for one hour and then buffer-exchanged into HSGG buffer. Ellman's reagent was used to check the status of cysteines.

Preparation of RNase B

Crude bovine pancreatic RNase B (Sigma-Aldrich) was first enriched for the $Man_8GlcNAc_2$-abundant species. Generally, 50 mg of crude RNase B was dissolved in EQ Buffer (20 mM HEPES pH 7.0, 150 mM NaCl, 5 mM $CaCl_2$, 5 mM $MgCl_2$, 5 mM $MnCl_2$) in 10 mg/ml concentration, and then mixed with 5 ml bed volume of EQ Buffer-equilibrated concanavalin A Sepharose beads (Sigma-Aldrich) at 4°C for 2 hours. The

slurry was subsequently transferred into an open column, washed sequentially with 15 ml EQ Buffer, 50 ml High-Salt Wash Buffer (20 mM HEPES pH 7.0, 500 mM NaCl, 1 mM $CaCl_2$, 1 mM $MgCl_2$, 1 mM $MnCl_2$), 10 ml EQ Buffer, and finally 200 ml Low-Glc Wash Buffer (20 mM HEPES pH 7.0, 150 mM NaCl, 50 mM Methyl-α-*D*-glucopyranoside). The column was first eluted 100 ml 200mM-Glc Buffer (20 mM HEPES pH 7.0, 150 mM NaCl, 200 mM Methyl-α-*D*-glucopyranoside) into 20 ml/fraction, and further eluted with 100 ml 1M-Glc Buffer (20 mM HEPES pH 7.0, 150 mM NaCl, 1 M Methyl-α-*D*-glucopyranoside). The N-glycan profile of RNase B from each step were checked by MALDI-TOF MS. Fractions containing the desired glycan species were pooled together, adjusted to pH 4.0 by acetic acid, and then loaded onto a 5-ml HiTrap-SP FF cation-exchange column (GE Healthcare Life Sciences) that had been equilibrated with Acidic Buffer (20 mM HEPES pH 4.0, 150 mM NaCl). The cation-exchange column was washed with 25 ml Acidic Buffer, and then eluted with Neutral Buffer (20 mM HEPES pH7.0, 500 mM NaCl). The eluent was buffer-exchanged into HSG Buffer by a PD10 desalting column (GE Healthcare Life Sciences). Purity was checked by size exclusion column chromatography.

For the preparation of RBsp, 1 mg RNase B was mixed with 20 μg freshly dissolved subtilisin (Sigma-Aldrich) in 2 ml HSG buffer. The mixture was kept at 4°C overnight, and 20 μg more subtilisin was added for another one-hour incubation at 4°C. The pH of the mixture was then adjusted to 2.0 with 1 M hydrochloric acid for one hour on ice to destroy subtilisin. Trichloroacetic acid (TCA) was then added to 10% (w/v), and the solution was warmed up to room temperature to allow RBsp precipitation overnight.

The mixture was centrifuged at 15,000 x *g* for 10 minutes, and the supernatant was removed. The pellet was dissolved with 9 M deionized urea, and then TCA-precipitated again to fully remove residual S-peptide. The pellet was dissolved with 9 M urea and buffer-exchanged into HSGG Buffer and stored at -30°C in aliquots. Disulfide-scrambling and carbamidomethylation of RNase B and RBsp were carried out with the same procedures as for Scr-CPY and Carb-CPY.

Circular dichroism analysis

RNase B variants were buffer-exchanged into 10 mM sodium phosphate, pH 7.0 to a final concentration of 10 μM. Measurement was conducted on a Jasco J-715 spectrometer in a 1-mm cuvette at 30°C. The spectrum was recorded over the range of 190-250 nm at a scanning speed of 20 nm/min with 1.0 nm bandwidth.

Limited proteolysis of RNase B variants

Trypsin (Sigma-Aldrich) was added to a final concentration of 50 ng/µl into 10 µM RNase B variants at the beginning of the time-course reaction at room temperature. At each time point, equal amount of sample was withdrawn and mixed with 1/10 volume of phenylmethylsulfonyl fluoride (Sigma-Aldrich) to stop the reaction for reducing SDS-PAGE analysis.

PNGase F sensitivity of RNase B variants

Glycerol-free PNGase F (New England Biolabs) was added to a final concentration of 0.5 unit/µl into 10 µM RNase B variants at the beginning of the time-course reaction at room temperature. At each time point, equal amount of sample was withdrawn and mixed with 4x SDS sample buffer to stop the reaction for reducing SDS-PAGE analysis.

Glycan profiling by MALDI-TOF MS

The procedure of N-glycan profiling by MALDI-TOF MS was based on published methods (Morelle and Michalski, 2007; Packer et al., 1998) with some modifications. N-glycoproteins were separated by SDS-PAGE and stained by Coomassie Blue R250. Individual gel bands were excised and destained twice with 100 µl 50% (v/v) acetonitrile with 10 mM Na_2CO_3 at 50°C for 30 minutes with vigorous shaking. The gels were then reduced by 50 mM DTT in 20 mM Na_2CO_3 at 50°C for 30 minutes, and then alkylated by adding iodoacetamide to 150 mM and incubated at dark at room temperature for 30 minutes. The gels were washed twice by 50% (v/v) acetonitrile with 10 mM Na_2CO_3 at room temperature for 30 minutes, dehydrated by 100% acetonitrile at room temperature for 10 minutes, and evaporated in a centrifugal evaporator for 10 minutes. To each dried gel piece, 5 units of glycerol-free PNGase F (New England Biolabs) in 20 µl of 20 mM Na_2CO_3 were added, and the mixture was incubated at 37°C overnight. To extract the released glycans, 100 µl of deionized H_2O was added, and the mixture was sonicated in the water-bath sonicator for 30 minutes. The solution was collected, and extraction was repeated for two more times. To desalt the pooled extract, each sample was loaded into a 20-µl filter tip filled with 10 mg of graphitized carbon (Grace Davidson Discovery

Sciences) that had been sequentially washed with 1 ml acetonitrile and 1 ml of deionized H_2O. After loading the sample, the tip-column was washed with 1 ml of deionized H_2O, and eluted with 100 µl of 25% (v/v) acetonitrile. For free glycans, the reaction solution was directly loaded onto the graphitized carbon tip-column and processed with the same procedure. The eluent was evaporated in the centrifugal evaporator at 60ºC. The dried sample was resuspended with 5 µl of deionized H_2O, and 1 µl of the sample was spotted on the MALDI target plate and vacuum dried. The plate was then washed with pure acetonitrile. 1 µl of 5 mg/ml 2.5-dihydroxybenzoic acid (DHB) (Sigma-Aldrich) dissolved in $50\%_{(v/v)}$ acetonitrile was then spotted onto each sample spot and dried. The mass spectrometric analysis was conducted on a Voyager Elite DE-STR Pro mass spectrometer (Applied Biosystems) or a Shimadzu AXIMA Performance mass spectrometer (Shimadzu) in the positive reflectron mode. For data collected in the Voyager mass spectrometer, the spectrum analysis was carried out with the bundled Data Explorer software to extract the values of peak area of the peak matched to each glycan. For spectra collected from the AXIMA Performance mass spectrometer, raw spectra were exported in the mzXML format, and then analyzed by the mMass software (Strohalm et al., 2010) to extract the values of peak intensity of the peak matched to each glycan.

Mannosidase assay

Unless otherwise specified, glycoprotein substrates in defined concentration (2 µM for CPY variants, 10 µM for RNase B isoforms) were mixed with 0.1 μM Htm1p-Pdi1p

and/or 0.1 μM Mns1p in Reaction Buffer (20 mM HEPES pH 7.0, 150 mM NaCl, 2 mM $CaCl_2$, 0.1% (v/v) NP-40). At each desired time-point, EDTA was added to 25 mM to stop demannosylation reaction. The mixture was separated by reducing SDS-PAGE and then subjected to N-glycan-profiling by MALDI-TOF MS.

NMR analysis

For the Man8-abundant RNase B control, 2 mg of RNase B was reduced by 10 mM DTT at 95ºC for 10min and then let cooled down. For the Htm1p-Pdi1p-treated RBsp, 2 mg of RBsp was first incubated with 50 μg of Htm1p-Pdi1p overnight. To both samples, 1000 units of PNGase F were then added for glycan release at 37ºC overnight. The next day, the reaction mixture was loaded onto a 200 mg of graphitized carbon column, washed with 5 ml water, and then eluted with 1.5 ml 25% acetonitrile. The eluent was lyophilized, and then dissolved by D_2O for lyophilization for two more times. The dried sample was then dissolved by D2O for NMR measure. The ^{1}H-NMR was carried out on a 400 MHz Bruker AvanceIII HD 2-channel instrument with a TopSpin v3.5 interface. Spectra were pre-collected using default proton method, calibrated to the reference chemical shift of water (4.79 ppm), and then collected with the presaturation method as described by the manufacturer to suppress the signal from water.

Acknowledgements

We would like to thank Tom Rapoport and Alexander Stein (Harvard Medical School) for providing the recombinant CPY plasmids and the detailed purification protocol; Peter Walter (UCSF) for providing anti-Pdi1p antibody; current and former members of the Fujimori lab and the Weissman lab for discussion and laboratory methods; Erin Quan Toyama and Jay Read for the initial tests on Htm1; Shoshana Bar-Nun (Tel Aviv University), Elizabeth Costa, Joshua Dunn, Christina Fitzsimmons, Calvin Jan, Kamena Kostova, Melanie Smith, Lindsey Pack, Dan Santos, and Erin Quan Toyama for critical comments on the manuscript; Yao-ming Huang (Kortemme group, UCSF) for the assistance with circular dichroism analysis; the UCSF Mass Spectrometry Facility, the DeGrado group, and the UCSF NMR laboratory for access to the mass spectrometers and the NMR instrument. We are grateful for the support from the Howard Hughes Medical Institute International Student Research Fellowship (Y.-C.L.), the Sandler Foundation-UCSF Program for Breakthrough Biomedical Research Award (D.G.F. and J.S.W.), the Howard Hughes Medical Institute (J.S.W.), and National Institute of Health (U01 GM098254 to J.S.W.).

Figures

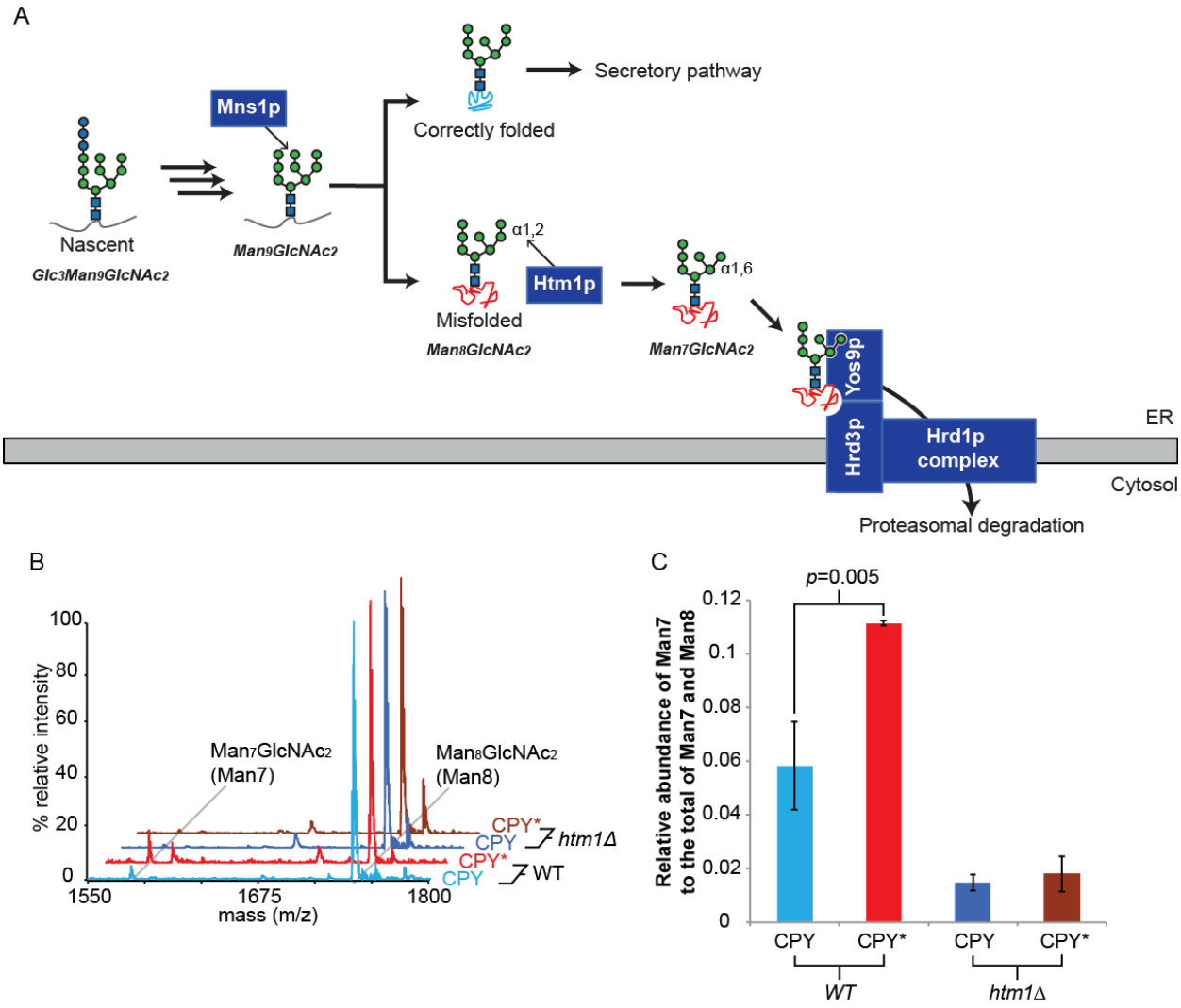

Figure 1. HTM1 mediates N-glycan processing for ERAD-L commitment.

(*A*) Scheme of N-glycan processing and ERAD-L commitment. Upon entering the ER, nascent N-glycoproteins acquire the $Glc_3Man_9GlcNAc_2$ *en bloc*, which is step-by-step deglycosylated as the nascent polypeptide folds. Mns1p catalyzes the last universal deglycosylation step to generate the $Man_8GlcNAc_2$ glycan. While native proteins are targeted for downstream secretory pathway, misfolded proteins are targeted by Htm1p, which removes the α1,2-linked mannose at the C branch from the $Man_8GlcNAc_2$ glycan.

The resulting terminally exposed α1,6-linked mannose and misfolded regions on the polypeptide chain are then read by Yos9p. Along with Hrd3p, Yos9p then permits the downstream retrotranslocation and polyubiquitination through the Hrd1p transmembrane complex for eventual proteasomal degradation.

(*B*) Examples of glycan profiles of CPY and CPY* expressed in wild type (*WT*) or *htm1Δ* yeast strains as measured by MALDI-TOF MS after the glycans were released from CPY/CPY* by PNGase F treatment. Each glycan was assigned to the m/z corresponding to its predicted $[M+Na]^+$ value.

(*C*) The relative abundance of Man7 is higher in CPY* than CPY in wild-type yeast, which is dependent on *HTM1*. The relative MS peak intensity of Man7, as found in (b), is normalized to the total of Man7 and Man8 as a proxy for its relative abundance. Shown are mean values ± one standard deviation (s.d.) from biological triplicates. The *p* value was calculated by unpaired *t* test.

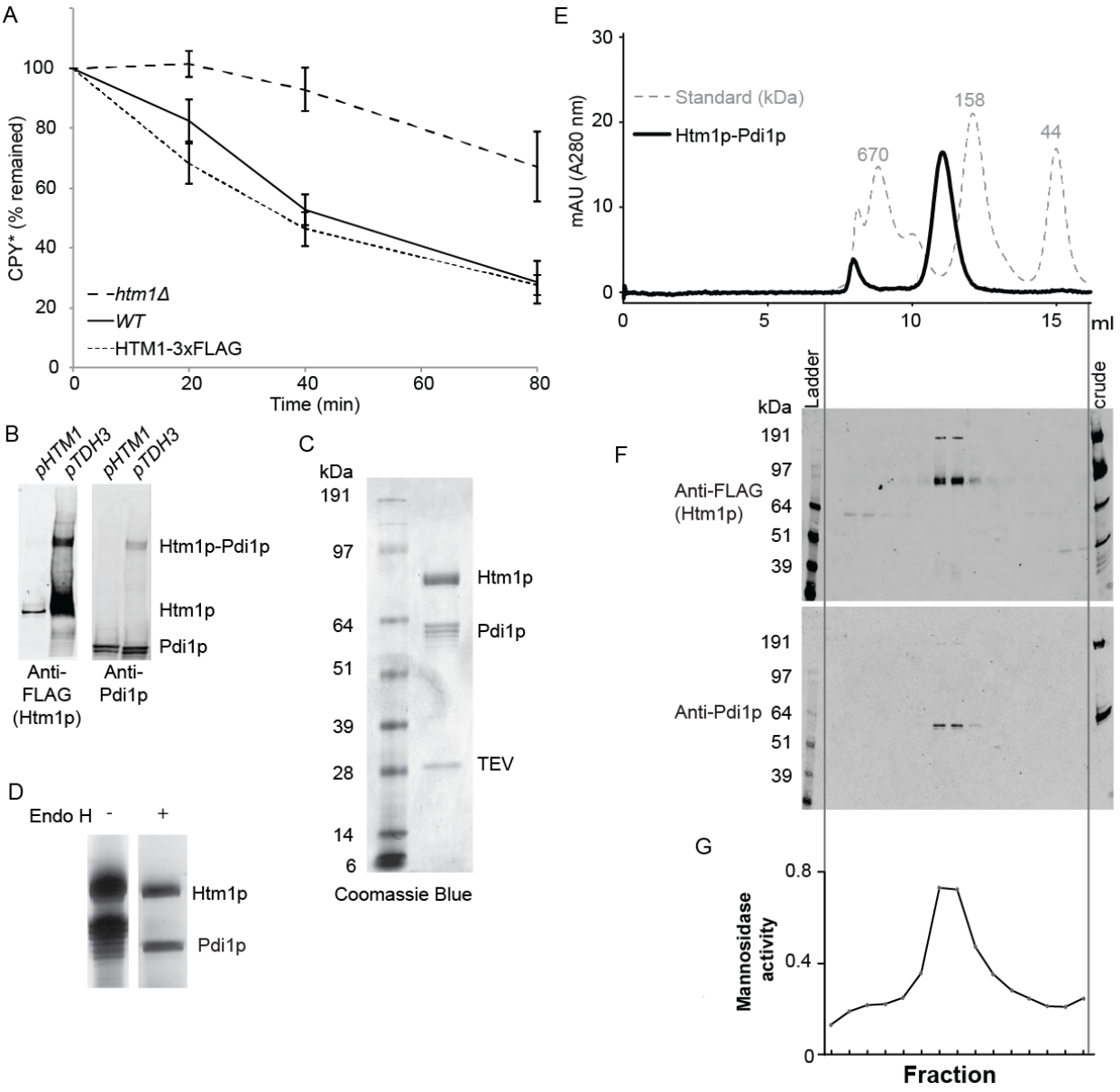

Figure 2. Recombinant preparation of Htm1-Pdi1p from *S. cerevisiae*.

(*A*) Degradation of HA-tagged CPY* is the same in a wild-type BY4741 (WT) and chromosomally 3xFLAG-HDEL-tagged *HTM1* (HTM1-tag). Equal amount of cells growing at mid-log phase were harvested, subjected to reducing SDS-PAGE, and quantitative western blot for the HA signal at each time point relative toe zero time point.

Shown are the mean values ± one standard error of the mean measured from four biological replicates.

(*B*) Expression levels of Htm1p-3xFLAG driven by either endogenous *HTM1* promoter (*pHTM1*) or chromosomally inserted *TDH3* promoter (*pTDH3*) as checked by non-reducing SDS-PAGE and western blot using anti-FLAG (mouse) and anti-Pd1ip (rabbit) primary antibodies and corresponding secondary IR-fluorescent antibodies.

(*C*) Specific interaction between Htm1p and Pdi1p after large-scale immunoprecipitation with anti-FLAG affinity resin followed by TEV protease treatment to release Htm1p. Shown is a Coomassie Blue R250-stained gel image after reducing SDS-PAGE.

(*D*) The N-glycosylation states of Htm1p and Pdi1p as checked by endoglycosidase H (Endo H) treatment.

(*E*) Superdex 200 10/300GL size exclusion column chromatography of Htm1p-Pdi1p eluted from anti-FLAG resin by 3xFLAG peptide.

(*F*) Western blot analysis for the distribution of Htm1p-3xFLAG and Pdi1p after non-reducing SDS-PAGE of the fractions separated by the size-exclusion column chromatography.

(*G*) The relative abundance of Man7 in the total of Man7 and Man8 on RBsp after one-hour incubation with individual fractions collected from the size-exclusion column chromatography of purified Htm1p-Pdi1p.

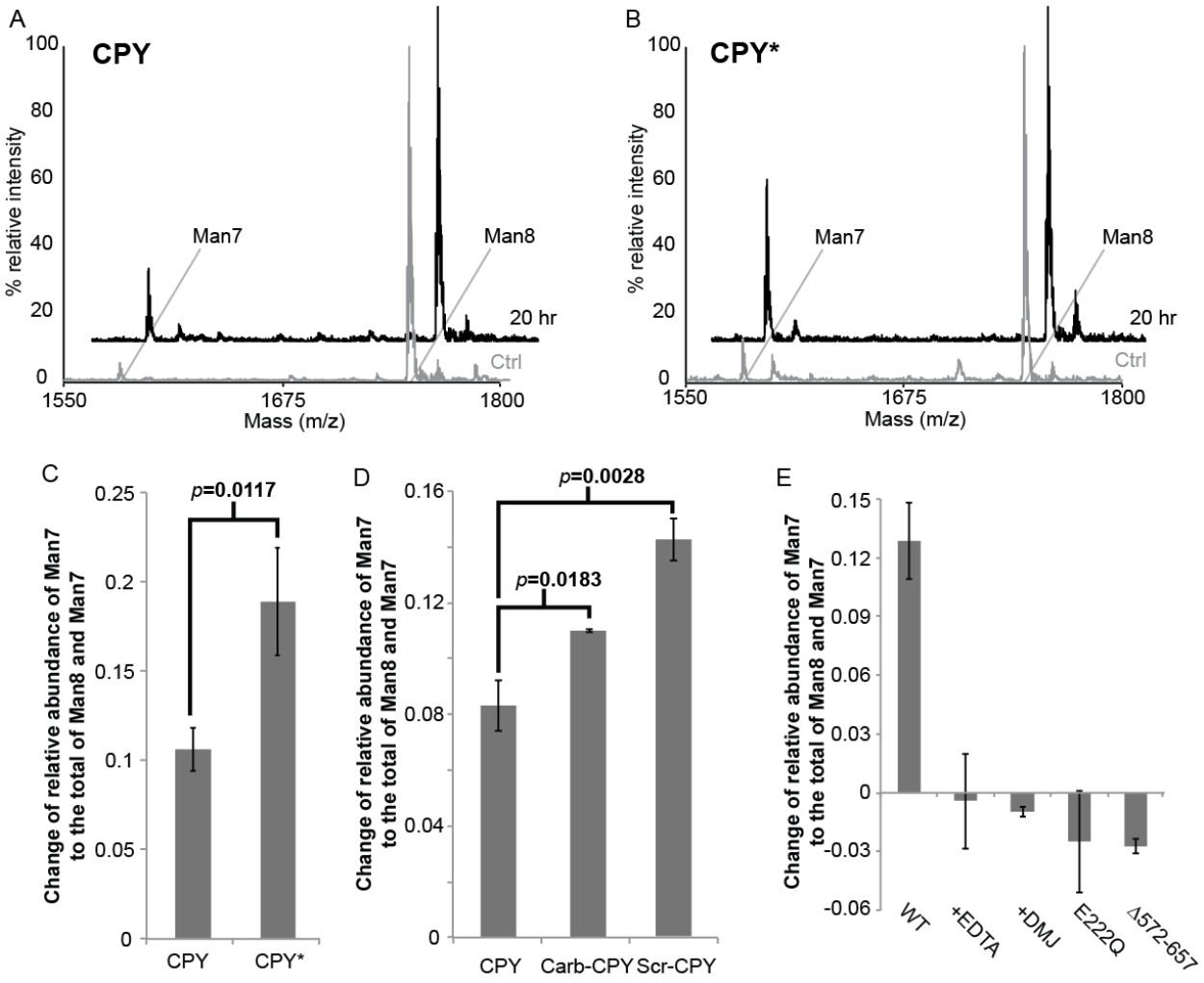

Figure 3. Htm1p-Pdi1p preferentially demannosylates nonnative CPY variants.

(***A* and *B***) Representative glycan profiles of CPY **(a)** and CPY* **(b)** before and after twenty-hour incubation with Htm1p-Pdi1p. 2 μM CPY or CPY* was incubated with 0.1 μM Htm1p-Pdi1p at 30°C for twenty hours, and then separated from Htm1-Pdi1p by SDS-PAGE for subsequent in-gel glycan release and MALDI-TOF MS analysis.

(*C*) Htm1p-Pdi1p generates more Man7 on CPY* than CPY after reaction. The mannosidase activity is measured based on the change of relative abundance of Man7 on CPY and CPY* after twenty-hour incubation with Htm1p-Pdi1p. Shown are the mean

values ± one s.d. from experimental triplicates. The *p* value was calculated by unpaired *t* test.

(***D***) Htm1p-Pdi1p generated more Man7 on Carb-CPY and Scr-CPY than CPY. Numbers shown are the mean ± one s.d. from experimental triplicates. The *p* value was calculated by unpaired *t* test.

(***E***) The mannosidase activity of Htm1p-Pdi1p against CPY* was inhibited by EDTA (+EDTA), 1-deoxymannojirimicin (+DMJ), mutations including E222Q and Δ572-657. Quantification was carried out as in (C). Shown are the mean values ± one s.d. from experimental triplicates.

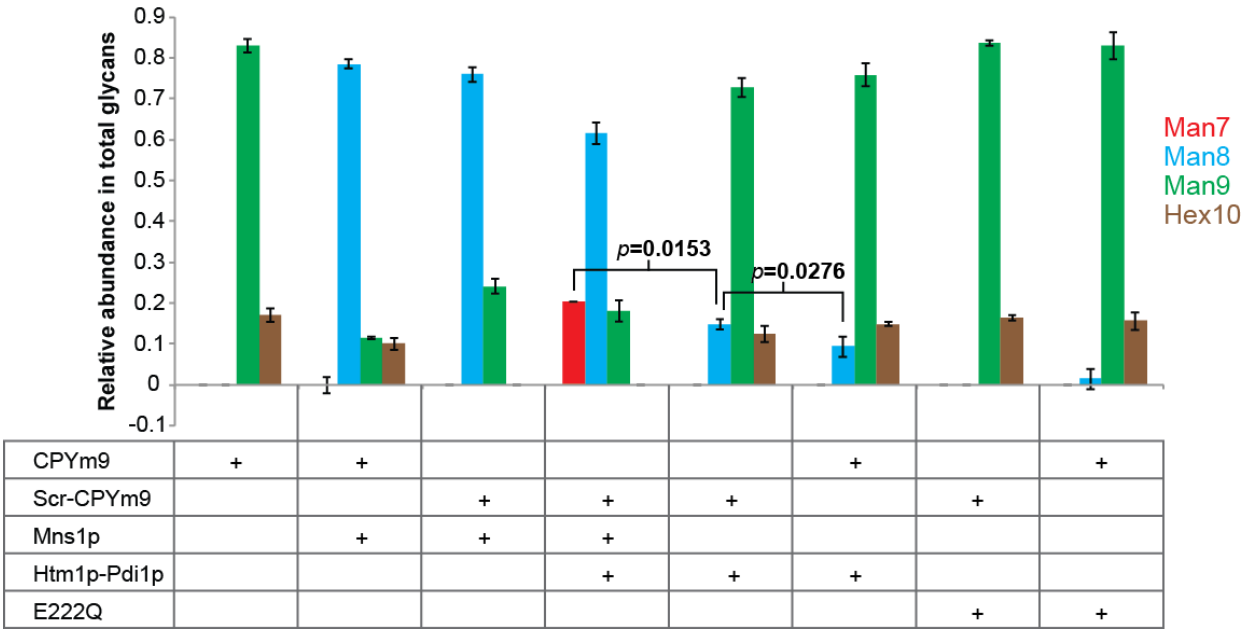

CPYm9	+	+				+		+
Scr-CPYm9			+	+	+		+	
Mns1p		+	+	+				
Htm1p-Pdi1p				+	+	+		
E222Q							+	+

Figure 4. Mns1p and Htm1p-Pdi1p have different sensitivities for folding states.

The relative abundance of each glycan on CPYm9 or Scr-CPYm9 after twenty-hour incubation with Mns1p and/or Htm1p-Pdi1p, or E222Q. Shown are the mean values ± one s.d. from experimental triplicates. The *p* value was calculated by unpaired *t* test.

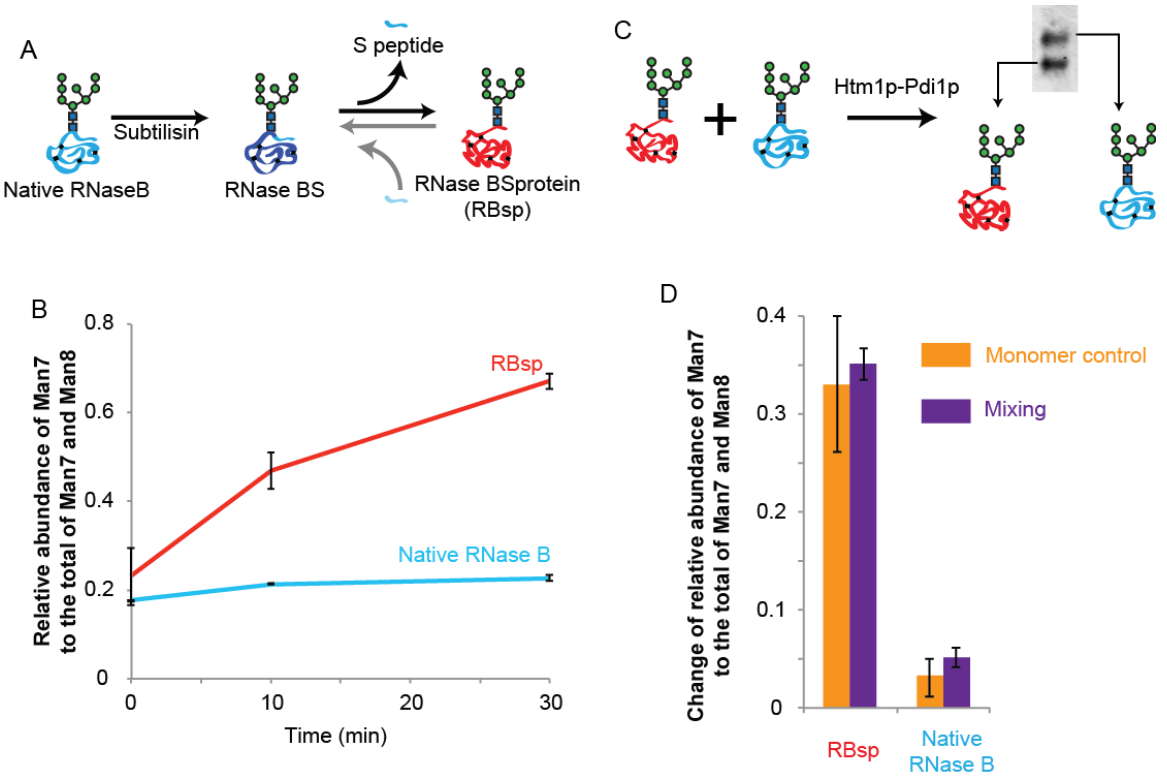

Figure 5. Htm1p-Pdi1p efficiently demannosylates RBsp.

(*A*) Schematic presentation of the generation of RBsp. Native RNase B was treated with subtilisin in a 100:1 ratio at 4ºC for twenty-four hours to generate RNase BS with a nick between the N-terminal S peptide and the rest of the protein (RBsp). RNase BS was then subjected to precipitation with 10% Trichloroacetic acid (TCA) to remove the soluble S peptide from the precipitated RBsp.

(*B*) Change of the relative abundance of Man7 on RBsp and native RNase B during a time course incubation with Htm1p-Pdi1p. Shown are the mean values ± one s.d. from experimental triplicates.

(*C*) Schematic presentation of the co-reaction of RBsp and native RNase B with Htm1p-Pdi1p. RBsp and native RNase B were pre-mixed at 1:1 ratio and incubated with

Htm1p-Pdi1p for twenty minutes, and subsequently separated by SDS-PAGE for MS analysis of the individual glycan profile.

(*D*) Change of the relative abundance of Man7 on premixed RBsp and native RNase B after incubation with Htm1p-Pdi1p for twenty minutes. Shown are the mean values ± one s.d. from experimental triplicates

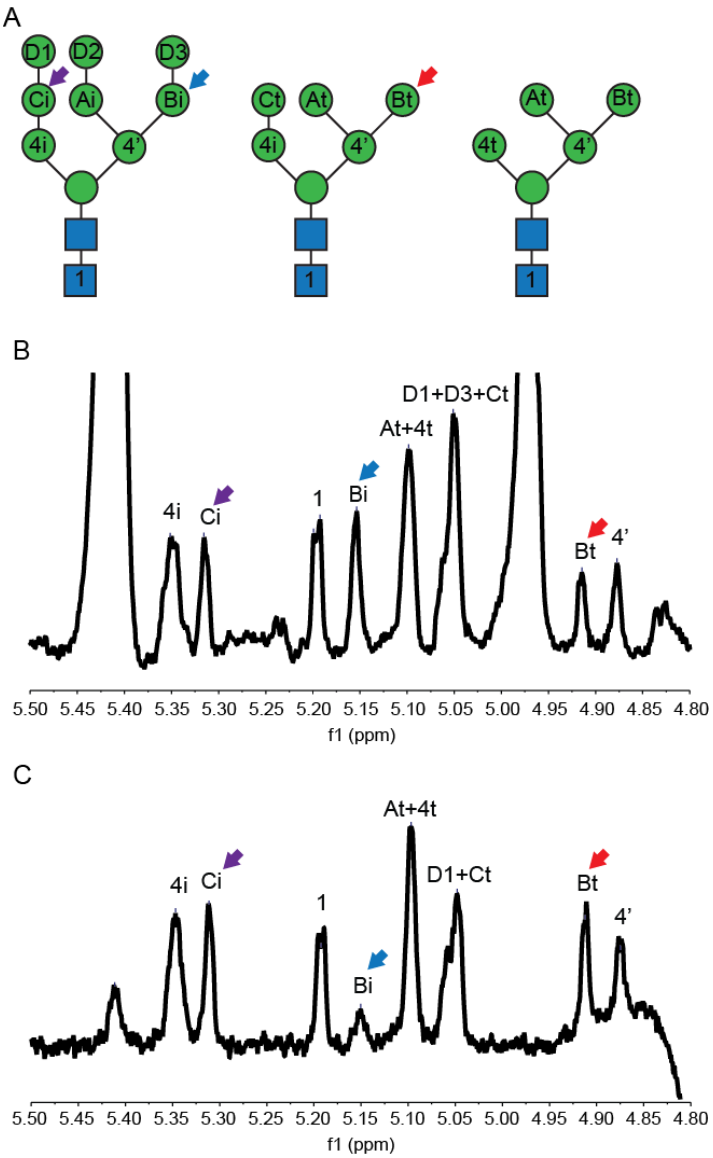

Figure 6. NMR analysis of the glycan released from RNase B before and after overnight incubation with Htm1p-Pdi1p.

(A) Representative N-glycan structures that cover all potential monosaccharide linakges to be found RBsp. The nonemclature and peak assignment is based on previous studies (Fu et al., 1994).

(B and C) The ^{1}H-NMR spectra of the glycans released from RBsp before **(B)** and after **(C)** Htm1p-Pdi1p treatment. Note the change of the height of the peaks corresponding

to the α1,6-linked mannose on the C branch with (Bi, blue arrow) or without (Bt, red arrow) the terminal α1,2-linked mannose (D3) after incubation with Htm1p-Pdi1p. In contrast, the level of the second α1,2-linked mannose on the A branch (Ci, purple arrow) did not change after Htm1p-Pdi1p treatment. Shown are the regions covering the H-1 on the anomeric carbon of each monosaccharide after solvent suppression by the presaturation method.

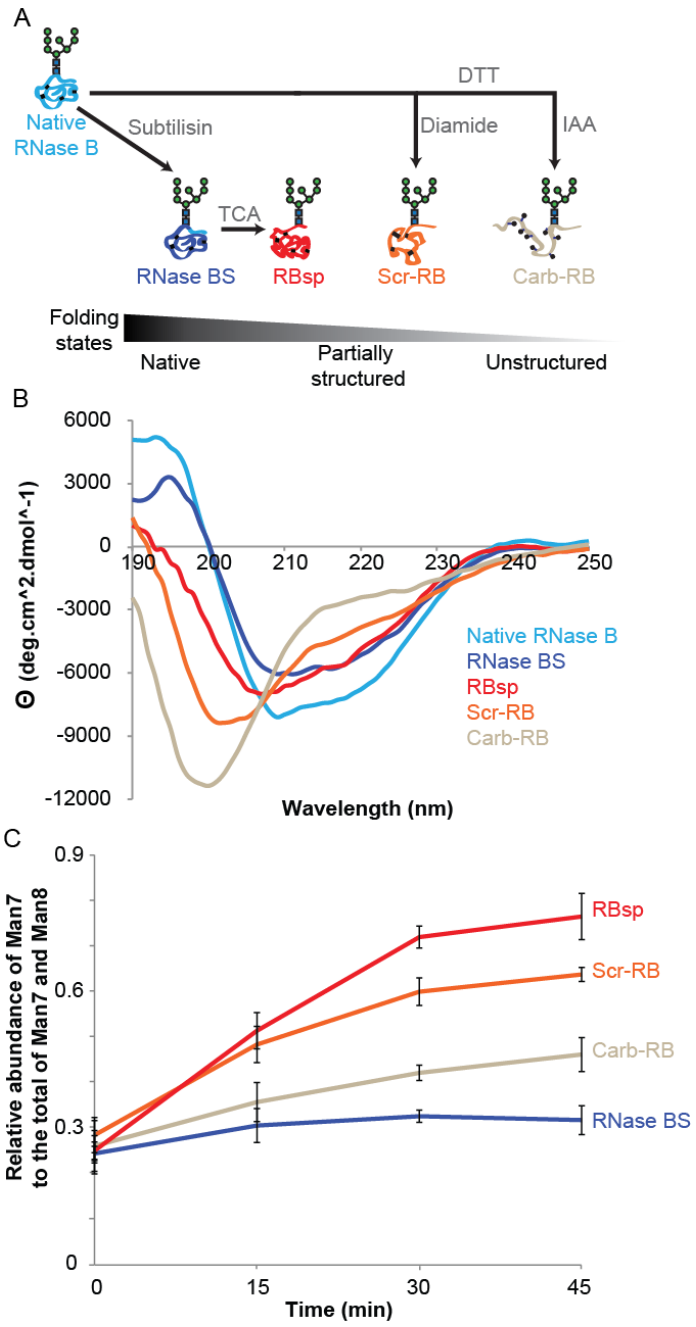

Figure 7. Htm1p-Pdi1p preferentially demannosylates partially structured RNase B variants.

(*A*) Schematic presentation of the generation of RNase B variants. RNase BS and RBsp are generated through subtilisin and TCA treatment as described in Fig.5a. Additionally, RNase B is reductively denatured by DTT in 6 M guanidine hydrochloride and then

either disulfide-scrambled by diamide to produce Scr-RB or blocked by iodoacetamide (IAA) to produce Carb-RB.

(*B*) Circular dichroism analysis of RNase B variants.

(*C*) The relative abundance of Man7 on RNase B variants during a time-course incubation with Htm1p-Pdi1p. Shown are the mean values ± one s.d. from experimental triplicates.

Supplementary Information

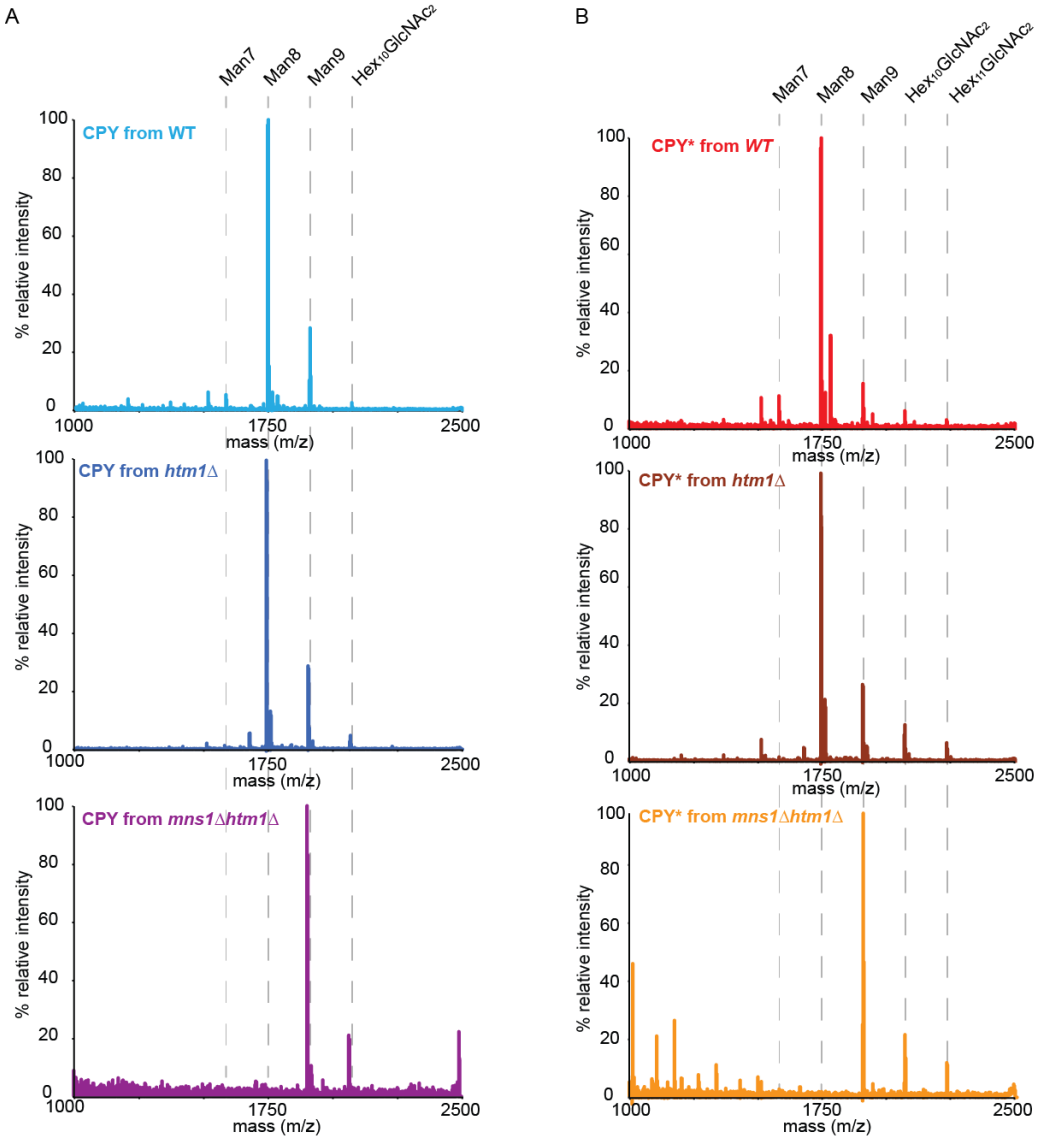

Figure S1. Full MS spectra of the glycan profiles on CPY and CPY* purified from different yeast strains.

As described in Fig. 1*B*, glycans of **(*A*)** CPY and **(*B*)** CPY* expressed in wild type (*WT*), *htm1Δ*, and *mns1Δhtm1Δ* yeast strains were released by PNGase F for subsequent analysis by MALDI-TOF MS. Each glycan was assigned according to the m/z corresponding to the predicted $[M+Na]^+$ value.

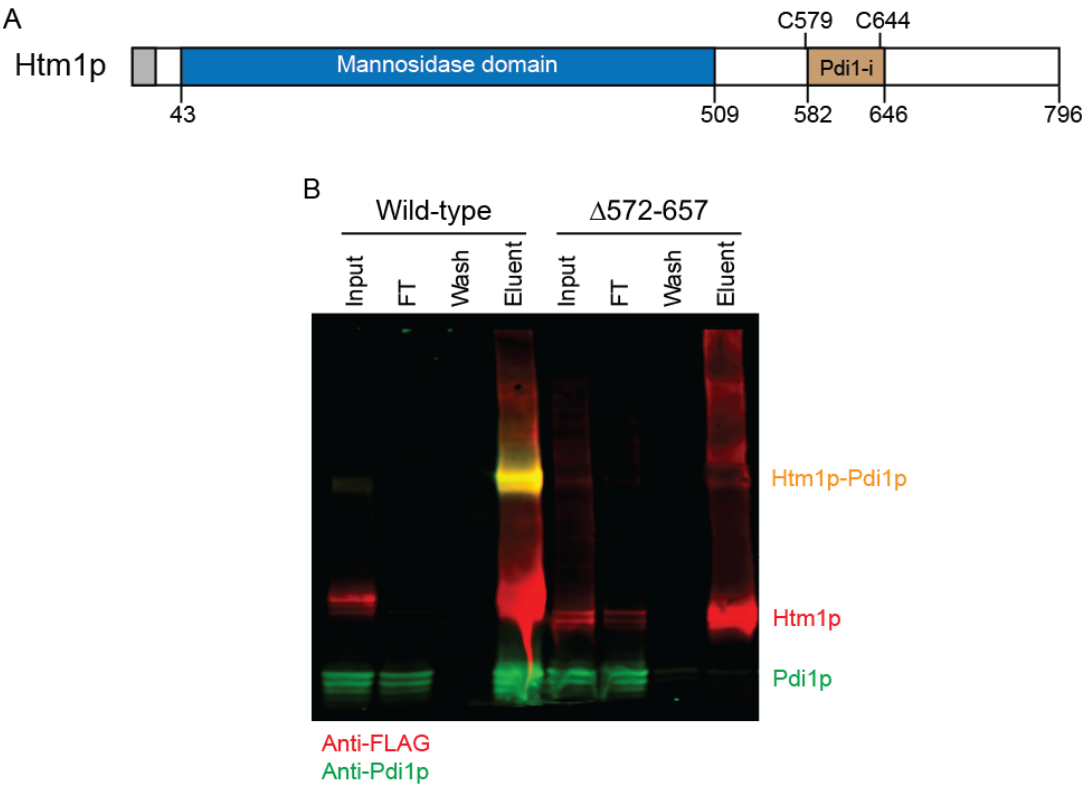

Figure S2. Deletion of the putative Pdi1p-interacting domain of Htm1p abolished the interaction between Htm1p and Pdi1p.

(*A*) Schematic representation of the domain structures of Htm1p. Htm1p consists of the N-terminal, conserved GH47 family mannosidase domain and the C-terminal, non-conserved region. Amino acyl region 582-646 (Pdi1-i) comprises the previously identified region required for non-covalent interaction, while Cys579 (C579) and Cys644 (C644) form disulfide-crosslinking with Pdi1p.

(*B*) Δ572-657 lost specific interaction with Pdi1p. Interaction of Pdi1p with wild-type Htm1p or Δ572-657 was analyzed by western blot after immunoprecipitation with anti-FLAG affinity resin followed by 3xFLAG peptide elution to release Htm1p.

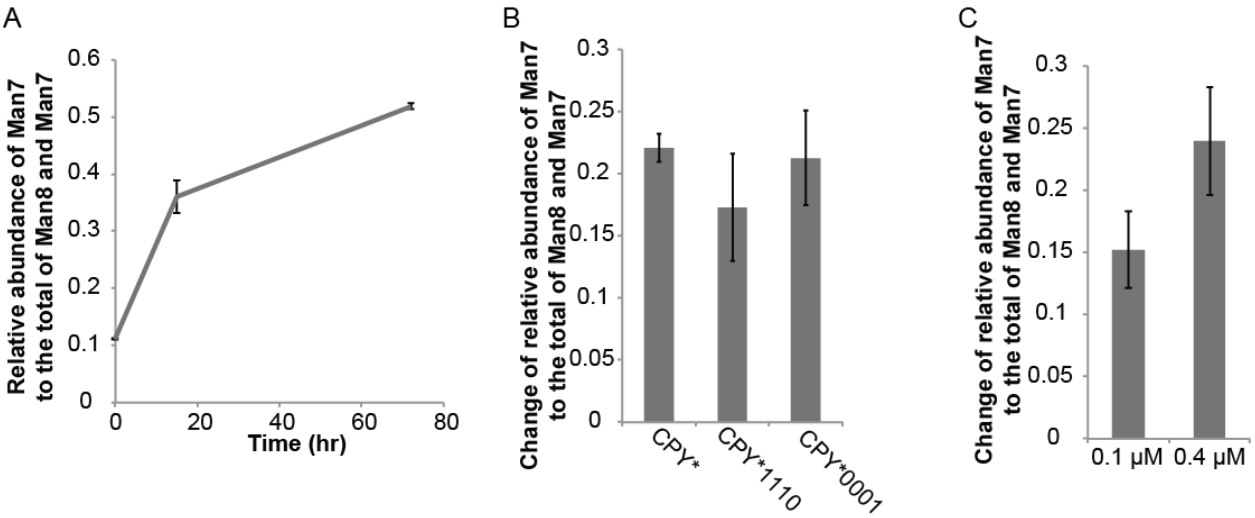

Figure S3. Glycosylation sites and concentration of Htm1p-Pdi1p are not the major limiting factors for demannosylation rates.

(***A***) The change of relative Man7 abundance to the sum of Man7 and Man8 on CPY* after 72-hour incubation with Htm1p-Pdi1p. Data are the mean values ± one s.d. from experimental triplicates.

(***B***) Htm1p-Pdi1p generated similar levels of Man7 on CPY* and CPY* variants with either the fourth (CPY*1110) or the first three (CPY*0001) glycosylation sites eliminated. Numbers shown are the mean ± one s.d. from three experimental replicates.

(***C***) Increasing the concentration of Htm1p-Pdi1p from 0.1 μM to 0.4 μM did not proportionally increase its Man8-to-Man7 mannosidase activity against CPY* after twenty-hour incubation. Shown are the mean values ± one s.d. from experimental triplicates.

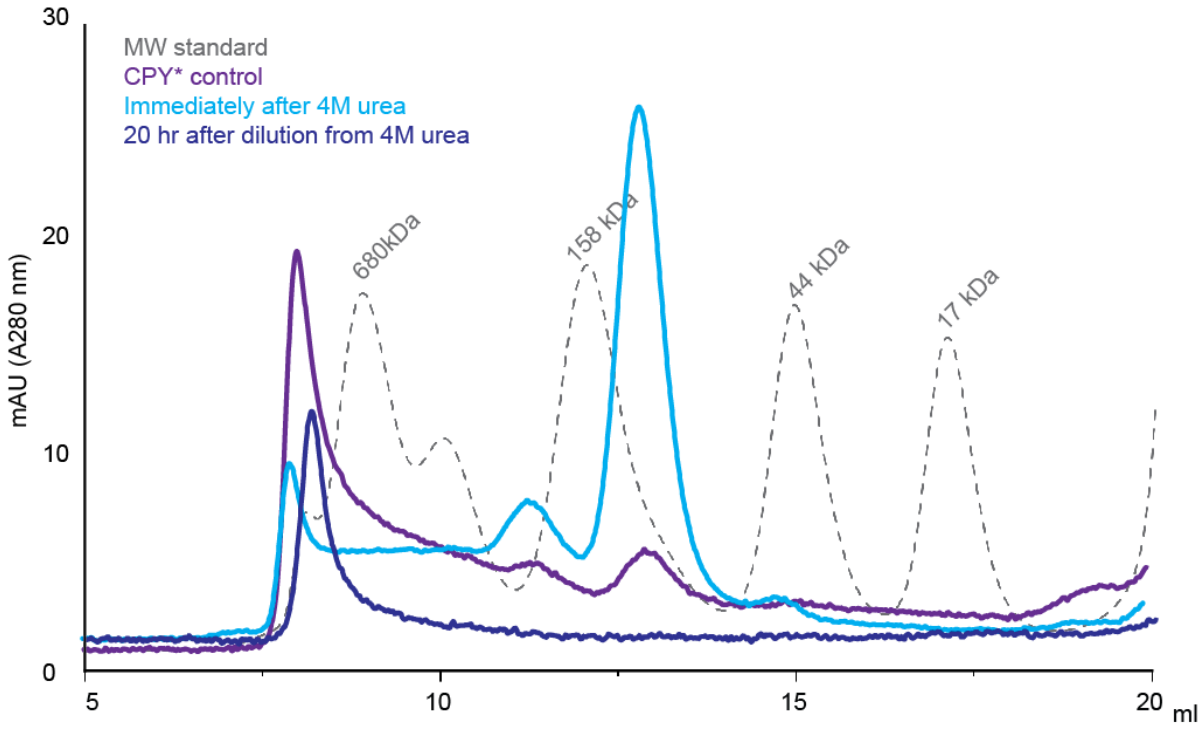

Figure S4. Size-exclusion column chromatography analysis of CPY*.

Size distribution of CPY* before (CPY* control) and immediately after solublization with 4 M urea, as well as twenty hours after dilution from 4 M urea treatment, as analyzed by Superdex 200 size exclusion chromatography.

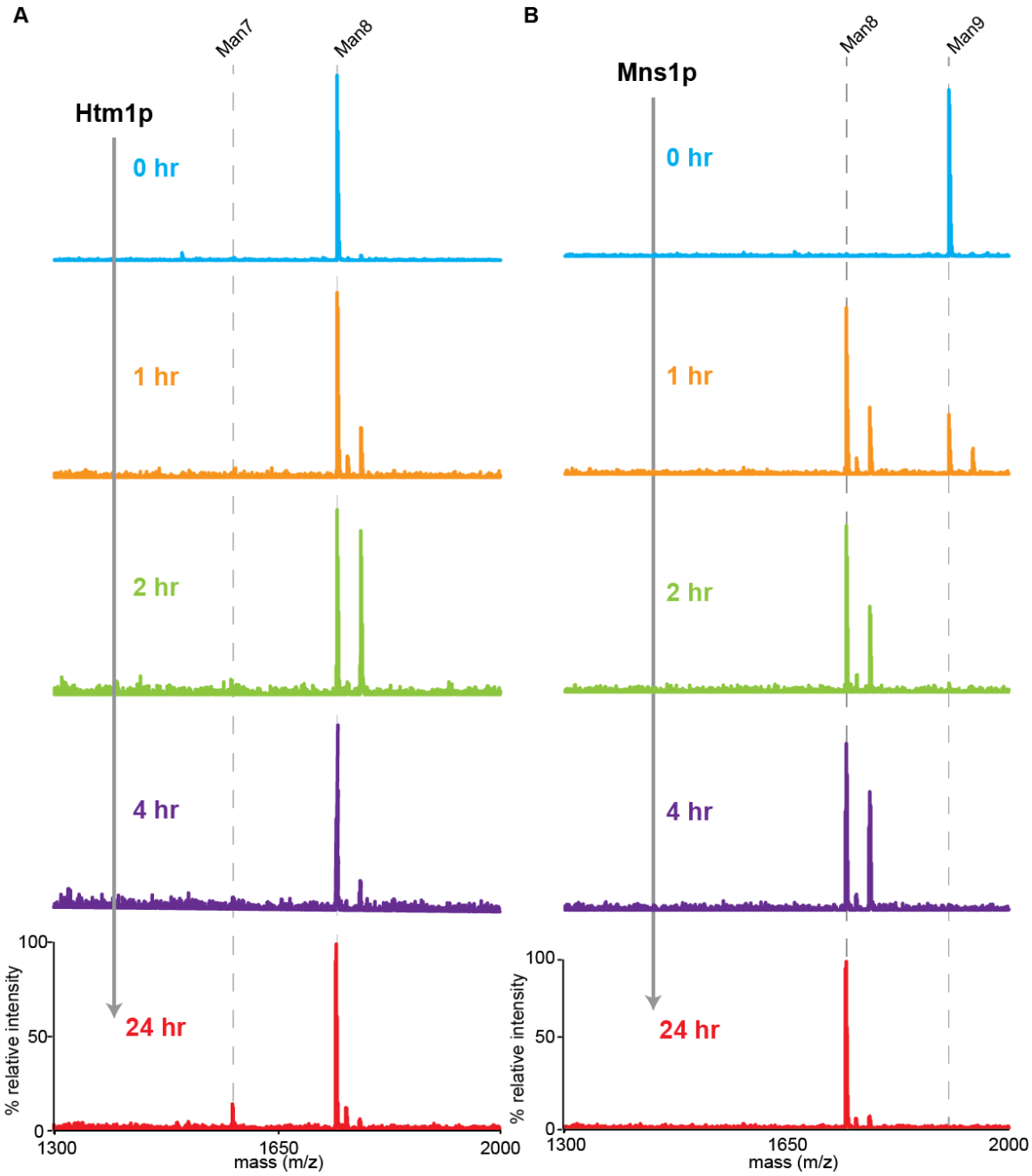

Figure S5. Htm1p-Pdi1p and Mns1p differently targets free glycans.

(*A*) 10 μM of free Man8 was incubated with 0.1 μM Htm1p-Pdi1p and collected for MS analysis at each indicated time point. Each glycan was assigned to the m/z corresponding to its $[M+Na]^+$ value. Note the occasional presence of the second peak

next to the $[M+Na]^+$ peak, which corresponds to the $[M+K]^+$ that does not influence overall quantification.

(B) 10 μM of free Man9 was incubated with 0.1 μM Mns1p and collected for MS analysis at each indicated time point. Each glycan was assigned to the m/z corresponding to its $[M+Na]^+$ value. Note the occasional presence of the second peak next to the $[M+Na]^+$ peak, which corresponds to the $[M+K]^+$ that does not influence overall quantification.

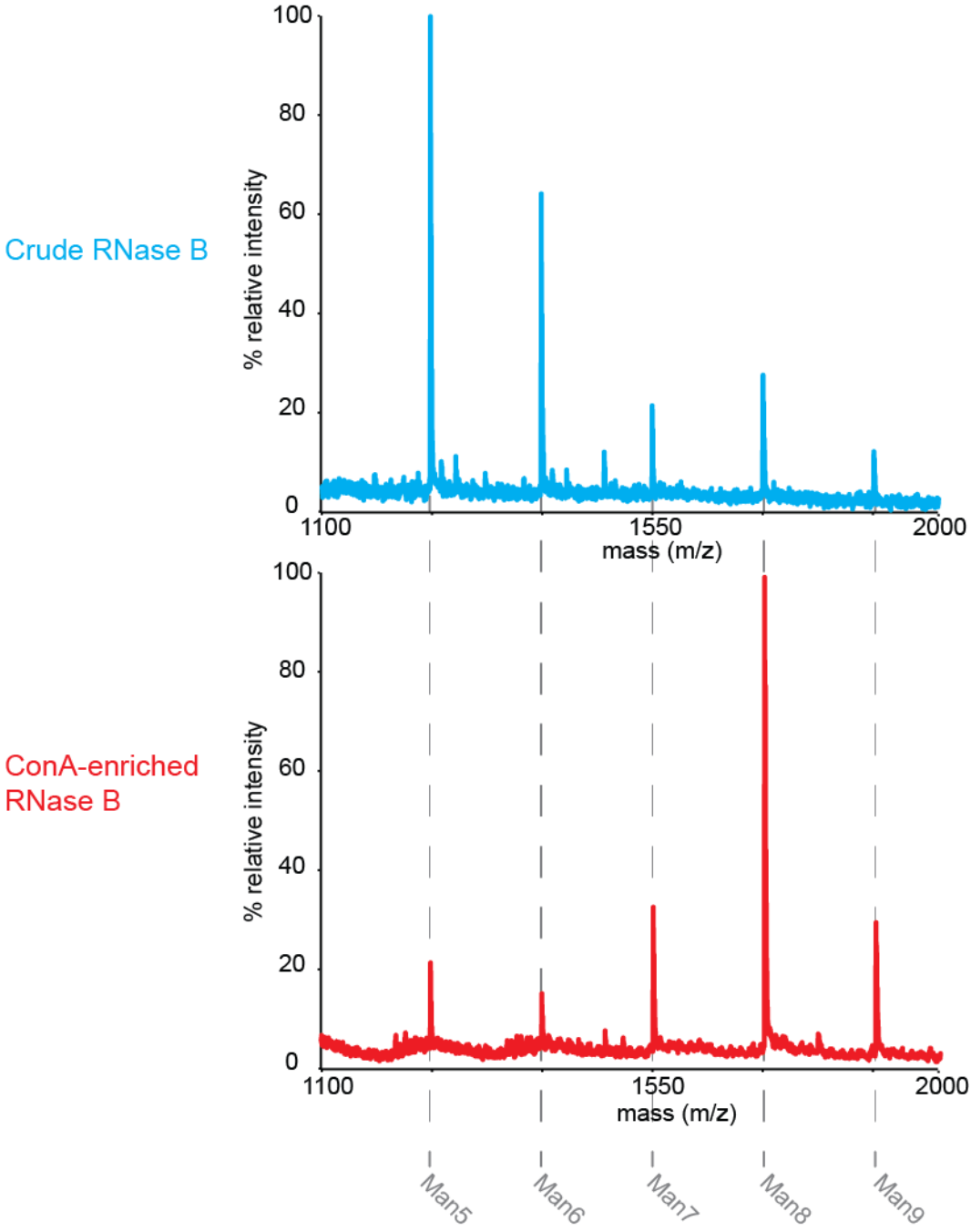

Figure S6. Concanavalin A (ConA) enrichment of Man8-abundant RNase B.

The glycan profiles of RNase B from the commercial source before and after affinity enrichment with ConA lectin column.

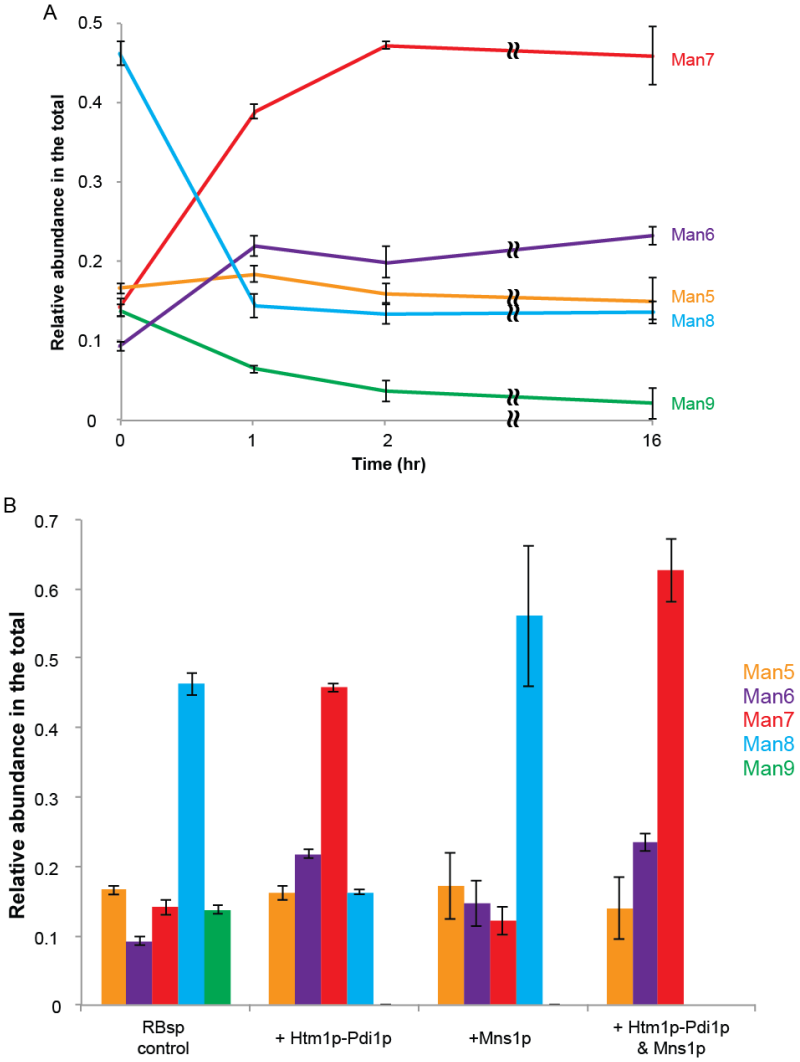

Figure S7. Mns1p and Htm1p-Pdi1p target different mannoses on RBsp.

(*A*) The relative abundance Man5 to Man9 normalized to the total glycans on RBsp over a 16-hr time course incubation with Htm1p-Pdi1p. Shown are the mean values ± one s.d. from experimental triplicates.

(*B*) The glycan distribution of RBsp before and after incubation with 0.1 μM Mns1p and/or Htm1p-Pdi1p for sixteen hours. Data are the mean values ± one s.d. from experimental triplicates.

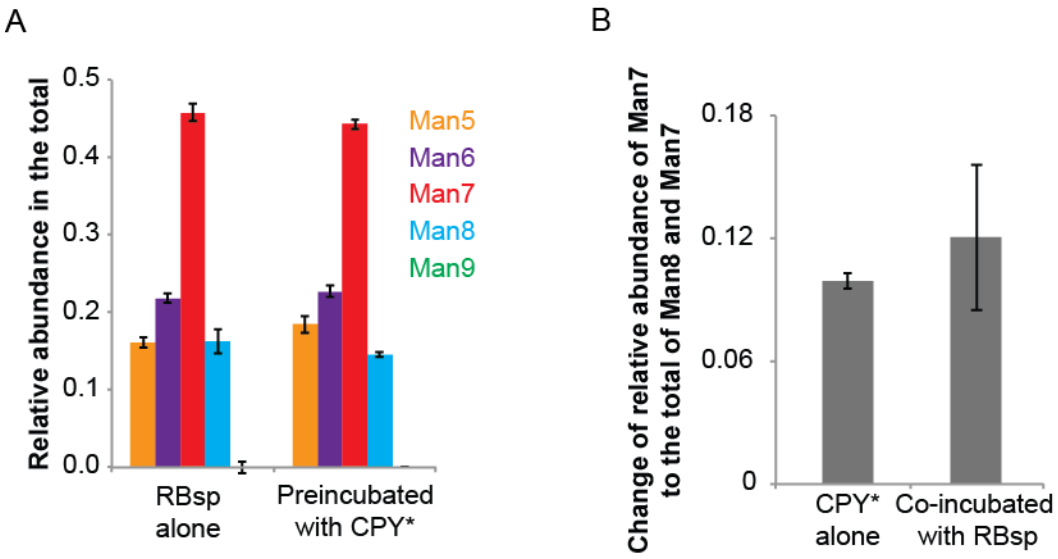

Figure S8. Htm1p-Pdi1p is not *trans* regulated by CPY* and RBsp.

(***A***) Htm1p-Pdi1p generated similar glycan profiles on RBsp with or without pre-incubation with CPY* after a sixteen-hour incubation. Numbers shown are the mean ± one s.d. from three experimental replicates.

(***B***) Htm1p-Pdi1p generated similar Man7 on CPY* in the presence or absence RBsp after a sixteen-hour incubation. Numbers shown are the mean ± one s.d. from three experimental replicates.

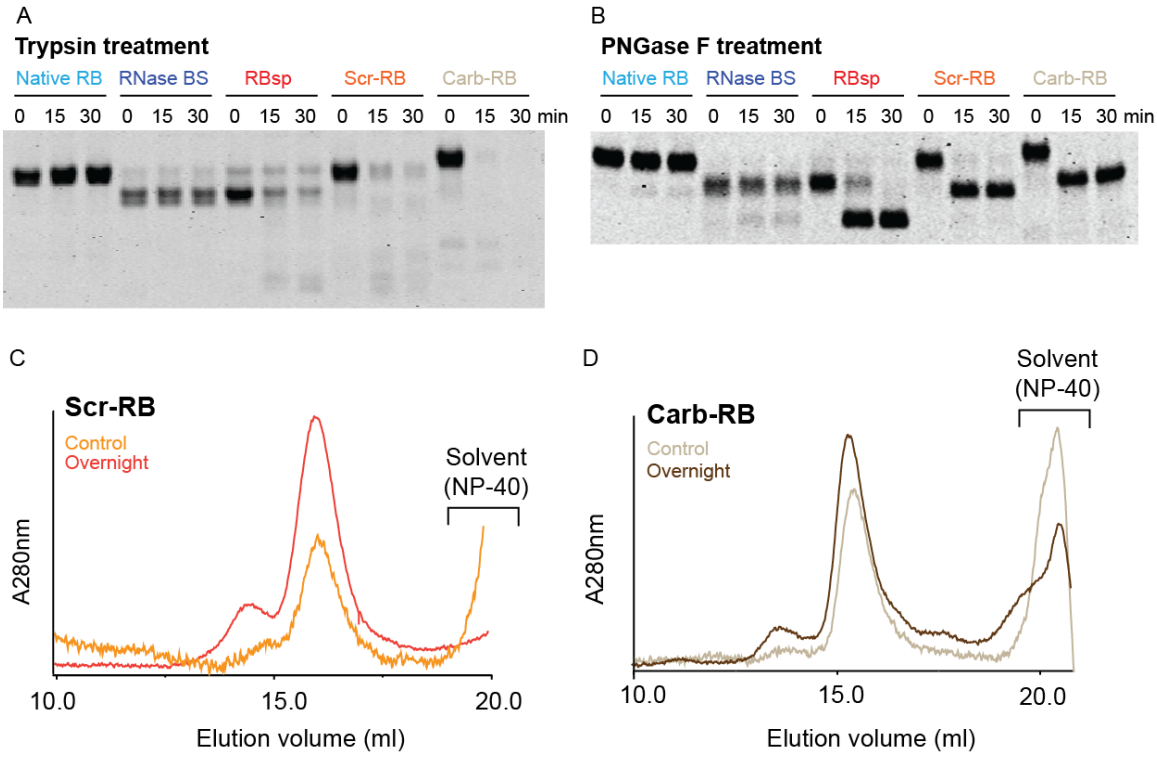

Figure S9. Folding states of RNase B variants.

(***A***) 10 μM of each RNase B variants were treated with 50 ng of trypsin in a total volume of 30 μl at room temperature. At the indicated time points, 10μl samples were collected and mixed with PMSF to stop proteolysis for subsequent SDS-PAGE analysis.

(***B***) 10 μM of each RNase B variants were treated with 1 unit of PNGase F in a total volume of 30 μl at 37ºC. At the indicated time points, 10μl samples were collected and mixed with 1x SDS-PAGE sample buffer to stop deglycosylation for subsequent SDS-PAGE analysis.

(***C***) Size distribution of Scr-RB before (control) and after (Overnight) overnight incubation with Htm1p-Pdi1p at 30ºC, as analyzed by Superdex 200 size exclusion chromatography.

(***D***) Size distribution of Carb -RB before (control) and after (Overnight) overnight incubation with Htm1p-Pdi1p at 30ºC, as analyzed by Superdex 200 size exclusion chromatography.

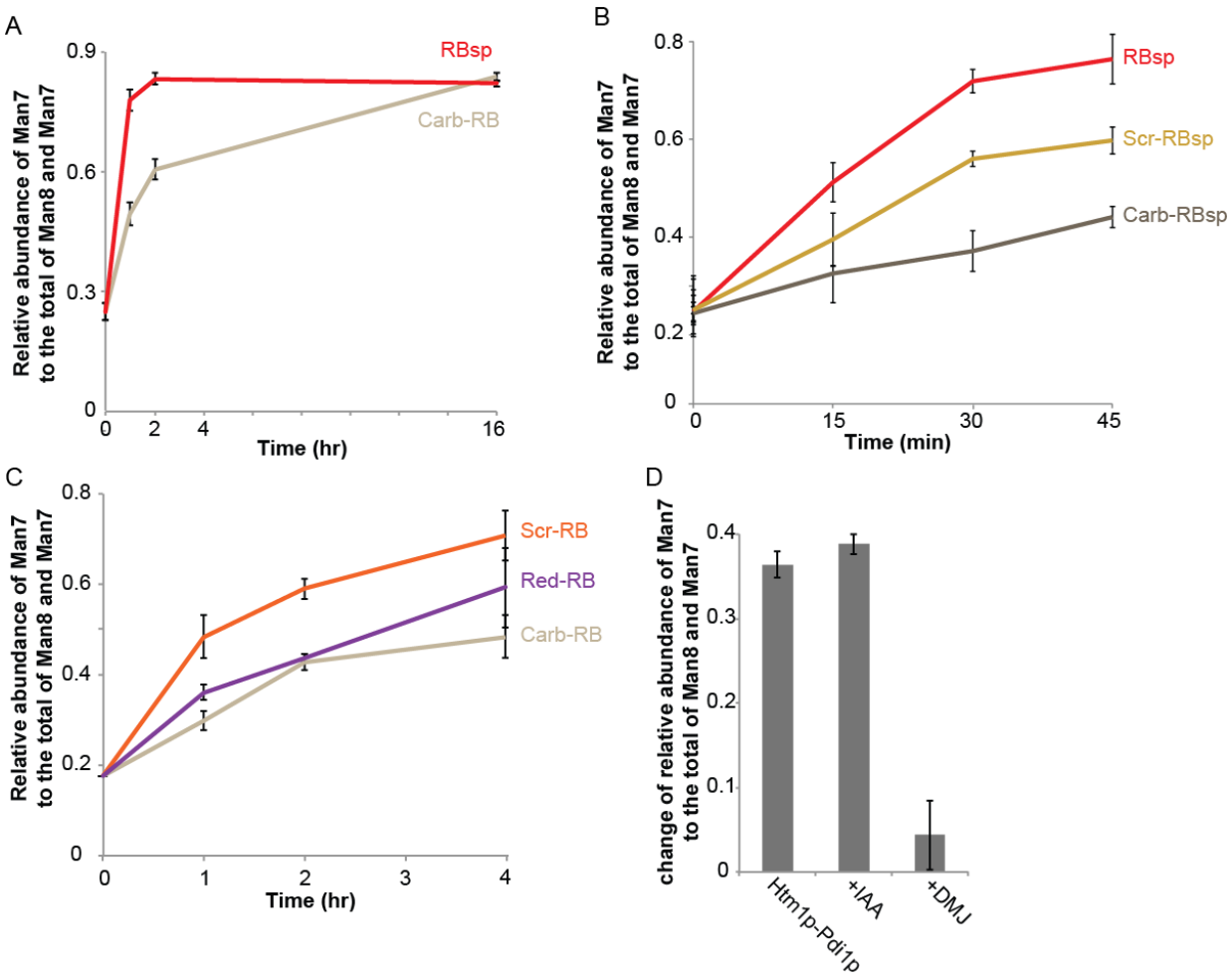

Figure S10. Additional experiments of demannosylation of RNase B variants by Htm1p-Pdi1p.

(***A***) The change of the relative Man7 abundance on RBsp and Carb-RB during along time-course incubation with Htm1p-Pdi1p. Data are the mean ± one s.d. from three experimental replicates.

(***B***) The changes of the relative Man7 abundance on Scr-RBsp and Carb-RBsp along a time-course incubation with Htm1p-Pdi1p in comparison to that of RBsp. Data are the mean ± one s.d. from three experimental replicates.

(***C***) The change of the relative Man7 abundance on Red-RB along a time-course incubation with Htm1p-Pdi1p, in comparison to those of Scr-RBsp and Carb-RBsp. Data are the mean ± one s.d. from three experimental replicates.

(***D***) The change of the relative Man7 abundance on RBsp after a thirty-minute incubation with Htm1p-Pdi1p, in the absence or presence of 10 mM iodoacetamide (+IAA), or 10 mM 1-deoxymannojirimicin (+DMJ). Data are the mean ± one s.d. from three experimental replicates.

Chapter 3

Investigating the roles of disulfides and Pdi1p in Htm1p-mediated ERAD-L

Abstract

Disulfide bond formation, a unique post-translational modification only found in the oxidative environment of the secretory pathway, has strong effects on the protein stability and conformation. In light of our discovery that Htm1p-Pdi1p preferentially targets misfolded proteins that are kept in partially folded states by disulfide bonds, we need to clarify whether disulfide is required for the action for the action of Htm1p-Pdi1p, and whether Pdi1p is involved in ERAD-L substrate recognition through its oxidoreductase function. We carried out a series of *in vivo* and *in vitro* experiments and showed that disulfide bonds are not a prerequisite for the N-glycan-dependent ERAD-L pathway mediated by Htm1p mannosidase function. Instead, Htm1p blocks the oxidoreductase activity of Pdi1p. Our findings suggest a potential mechanism of how Htm1p interacts with Pdi1p to mediate substrate recognition.

Introduction

For our *in vitro* enzymatic assay of Htm1p-Pdi1p, as described in chapter two, we essentially relied on the formation of intramolecular disulfide bonds to achieve and maintain protein of partially structured states. Disulfide bonds comprise a unique type of post-translational modification that is found in the oxidizing environment in the ER. As a covalent modification, disulfide bond formation is known to help populate folding intermediates (Chang, 2011; Mamathambika and Bardwell, 2008), it is possible that Htm1p intrinsically prefers disulfide-linked proteins. Also, mixed disulfide bonds between misfolded proteins and ER chaperones ensure that misfolded proteins are retained and retrieved to the ER for subsequent ERAD targeting (Hurtley and Helenius, 1989; Mamathambika and Bardwell, 2008). To further understand the conformational basis for ERAD targeting, we aim to further investigate the association between the ERAD functions of Htm1p and ERAD-L substrates with different capabilities to form disulfide bonds.

The correlation between disulfide bonds and Htm1p-mediated ERAD is particularly interesting given the essential role of Pdi1p, a well-characterized ER oxidoreductase, in the function of Htm1p (Clerc et al., 2009; Gauss et al., 2011; Sakoh-Nakatogawa et al., 2009b). Pdi1p belongs to the highly conserved protein disulfide isomerase (PDI) family that possesses both molecular chaperone and oxidoreductase functions to promotes disulfide bond formation and rearrangement during protein folding in the ER (Hatahet and Ruddock, 2009). Among the five PDIs found in budding yeast, Pdi1p is the only essential PDI in *Saccharomyces cerevisiae* (Nørgaard et al., 2001).

Potential ERAD functions of PDI have been suggested among various eukaryotic systems, such as preventing misfolded proteins from ER export and facilitating their unfolding and retrotranslocation (Gillece et al., 1999; Grubb et al., 2012; Izawa et al., 2012; Tsai et al., 2001; Ushioda et al., 2008). One of the most widely proposed ERAD roles of PDIs is to mediate unfolding of proteins to promote their retrotranslocation, such as the example of the mammalian reductase ERdj5 (Hagiwara et al., 2011; Tsai et al., 2001; Ushioda et al., 2008). Interestingly, ERdj5 also interacts with EDEM1, the mammalian Htm1p homolog, which raises a question of whether there is a conserved role of the interaction between PDI family proteins and ERAD-committing mannosidases to promote reduction of misfolded proteins.

Specific to Htm1p, Pdi1p has been suggested to be critical for structural formation and stability of Htm1p (Sakoh-Nakatogawa et al., 2009b). The molecular chaperone function of Pdi1p makes it a plausible candidate for mediating partially structured substrate recruitment by Htm1p (Denic, 2011; Gauss et al., 2011; Sakoh-Nakatogawa et al., 2009b), a mechanism that has been elusive among all the known chaperones with this specificity. However, with many described ER folding functions and the essentiality of Pdi1p, as well as the differences in the endogenous abundance between Pdi1p and Htm1p (near three orders of magnitude) (Kulak et al., 2014), it is hard to distinguish the specific role of Pdi1p to Htm1p from other *in vivo* ERAD functions of Pdi1p that are independent of Htm1p. In addition, not all secretory proteins form disulfide bonds, nor do all known ERAD substrates (Gillece et al., 1999). The question of whether formation of disulfide bonds is required for Htm1p-mediated ERAD thus

needs to be clarified. Also, if cysteines are not required for Htm1p-mediated N-glycan process and ERAD, we will be able to use cysteine-based chemistry to conjugate chemically synthesized glycans to explore the specificity of Htm1p-Pdi1p against more prototypical folding intermetidates that do not require disulfide bonds to populate in partially folded states (Alexandrescu and Shortle, 1994; Alexandrescu et al., 1994; Chakraborty et al., 2010; Matsuo et al., 2003; Tang et al., 2006; Totani et al., 2006).

Here, we carry out *in vivo* and *in vitro* analysis to clarify whether disulfide bonds are directly involved in the N-glycan-dependent ERAD-L process mediated by Htm1p-Pdi1p. We found that the prototypical ERAD-L substrate CPY* can still be targeted for the N-glycan-dependent ERAD-L after the removal of all of its eleven cysteines, suggesting that the disulfide bond is not a required feature for ERAD-L. In addition, we discovered a secondary effect of Htm1 in promoting ERAD through blocking the oxidoreductase activities of Pdi1p. Our results suggest a potential mechanism of how Htm1p coordinates with Pdi1p to recognize substrates.

Results

Cysteines on the substrate are not required for the N-glycan-dependent ERAD-L pathway

To test whether cysteines are required for Htm1p-mediated ERAD, we designed a cysteine-null CPY* (CPY*noCys) whose eleven cysteines are all replaced by alanines. When we purified CPY*noCys from WT yeast, we found no signal of Man7 (Fig. 1 A and B). Consistent with our *in vitro* studies in chapter two, we found that Htm1p-Pdi1p

generated a level of Man7 on CPY*noCys that is significantly lower than that of CPY* (Fig. 1C), suggesting that CPY*noCys is less preferred by Htm1p-Pdi1p than CPY* *in vitro*. On the other hand, similar to CPY*, CPY*noCys underwent degradation *in vivo* through an *HTM1*-/*HRD1*-dependent manner (Fig. 1D). Removal of the glycosylation sites also prevented *HRD1*-dependnent degradation (Fig. 1E), suggesting that the cysteine-null CPY*noCys can still be targeted for ERAD through an N-glycan-dependent manner.

If disulfide bonds significantly impact conformations of the substrates of Htm1p-Pdi1p *in vivo* similarly to those *in vitro*, we expect that the demannosylation step will be the rate-limiting step for ERAD of CPY*noCys. In this scenario, we expect to see accelerated turnover of CPY*noCys when we promote the mannosidase activity by overexpressing *HTM1 in vivo* (*oeHTM1*). Instead, we found that the turnover rate of CPY*noCys in *oeHTM1* was indistinguishable to that in wild-type (Fig. 1F). Consistent to this finding, we have seen previously that addition of a thiol-blocking reagent did not inhibit demannosylation *in vitro* (Chapter two, Fig. S10D), further ruling out the direct requirement for disulfide formation for N-glycan-mediated ERAD-L. Taken together, the absence of disulfide bonds does not limit N-glycan-dependent ERAD of CPY*noCys *in vivo*.

Of a note, CPY*noCys underwent *HRD1*-independnet degradation. This degradation event is likely mediated through a post-ER pathway as shown by the steady increase of molecular mass of CPY*noCys along the chase time-course, a sign of extension of N-glycans in the Golgi (Fig. 2A). Endo H treatment collapsed the higher

molecular mass signal of CPY*noCys into a single band that is similar to Endo H-treated CPY* (Fig. 2B). On the other hand, treatment with barium hydroxide, which promote β-elimination of O-linked modifications, did not collapse the high molecular-mass smear of CPY*noCys (Fig. 2B), suggesting that, different from other ERAD-L substrates (Vashist, 2001; Xu et al., 2013), CPY*noCys is not trapped in a futile ER folding cycle and O-mannosylated.

Overexpression of *HTM1* promotes an N-glycan-independent, cysteine-dependent ERAD mechanism

Our experiments with CPY*noCys suggest that demannosylation is not the rate-limiting step for ERAD-L *in vivo*. However, it has been found that overexpressed *HTM1* can enhance the turnover rate of CPY* *in vivo* (Gauss et al., 2011). We were able to reproduce the accelerated degradation of CPY* in the *oeHTM1* yeast strain (Fig. 3A). The enhanced turnover of CPY* by *oeHTM1* was completely abolished when we blocked the downstream ERAD action with *der1* deletion, suggesting that this ERAD enhancement is still dependent on the canonical ERAD-L system.

One potential mechanisms to explain that *oeHTM1* meditates the enhanced turnover of CPY* but not CPY*noCys is that Htm1p prefers cysteine- or disulfide-bond-containing proteins, and increasing the normally limited amount of Htm1p *in vivo* enhanced demannosylation of these preferred cysteine-containing substrates. We reasoned that if the effect of *oeHTM1* resulted from enhanced demannosylation, we would expect no effect from *oeHTM1* in the *alg9Δ oeALG12* strain that directly produces

Man7 (Quan et al., 2008). Still, we found that *oeHTM1* accelerated the degradation of CPY* in *alg9Δ oeALG12* (Fig. 3B). We further tested the effect of *oeHTM1* on the turnover of CPY*0000, which is void of all glycosylation sites and is thus resistant to N-glycan-dependent ERAD (Knop et al., 1996). Again, *oeHTM1* promoted degradation of CPY*0000 (Fig. 3C), suggesting that the *oeHTM1* enhances ERAD through a mechanism that is independent of N-glycans. In addition, we found that *yos9Δ* was partially bypassed by *oeHTM1* to promote ERAD of CPY* (Fig. 3D). The rates of degradation of CPY* and CPY*0000 were indistinguishable in *yos9Δ oeHTM1* (Fig. 3E). On the other hand, oe*HTM1* cannot bypass *yos9Δ* to promote ERAD of CPY*noCys (Fig. 3F). Collectively, the paradoxical effect of *oeHTM1* on promoting ERAD of CPY* but not CPY*noCys is mediated in a cysteine-dependent but N-glycan-independent manner.

Htm1p blocks the oxidoreductase activities of Pdi1p

Given its essential interaction with Htm1p, as well as its well-characterized oxidoreductase activities, Pdi1p is likely involved in this cysteine-dependent ERAD event mediated by *oeHTM1*. Indeed, studies from the Endo group has suggested that disulfide crosslinks between Htm1p and Pdi1p is critical for *in vivo* function and stability of Htm1p (Sakoh-Nakatogawa et al., 2009b). In addition, when in complex with Htm1p, Pdi1p is at different oxidative states from its free form. The involvement of Pdi1p may explain why CPY*noCys is not targeted by the N-glycan-independent ERAD due to the loss of mixed disulfide-mediated interaction with Pdi1p.

The first model of how increase *in vivo* abundance of Htm1p can enhance ERAD through Pdi1p is that Htm1p uses Pdi1p as a reductase to facilitate retrotranslocation. We examined the reductase activity of free Pdi1p and Htm1p-Pdi1p against misfolded RBsp in the presence of reducing agents. The presence of free cysteines was monitored by 4-acetamido-4'-maleimidylstilbene-2,2'-disulfonic acid (AMS) labeling, which increases molecular mass by roughly 0.5 kDa for each labeled sulfhydryl group. Free Pdi1p efficiently promoted reduction of the partially structured RBsp (Fig. 4A), suggesting that free Pdi1p can act as a reductase for misfolded proteins. By contrast, the rate of reduction of RBsp was indistinguishable in the presence of Htm1p-Pdi1p from that seen in a buffer control, suggesting the lack of reductase activity of Htm1p-Pdi1p.

The absence of reductase activity of Htm1p-Pdi1p prompted us to explore whether Htm1p-Pdi1p retains Pdi1p's function as a catalyst of oxidative folding. We monitored the rate of oxidative refolding of reduced RNase A to the native form by the same AMS-labeling assay, but here the decrease of molecular mass reports on the rate of oxidation. While free Pdi1p significantly accelerated disulfide formation of reduced RNase A, Pdi1p in complex with Htm1p had no effect on this reaction in comparison to the control (Fig. 4B). In addition to promoting oxidative folding, it has been reported that the mammalian PDI also has a paradoxical activity which promotes protein aggregation under specific biochemical conditions (Puig and Gilbert, 1994; Puig et al., 1994; V. Sideraki and Gilbert, 2000). We further explored *in vitro* reconstitution of this event with CPY*. Under oxidative conditions, fully reduced CPY* slowly oligomerized into high

molecular-mass oligomers that are cross-linked by disulfide as resolved by non-reducing SDS-PAGE (Fig. 4C). The presence of free Pdi1p markedly accelerated oligomerization. By contrast, not only did Htm1p-Pdi1p fail to accelerate CPY* oligomerization, but Htm1p-Pdi1p also suppressed CPY* oligomerization. Taken together, the oxidoreductase activity of Pdi1p in inhibited when in complex with Htm1p.

One major consequence of blocking oxidoreductase activities of Pdi1p is the disruption of oxidative folding and thus the activation of the unfolded protein response (UPR) (Braakman et al., 1992; Cox et al., 1993; Jämsä et al., 1994; Mori et al., 1993; Nørgaard et al., 2001). Indeed, using an UPRE-driven β-galactosidase assay (Cox et al., 1993), we found that *oeHTM1* caused activation of UPR (Fig. 5). The effect of *oeHTM1* was specific since overexpression of *PDI1* did not induce UPR through the same overexpression system. Co-overexpression of *HTM1* and *PDI1* attenuated UPR, confirming that *oeHTM1* induced UPR by sequestering endogenous Pdi1p. Overexpression of *ERO1*, which encodes Ero1p, the FAD-dependent oxidase responsible for generating oxidative equivalents for Pdi1p (Frand and Kaiser, 1998; Pollard et al., 1998; Tu, 2000), also partially attenuated the activation of UPR by *oeHTM1*, further validating that *oeHTM1* activated UPR through interfering oxidative folding (Fig. 5). These *in vivo* observations are consistent with our *in vitro* results to support that by forming a tight complex, Htm1p blocks the functions of Pdi1p in promoting reduction and oxidation.

If the effect of *oeHTM1* in promoting N-glycan-independent ERAD is mediated through the excessive level of Htm1p that sequesters endogenous Pdi1p, we will be

able to prevent this ERAD event by abolishing the interaction between Htm1p and Pdi1p. We followed the degradation of CPY* in the genetic background with overexpressed htm1-Δ572-657 (*oeΔ56*), which is void of interaction with Pdi1p. Indeed, CPY* was mostly stabilized in *oeΔ56* (Fig. 6), confirming that the interaction with Pdi1p is essential for Htm1p to mediate ERAD. Overexpression of catalytically dead htm1-E222Q (*oeE222Q*), on the other hand, still promoted N-glycan-independent ERAD-L (Fig. 6), suggesting that the effect of sequestering Pdi1p is independent of the mannosidase function of Htm1p. Taken together, we conclude that *oeHTM1* promotes the N-glycan-independent ERAD by generating excessive Htm1p that sequesters endogenous Pdi1p.

Discussion

Disulfide bond formation is one of the unique post-translational modifications in the ER that are closely relevant to protein folding. The covalent and controllable nature of disulfide bonds also provides a widely applicable system to produce folding intermediates for *in vitro* studies (Chang, 2011; Mamathambika and Bardwell, 2008). For our purpose in studying the targeting of misfolded proteins by Htm1p-Pdi1p for ERAD commitment, the availability of disulfide bond-stabilized partially folded states has been instrumental for our discovery for the conformational preference of Htm1p-Pdi1p. At the same time, it is known that disulfide formation is common found in misfolded proteins in the ER (Haynes et al., 2004; Hosokawa et al., 2006). Using the cysteine-null CPY*noCys, here we show that disulfide bonds are not required for the N-glycan-

dependent ERAD-L process. Thus, the demannosylation process by Htm1p-Pdi1p is unlikely to be the main rate-limiting step for targeting CPY*noCys to N-glycan-dependent ERAD-L. Indeed, previous studies have found that the turnover rates of misfolded proteins were not accelerated in the yeast strains that constitutively produces N-glycoproteins with a terminally exposed α1,6-linked mannose (Quan et al., 2008; Xie et al., 2009).

We also found that overexpression of *HTM1* can promote ERAD in an N-glycan-independent mechanism. One possible mechanism of how *oeHTM1* promotes ERAD is through activating UPR (Travers et al., 2000). However, UPR-mediated ERAD is insufficient to explain why ERAD of CPY*noCys is not similarly accelerated by *oeHTM1*. How, then, can we explain the N-glycan-independent but cysteine-dependent ERAD effect promoted by *oeHTM1*? Our *in vitro* investigation demonstrates that the Htm1p-Pdi1p complex exhibits minimal reductase activities to reduce misfolded RBsp, as well as minimal oxidase to promote disulfide-linked oligomerization of CPY*. The activation of UPR by overexpression of *HTM1* further suggests that extra copies of Htm1p sequesters Pdi1p and thus disrupts oxidative folding. Previous studies have found that Pdi1p, as well as mammalian PDIs, retains misfolded proteins in the ER, promotes oxidative oligomerization, and reduces ERAD efficiency (Hosokawa et al., 2006; Izawa et al., 2012). It has also been shown that Pdi1p has prolonged interaction with CPY* that is conjugated with the oxidative folding cycle (Haynes et al., 2004). Taken together, we propose that by sequestering the endogenous Pdi1p, extra copies of Htm1p prevent

cysteine-mediated retention of CPY* in the ER and thus facilitate the retrotranslocation process.

As Pdi1p does not play the role as an oxidoreductase for substrates of Htm1p, the chaperone activity of Pdi1p to recognize unfolded proteins suggests a potential role of Pdi1p in mediating substrate recruitment for Htm1p-Pdi1p (Clerc et al., 2009; Gauss et al., 2011; Sakoh-Nakatogawa et al., 2009b). If so, how does it achieve the process? While Pdi1p is known to have peptide binding activity for misfolded proteins (Gillece et al., 1999), our findings argue against a simple model in which Pdi1p acts an independent module to bind substrates for Htm1p. First, the preference of Htm1p-Pdi1p for partially folded proteins is different from that of uncomplexed Pdi1p, which likely prefers unfolded polypeptides over partially folded ones similarly to human PDI (Irvine et al., 2014). Second, by forming tight complex with Pdi1p and blocking its oxidoreductase functions, Htm1p may manipulate the substrate binding mode of Pdi1p, which is tightly coupled to its redox state (Nakasako et al., 2010; Sakoh-Nakatogawa et al., 2009b; Serve et al., 2010; Wang et al., 2012). Also, Gauss et al. have reported a Leu_{313} to Pro mutation on Pdi1p that interferes with its interaction with Htm1p (Gauss et al., 2011). Based on the crystal structure of Pdi1p (Tian et al., 2006), the Leu_{313} residue resides in the hydrophobic pocket of the b' peptide binding domain, suggesting that Htm1p makes critical contact with this domain of Pdi1p. Third, in addition to not accelerating disulfide crosslinking of CPY*, the Htm1p-Pdi1p complex suppresses this process, presumably through the same mechanism that allows it to specifically act on partially folded substrates. We therefore propose that together the Htm1p-Pdi1p is able to recruit

desired substrates through the peptide-binding pocket of Pdi1p, whose specificity is changed to accommodate the preferred partially structured proteins.

It has been reported that in mammalian cells, EDEM1 interacts with misfolded proteins through a mannosidase-independent manner, and overexpression of *EDEM1* enhanced ERAD in a glycan-independent manner (Cormier et al., 2009; Hagiwara et al., 2011; Hosokawa et al., 2006, 2010; Olivari et al., 2006; Ron et al., 2011; Shenkman et al., 2013). Our findings argue against a model that the major role of Pdi1p in the Htm1p-Pdi1p complex is to promote substrate remodeling or recruitment by disulfide-crosslinking mechanisms. The present work could serve as model for analogous efforts to define how and if EDEM1 repurposes ERdj5 to aid ERAD function (Hagiwara et al., 2011; Ushioda et al., 2008). Recently, two paralogs of EDEM1, EDEM2/3, were also found to interact with a newly identified PDI-like protein, TXNDC11 (Timms et al., 2016). The conserved interaction between these ERAD-mediating mannosidases and PDI-like protein supports a critical role for this interaction. Our ability to purify Htm1p-Pdi1p will allow future structural investigations of how this potential substrate recruitment mechanism is achieved.

Our findings that CPY*noCys is exported from the ER provides an interesting case on the mechanisms of how protein folding quality control mediates ER retention/export. Previous studies have suggested for protein mutants, the most stable or structured nonnative forms can be exported from the ER while the most destabilized ones are retained and targeted for ERAD (Sekijima et al., 2005). As CPY*noCys lacks any cysteine pair to form disulfide bonds to partially stabilize structures, the differences

of ER retention between CPY* and CPY*noCys are mechanistically different from this existing model. The export mechanism is not mediated through glycan-recognition by lectin cargo receptors, since CPY*noCys0000 is similar exported (Dancourt and Barlowe, 2010; Helenius and Aebi, 2004). A potential mechanism for ER export of CPY*noCys is that the absence of mixed disulfide bonds with Pdi1p or other ER PDIs diminishes the ER retention, in reminiscent to mammalian PDIs that forms mixed disulfide with nonnative proteins (Anelli et al., 2003; Fra et al., 1993; Guenzi et al., 1994). This disulfide-mediated retention/retrieval model predicts that there is no folding sensor to safeguard the export of CPY*noCys; CPY*noCys escapes from the ER through a bulk-flow mechanism (Wieland et al., 1987). The bulk flow alone, though, cannot fully explain the absence of ER export of CPY* in *der1Δ oeHTM1*, if the only difference between CPY* and CPY*noCys is the presence of cysteines for mixed disulfide crosslinking with Pdi1p. Future studies on this clear difference will be critical to further our understandings on the association between ER quality control and ER export/retention. The availability of CPY variants with this diverse set of ER retention/export properties will be useful to pinpoint the molecular details of how one switch from retention to export, and how ERAD and ER export communicate with each other to maintain protein quality in the ER.

Materials and Methods

Yeast strains

YOS9, *DER1* or *HRD1* was deleted from wild-type BY4741 with the *Candida glabrata LEU2* gene using the standard PCR-mediated method at the genomic level as previously described (Quan et al., 2008).

Cycloheximide degradation assay

The degradation assay was carried out as described before (Quan et al., 2008). Briefly, the CEN/ARS plasmid carrying a *PRC1* promoter-driven HA-tagged CPY* variant was introduced into the desired yeast strains. Four individual colonies of each strain were parallel inoculated and grown in selection media until mid-log phase. At the zero time point, cycloheximide was added to a final concentration of 200 μg/ml to stop translation. 1 ml liquid culture was collected at each time point and subjected to SDS-PAGE and western blot. The level of CPY* was detected with anti-HA primary antibody and the corresponding IR fluorescent secondary antibody for scanning on a LI-COR Odyssey scanner. The endogenous hexokinase was parallel detected on the same nitrocellulose membrane as a loading control. The level of HA and hexokinase on each lane was determined by the Odyssey Image Studio software. The HA signal was divided by the hexokinase signal on each lane, and then normalized to the zero time point to represent as percentage remained along the time course. Each time point represents the average of four measurements from the four biological replicates with one standard error of the mean indicated.

Recombinant preparation of Pdi1p

For N-glycan profiling of endogenous Pdi1p, C-terminally 6xHis-tagged Pdi1p was purified through the same procedure as native CPY. For the *in vitro* Pdi1p activity assay, C-terminally 6xHis-tagged Pdi1p was expressed in *E. coli* BL-21 and purified with Ni-NTA agarose beads as previously described (Tu, 2000). After purification, Pdi1p was buffer-exchanged to HSG buffer for storage.

RBsp reduction assay

RBsp was prepared at 10 μM in Reaction Buffer. At the beginning of the assay DTT was added at the indicated concentrations, and free Pdi1p or Htm1p-Pdi1p was added to 100 nM. The mixtures were incubated at 30°C for one hour. To stop the reaction, 4-acetamido-4'-maleimidylstilbene-2,2'-disulfonic acid (AMS) (Life Technologies) was added to 5 mM to block and label free cysteines. The samples were separated by non-reducing SDS-PAGE and visualized by Coomassie blue R250 stain.

RNase A oxidation assay

Commercially available bovine pancreatic RNase A (Sigma-Aldrich) was reduced by 5mM DTT in 6 M guanidine hydrochloride 42°C for one hour, buffer-exchanged into HSG Buffer, and immediately used for the refolding assay. At the beginning of the time course, freshly reduced RNase A was added to a final concentration of 15 μM into HSG Buffer (20 mM HEPES pH 7.0, 150 mM NaCl, 15% (v/v) glycerol)-based reaction buffer

containing 1 mM reduced glutathione and 0.2 mM oxidized glutathione, along with 0.9 μM free Pdi1p, BSA, or Htm1p-Pdip1, at 30°C, At each time point, equal amount of sample was taken and mixed with 5 mM AMS. The samples were separated by non-reducing SDS-PAGE and visualized by Coomassie blue R250 stain.

CPY* oxidative aggregation assay

2.5 μM CPY* was reduced by 50 mM DTT in 6 M guanidine hydrochloride at room temperature for one hour and then buffer-exchanged to HSG Buffer immediately before the assay. At the zero time point, freshly reduced CPY* was mixed with 100 μM oxidized glutathione (GSSG) at 30°C, and free Pdi1p or Htm1p-Pdi1p was added to 100 nM as indicated. At each time point, the same amount of sample was withdrawn and mixed with 10 mM AMS. The samples were separated by non-reducing SDS-PAGE and detected by western blotting with anti-SBP primary antibody against the SBP-tag on CPY*. For quantitative analysis, the percentage of aggregation was calculated by dividing the SBP signal of the oligomeric aggregate region to the total SBP signal on each lane. Each time point represents the mean from an experimental triplicate with one SD indicated.

UPR assay

The UPR assay was carried out according to a previously published protocol (Pollard et al., 1998). Briefly, the pJC005 (pJW464) 2μm plasmid containing UPRE-LacZ reporter (Cox et al., 1993) was introduced into each desired yeast strains: *BY4741* (wild-type,

yJW1819), *oeHTM1* (yJW1820), *oeE222Q* (yJW1835), and *oeΔ56* (yJW1836). For overexpression of *PDI1* (*oePDI1)*, a 2*μ*m plasmid carrying pTEF2-PDI1 (pYL107) was co-transformed with pJC005, and the same for *oeERO1* (pJW672) (Tu, 2000).

One colony of transformed yeast was inoculated in 5 ml selection medium at 30ºC overnight, diluted to OD600 =0.1 in 15 ml medium, and allowed to grow to mid-log phase (OD6000 = 0.6~1.0). 10 ml culture was harvested by centrifugation at 3,000 x g for 5 minutes. After being washed twice with cold 1 ml U Buffer (1x PBS containing 1mM MgCl2 and 1x *cOmplete* EDTA-free protease inhibitor cocktail (Roche)), the cell pellet was resuspended in 200 *μ*l U Buffer. 50*μ*l of glass beads was added, and the cells were agitated by vortexing at maximal speed for one minute at 4ºC with one-minute rest on ice twice. The lysate was centrifuged at 500 x g for one minute. The supernatant was collected and centrifugation at 10,000 x g for another five minutes. The protein concentration in the clarified supernatant was measured by Pierce BCA protein assay. 5 *μ*l of the clarified supernatant was then taken into a 384-well clear plate. 45 *μ*l 2 mM chlorophenol red-β-*D*-galactopyranoside (CPRG) in U Buffer was added immediately before the measurement. The measurement of the absorption at 595 nm was carried out in real time on the VMax Kinetic ELISA Absorbance Microplate Reader (Molecular Devices, Sunnyvale, CA) for thirty minutes. The specific activity of β-galactosidase was calculated as:

Units (nmol/mg/min) = $55 \times \frac{\Delta OD595}{\Delta T \times [lysate\ concentration]}$

Figures

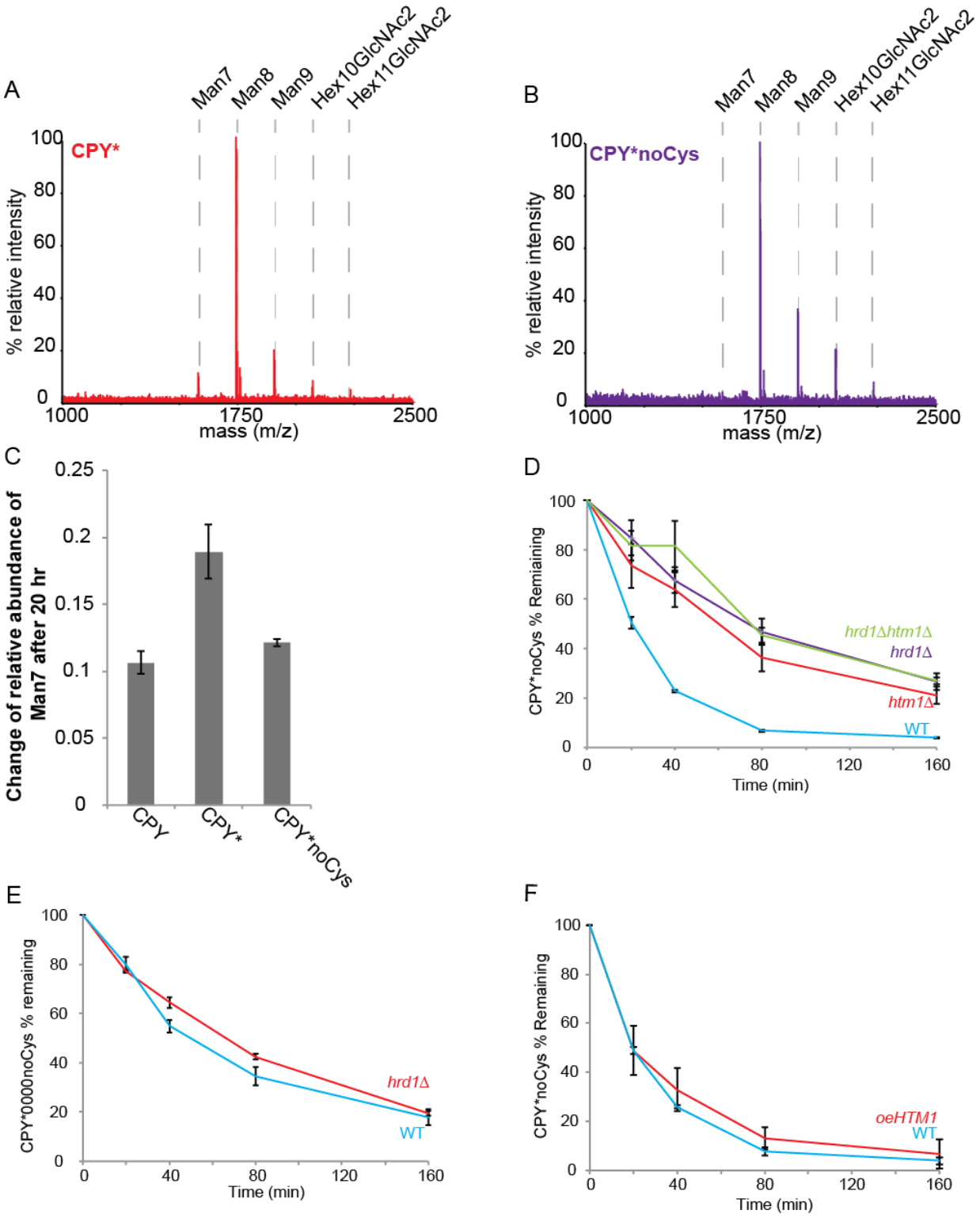

Figure 1. CPY*noCys undergoes N-glycan-dependent ERAD-L pathway.

(A and B) The glycan profiles of glycans released from CPY* **(A)** in comparison to those from CPY*noCys **(B)**

(C) The change of the relative abundance of Man7 in the total of Man8 and Man7 on different CPYs after 20-hour incubation with Htm1p-Pdi1p. Shown are the means ± standard deviation (S.D.) from biological triplicate.

(D) The % remaining of CPY*noCys after addition of cycloheximide (CHX) normalized to the zero time point in different yeast strains as indicated. Shown are the means ± one standard error of the mean (S.E.M.) from four biological replicates.

(E) The % remaining of glycan-null CPY*noCys (CPY*noCys0000) after addition of cycloheximide (CHX) normalized to the zero time point in different yeast strains as indicated. Shown are the mean ± S.E.M. from four biological replicates.

(F) The % remaining of CPY*noCys after addition of cycloheximide (CHX) normalized to the zero time point in wild-type and *oeHTM1* as indicated. Shown are the means ± S.E.M. from four biological replicates.

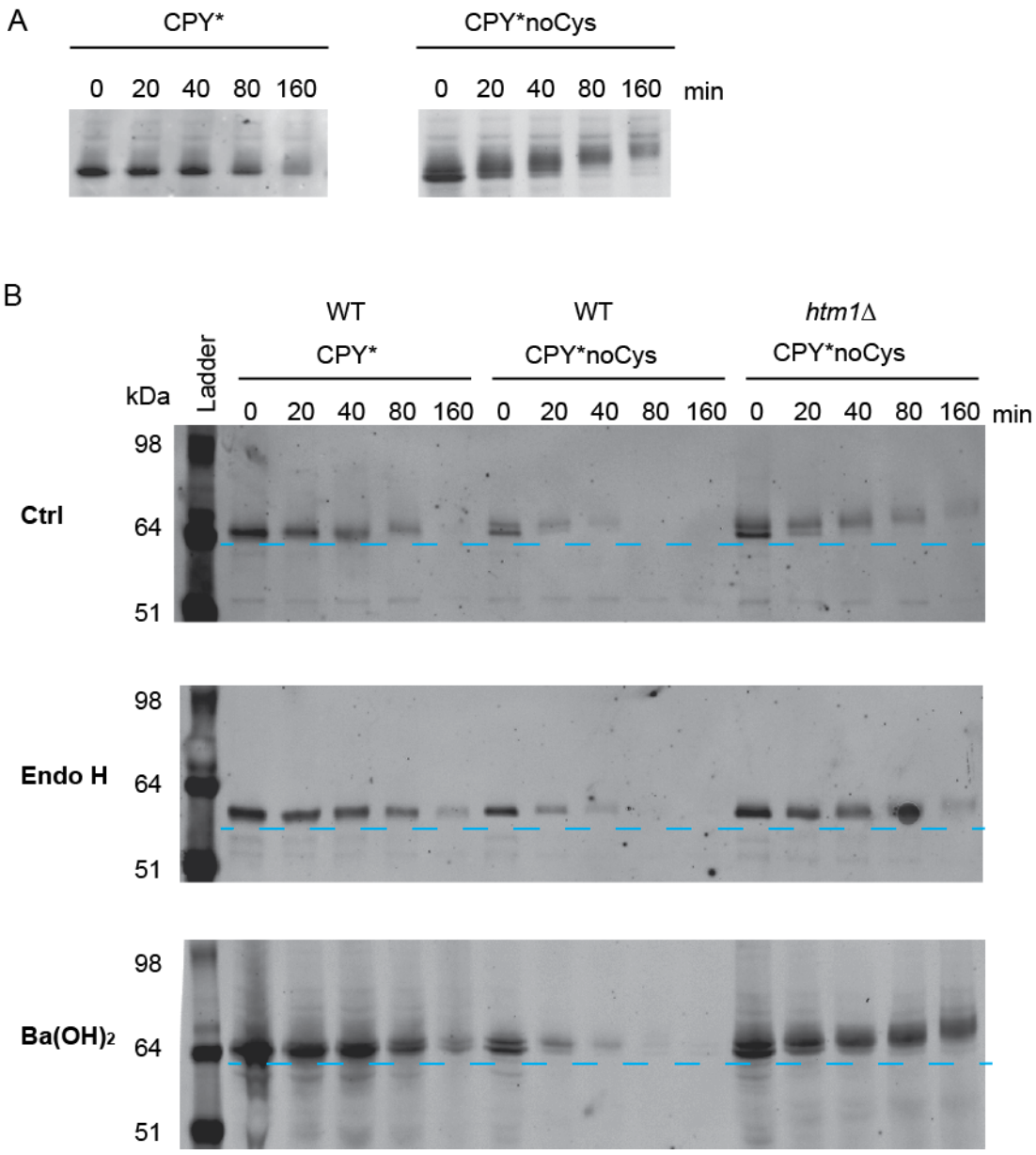

Figure 2. CPY*noCys is exported from the ER to the Golgi.

(A) The SDS-PAGE mobility of CPY* in comparison of CPY*noCys along the CHX chase timecourse as found in Fig. 1D.

(B) The SDS-PAGE mobility of CPY* and CPY*noCys along the CHX chase timecourse before (Ctrl) and after treatment with Endo H to remove N-glycans, or 0.1 M $Ba(OH)_2$ to removes O-glycans.

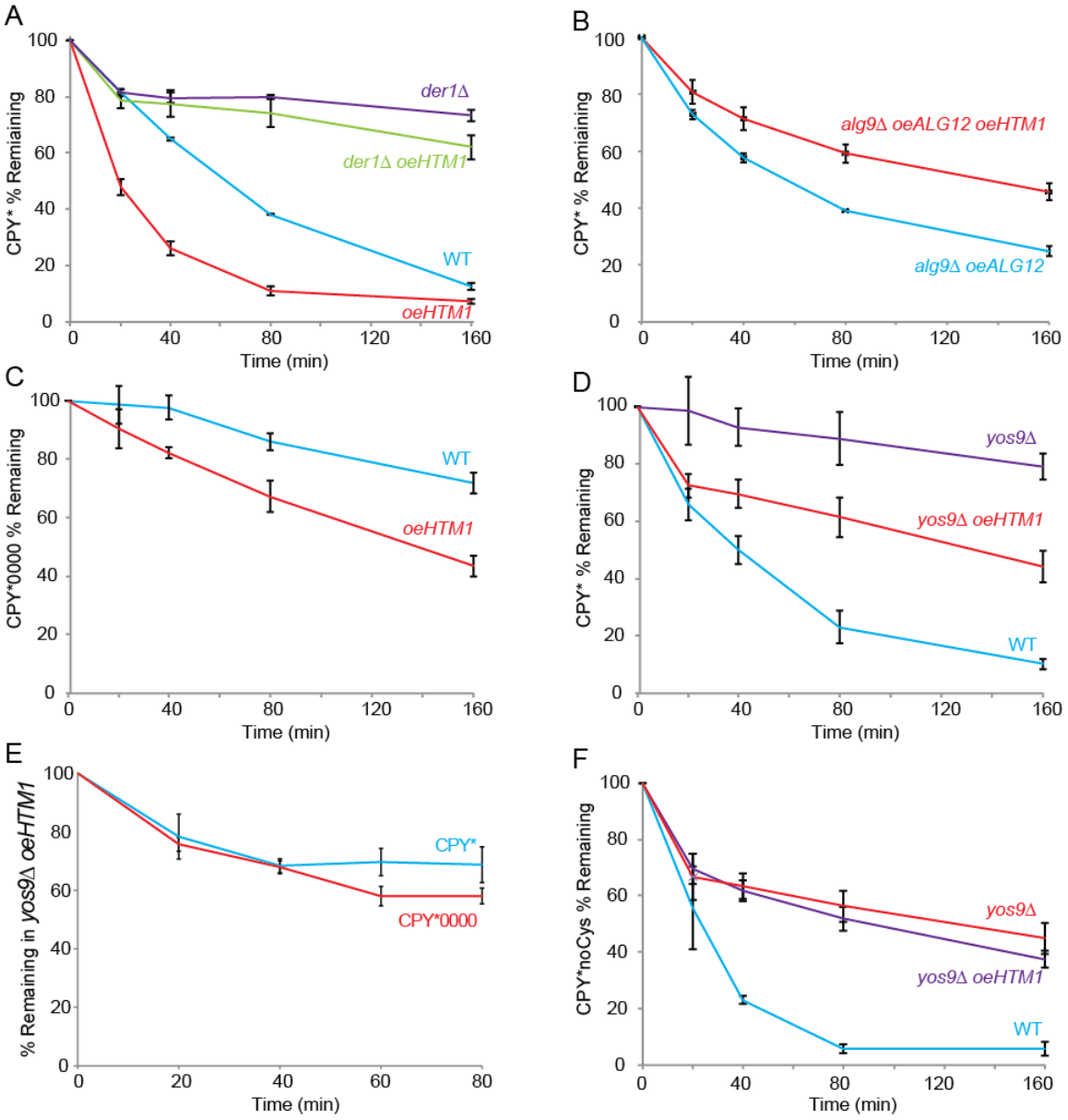

Figure 3. Overexpression of *HTM1* targets CPY* for an N-glycan-independent but cysteine-dependent ERAD-L pathway.

(A) The % remaining of CPY* after addition of cycloheximide (CHX) normalized to the zero time point in wild-type and *oeHTM1*. Shown are the means ± S.E.M. from four biological replicates.

(B) The % remaining of CPY* after addition of cycloheximide (CHX) normalized to the zero time point in *alg9Δ oeALG12* and *alg9Δ oeALG12 oeHTM1*.

(C) The % remaining of glycan-null CPY*0000 after addition of cycloheximide (CHX) normalized to the zero time point in wild-type and *oeHTM1.*

(D) The % remaining of CPY* after addition of cycloheximide (CHX) normalized to the zero time point in wild-type, *yos9Δ* and *yos9Δ oeHTM1.*

(E) The % remaining of CPY* and CPY*0000 after addition of cycloheximide (CHX) normalized to the zero time point in *yos9Δ oeHTM1.*

(F) The % remaining of CPY*noCys after addition of cycloheximide (CHX) normalized to the zero time point in wild-type, *yos9Δ* and *yos9Δ oeHTM1.*

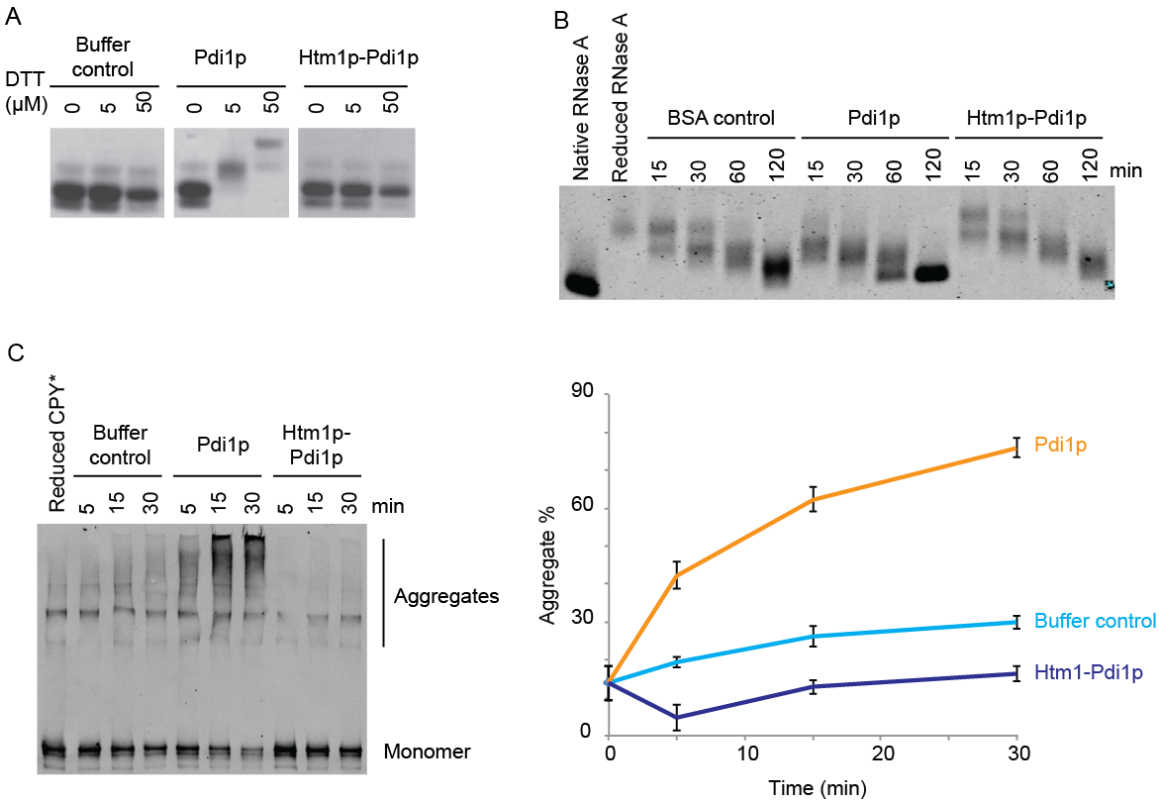

Figure 4. Htm1p blocks oxidoreductase activities of Pdi1p.

(A) Cysteins-labeling time-course of RBsp in the presence of Pdi1p, Htm1p-Pdi1p or neither (Buffer only), as resolved by non-reducing SDS-PAGE. The steady decrease of SDS-PAGE mobility is a sign of increase labeling by thiol-react AMS, as an indicator of reduction of RBsp.

(B) The oxidative refolding of reduced RNase A by BSA, uncomplexed Pdi1p, or Htm1p-Pdi1p as monitored by AMS labeling and non-reducing SDS-PAGE. The steady increase of SDS-PAGE mobility is a sign of increase oxidation of reduced RNase A.

(C) Oxidative oligomerization of freshly reduced CPY* in the presence of free Pdi1p, Htm1p-Pdi1p, or neither (Buffer only) in an oxidative environment (100 μM GSSG) along a time course. The products from each time point were collected and resolved by non-

reducing SDS-PAGE and visualized by western blot with anti-SBP antibody. Shown are the means ± S.D. from an experimental triplicate.

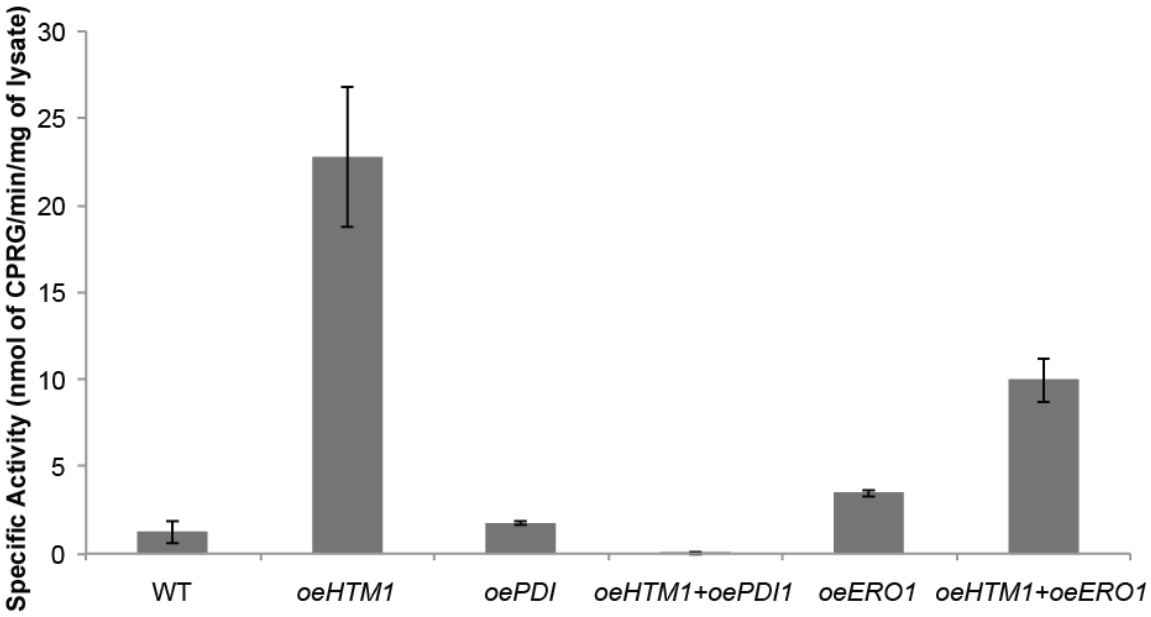

Figure 5. Overexpression of HTM1 induces UPR by sequestering Pdi1p.

The activation of UPR was measure by the activity of an UPRE-LacZ reporter as a function of the hydrolysis of CPGR in different yeast strains as indicated. Shown are the means ± S.D. from a technical replicate of a biological triplicate (total n=6).

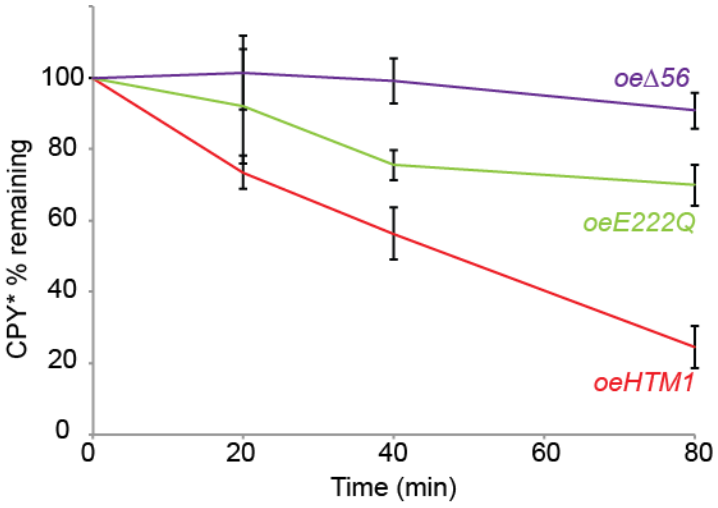

Figure 6. Pdi1p interaction is required for oeHTM1 to promote N-glycan-independent ERAD-L.

The % remaining of CPY* after addition of cycloheximide (CHX) normalized to the zero time point in wild-type and *oeHTM1*. Shown are the means ± S.E.M. from four biological replicates.

Chapter 4

Conclusions

Following our initial work in discovering an N-glycan degradation signal to license misfolded proteins for degradation via ERAD, we demonstrate that not only does the Htm1p-Pdi1p mannosidase complex preferentially target nonnative glycoproteins to generate this degradation signal, but it also differentiates different types of nonnative proteins. Particularly, the fact that Htm1p-Pdi1p prefers partially structured proteins over globally unfolded ones, as well as that it is specific to glycoproteins but not free glycans, provides a strong argument that Htm1p-Pdi1p recognizes ERAD substrates by their three-dimensional folding states, rather than general accessibility to glycosylation sites or surface exposed hydrophobic residues. Together with the existing knowledge on the enzyme specificity of UGGT (D'Alessio et al., 2010b), this conformational preference of Htm1p-Pdi1p suggests that there may exist a general conformational standard in ER that defines misfolded/incompletely folded proteins for quality control ER.

A key issue that needs to be further investigated is whether and how partially structured forms of misfolded proteins are differentiated from productive folding intermediates. To answer this question, we will need to quantitatively describe the kinetic and thermodynamic parameter that defines a misfolded protein by Htm1p-Pdi1p. So far as RBsp mimics a kinetically trapped, partially folded state, it provides only a snapshot of the folding intermediate. In addition, while the timer theory proposes that Htm1p only acts after Mns1p, our work has shown that it Htm1p-Pdi1p can bypass Mns1p in vitro, and in vivo studies have also suggested that Mns1p is not as essential as Htm1p or Yos9p in mediating ERAD (Bhamidipati et al., 2005; Hosomi et al., 2010). One possible mechanism to explain the correlation between Mns1p and Htm1p is that

Htm1p prefers Man8 to Man9. If so, instead of being considered as a timer that protects proteins from Htm1p before the generation of Man8 as proposed (Helenius and Aebi, 2004), the N-glycan processing is more like a stopwatch, that gradually increase the propensity of a protein to be targeted to ERAD as the deglycosylation proceeds. We will need to expand our substrate pool, such as combining the chemical approach to reconstitute glycan-specific N-glycoproteins with a full, well-described folding pathway and apparent kinetic trapped intermediate states (Chakraborty et al., 2010; Dedola et al., 2014; Izumi et al., 2012, 2016; Shortle, 2002; Tang et al., 2006; Totani et al., 2009; Weissman and Kim, 1991).

With the reconstitution systems of multiple ERAD-L factors established (Quan et al., 2008; Smith et al., 2014; Stein et al., 2014), we can start to ask the biochemical mechanism of how do ERAD factors communicate with each other, and how the kinetic proofreading mechanism is used by the ER to tell the right from the wrong. Furthermore, as the input from ER chaperones has been found to contribute to ERAD (Gillece et al., 1999; Grubb et al., 2012; Nakatsukasa et al., 2001; Wiseman et al., 2007), it will also be critical to understand how ERAD communicates with the ER folding machinery, and how ER chaperones affect the folding pathways to facilitate ERAD identification of terminally misfolded proteins while preventing wrongfully targeting productive folding intermediates for degradation.

To conclude, by establishing the association between the mannosidase activity of Htm1p-Pdi1p and the conformations of N-glycoprotein substrates, we will be able to apply this criterion to systematically identify endogenous ERAD-L substrates in an

unperturbed manner. Particularly, advances in mass spectrometry have now allowed concurrent characterization of both the peptide identity and the glycan structure of intact glycopeptides (Woo et al., 2015). Future integration of this approach with quantitative mass spectrometry may allow us to obtain systematic view of how the generation of α1,6-linked mannoses is coordinated with the turnover of endogenous N-glycoproteins.

References

Aebi, M., Bernasconi, R., Clerc, S., and Molinari, M. (2010). N-glycan structures: recognition and processing in the ER. Trends Biochem. Sci. *35*, 74–82.

Alexandrescu, A.T., and Shortle, D. (1994). Backbone dynamics of a highly disordered 131 residue fragment of staphylococcal nuclease. J. Mol. Biol. *242*, 527–546.

Alexandrescu, A.T., Abeygunawardana, C., and Shortle, D. (1994). Structure and dynamics of a denatured 131-residue fragment of staphylococcal nuclease: a heteronuclear NMR study. Biochemistry (Mosc.) *33*, 1063–1072.

Anelli, T., Alessio, M., Bachi, A., Bergamelli, L., Bertoli, G., Camerini, S., Mezghrani, A., Ruffato, E., Simmen, T., and Sitia, R. (2003). Thiol-mediated protein retention in the endoplasmic reticulum: the role of ERp44. EMBO J. *22*, 5015–5022.

Anfinsen, C.B., Haber, E., Sela, M., and White, F.H. (1961). The kinetics of formation of native ribonuclease during oxidation of the reduced polypeptide chain. Proc. Natl. Acad. Sci. U. S. A. *47*, 1309–1314.

Araki, K., and Nagata, K. (2011). Protein Folding and Quality Control in the ER. Cold Spring Harb. Perspect. Biol. *3*, a007526–a007526.

Bays, N.W., Gardner, R.G., Seelig, L.P., Joazeiro, C.A., and Hampton, R.Y. (2001a). Hrd1p/Der3p is a membrane-anchored ubiquitin ligase required for ER-associated degradation. Nat. Cell Biol. *3*, 24–29.

Bays, N.W., Wilhovsky, S.K., Goradia, A., Hodgkiss-Harlow, K., and Hampton, R.Y. (2001b). HRD4/NPL4 is required for the proteasomal processing of ubiquitinated ER proteins. Mol. Biol. Cell *12*, 4114–4128.

Bhamidipati, A., Denic, V., Quan, E.M., and Weissman, J.S. (2005). Exploration of the Topological Requirements of ERAD Identifies Yos9p as a Lectin Sensor of Misfolded Glycoproteins in the ER Lumen. Mol. Cell *19*, 741–751.

Biederer, T., Volkwein, C., and Sommer, T. (1997). Role of Cue1p in Ubiquitination and Degradation at the ER Surface. Science *278*, 1806–1809.

Blanchard, V., Frank, M., Leeflang, B.R., Boelens, R., and Kamerling, J.P. (2008). The structural basis of the difference in sensitivity for PNGase F in the de-N-glycosylation of the native bovine pancreatic ribonucleases B and BS. Biochemistry (Mosc.) *47*, 3435–3446.

Bole, D.G., Hendershot, L.M., and Kearney, J.F. (1986). Posttranslational association of immunoglobulin heavy chain binding protein with nascent heavy chains in nonsecreting and secreting hybridomas. J. Cell Biol. *102*, 1558–1566.

Bonifacino, J.S., and Lippincott-Schwartz, J. (1991). Degradation of proteins within the endoplasmic reticulum. Curr. Opin. Cell Biol. *3*, 592–600.

Braakman, I., and Bulleid, N.J. (2011). Protein Folding and Modification in the Mammalian Endoplasmic Reticulum. Annu. Rev. Biochem. *80*, 71–99.

Braakman, I., Helenius, J., and Helenius, A. (1992). Manipulating disulfide bond formation and protein folding in the endoplasmic reticulum. EMBO J. *11*, 1717–1722.

Brockwell, D.J., and Radford, S.E. (2007). Intermediates: ubiquitous species on folding energy landscapes? Curr. Opin. Struct. Biol. *17*, 30–37.

Carvalho, P., Goder, V., and Rapoport, T.A. (2006). Distinct ubiquitin-ligase complexes define convergent pathways for the degradation of ER proteins. Cell *126*, 361–373.

Carvalho, P., Stanley, A.M., and Rapoport, T.A. (2010). Retrotranslocation of a Misfolded Luminal ER Protein by the Ubiquitin-Ligase Hrd1p. Cell *143*, 579–591.

Chakraborty, K., Chatila, M., Sinha, J., Shi, Q., Poschner, B.C., Sikor, M., Jiang, G., Lamb, D.C., Hartl, F.U., and Hayer-Hartl, M. (2010). Chaperonin-catalyzed rescue of kinetically trapped states in protein folding. Cell *142*, 112–122.

Chang, J.-Y. (2011). Diverse pathways of oxidative folding of disulfide proteins: underlying causes and folding models. Biochemistry (Mosc.) *50*, 3414–3431.

Chantret, I., Kodali, V.P., Lahmouich, C., Harvey, D.J., and Moore, S.E.H. (2011). Endoplasmic reticulum-associated degradation (ERAD) and free oligosaccharide generation in Saccharomyces cerevisiae. J. Biol. Chem. *286*, 41786–41800.

Cheng, S.H., Gregory, R.J., Marshall, J., Paul, S., Souza, D.W., White, G.A., O'Riordan, C.R., and Smith, A.E. (1990). Defective intracellular transport and processing of CFTR is the molecular basis of most cystic fibrosis. Cell *63*, 827–834.

Chiti, F., and Dobson, C.M. (2006). Protein misfolding, functional amyloid, and human disease. Annu. Rev. Biochem. *75*, 333–366.

Christianson, J.C., Shaler, T.A., Tyler, R.E., and Kopito, R.R. (2008). OS-9 and GRP94 deliver mutant α1-antitrypsin to the Hrd1?SEL1L ubiquitin ligase complex for ERAD. Nat. Cell Biol. *10*, 272–282.

Christianson, J.C., Olzmann, J.A., Shaler, T.A., Sowa, M.E., Bennett, E.J., Richter, C.M., Tyler, R.E., Greenblatt, E.J., Wade Harper, J., and Kopito, R.R. (2011). Defining human ERAD networks through an integrative mapping strategy. Nat. Cell Biol. *14*, 93–105.

Clerc, S., Hirsch, C., Oggier, D.M., Deprez, P., Jakob, C., Sommer, T., and Aebi, M. (2009). Htm1 protein generates the N-glycan signal for glycoprotein degradation in the endoplasmic reticulum. J. Cell Biol. *184*, 159–172.

Copeland, C.S., Doms, R.W., Bolzau, E.M., Webster, R.G., and Helenius, A. (1986). Assembly of influenza hemagglutinin trimers and its role in intracellular transport. J. Cell Biol. *103*, 1179–1191.

Cormier, J.H., Tamura, T., Sunryd, J.C., and Hebert, D.N. (2009). EDEM1 Recognition and Delivery of Misfolded Proteins to the SEL1L-Containing ERAD Complex. Mol. Cell *34*, 627–633.

Cox, J.S., Shamu, C.E., and Walter, P. (1993). Transcriptional induction of genes encoding endoplasmic reticulum resident proteins requires a transmembrane protein kinase. Cell *73*, 1197–1206.

D'Alessio, C., Caramelo, J.J., and Parodi, A.J. (2010a). UDP-GlC:glycoprotein glucosyltransferase-glucosidase II, the ying-yang of the ER quality control. Semin. Cell Dev. Biol. *21*, 491–499.

D'Alessio, C., Caramelo, J.J., and Parodi, A.J. (2010b). UDP-GlC:glycoprotein glucosyltransferase-glucosidase II, the ying-yang of the ER quality control. Semin. Cell Dev. Biol. *21*, 491–499.

Dancourt, J., and Barlowe, C. (2010). Protein Sorting Receptors in the Early Secretory Pathway. Annu. Rev. Biochem. *79*, 777–802.

Dedola, S., Izumi, M., Makimura, Y., Seko, A., Kanamori, A., Sakono, M., Ito, Y., and Kajihara, Y. (2014). Folding of Synthetic Homogeneous Glycoproteins in the Presence of a Glycoprotein Folding Sensor Enzyme. Angew. Chem. Int. Ed. *53*, 2883–2887.

Denic, V. (2011). No country for old misfolded glycoproteins. Mol. Cell *42*, 715–717.

Denic, V., Quan, E.M., and Weissman, J.S. (2006). A Luminal Surveillance Complex that Selects Misfolded Glycoproteins for ER-Associated Degradation. Cell *126*, 349–359.

Eichner, T., and Radford, S.E. (2011). A Diversity of Assembly Mechanisms of a Generic Amyloid Fold. Mol. Cell *43*, 8–18.

Ellgaard, L., and Helenius, A. (2003). Quality control in the endoplasmic reticulum. Nat. Rev. Mol. Cell Biol. *4*, 181–191.

Endrizzi, J.A., Breddam, K., and Remington, S.J. (1994). 2.8-A structure of yeast serine carboxypeptidase. Biochemistry (Mosc.) *33*, 11106–11120.

Fernández, F.S., Trombetta, S.E., Hellman, U., and Parodi, A.J. (1994). Purification to homogeneity of UDP-glucose:glycoprotein glucosyltransferase from Schizosaccharomyces pombe and apparent absence of the enzyme fro Saccharomyces cerevisiae. J. Biol. Chem. *269*, 30701–30706.

Fewell, S.W., Travers, K.J., Weissman, J.S., and Brodsky, J.L. (2001). The action of molecular chaperones in the early secretory pathway. Annu. Rev. Genet. *35*, 149–191.

Fink, A.L. (1995). Compact intermediate states in protein folding. Annu. Rev. Biophys. Biomol. Struct. *24*, 495–522.

Foresti, O., Rodriguez-Vaello, V., Funaya, C., and Carvalho, P. (2014). Quality control of inner nuclear membrane proteins by the Asi complex. Science *346*, 751–755.

Fra, A.M., Fagioli, C., Finazzi, D., Sitia, R., and Alberini, C.M. (1993). Quality control of ER synthesized proteins: an exposed thiol group as a three-way switch mediating assembly, retention and degradation. EMBO J. *12*, 4755–4761.

Frand, A.R., and Kaiser, C.A. (1998). The ERO1 gene of yeast is required for oxidation of protein dithiols in the endoplasmic reticulum. Mol. Cell *1*, 161–170.

Fu, D., Chen, L., and O'Neill, R.A. (1994). A detailed structural characterization of ribonuclease B oligosaccharides by 1H NMR spectroscopy and mass spectrometry. Carbohydr. Res. *261*, 173–186.

Gauss, R., Jarosch, E., Sommer, T., and Hirsch, C. (2006). A complex of Yos9p and the HRD ligase integrates endoplasmic reticulum quality control into the degradation machinery. Nat. Cell Biol. *8*, 849–854.

Gauss, R., Kanehara, K., Carvalho, P., Ng, D.T.W., and Aebi, M. (2011). A Complex of Pdi1p and the Mannosidase Htm1p Initiates Clearance of Unfolded Glycoproteins from the Endoplasmic Reticulum. Mol. Cell *42*, 782–793.

Gershenson, A., Gierasch, L.M., Pastore, A., and Radford, S.E. (2014). Energy landscapes of functional proteins are inherently risky. Nat. Chem. Biol. *10*, 884–891.

Gething, M.J., McCammon, K., and Sambrook, J. (1986). Expression of wild-type and mutant forms of influenza hemagglutinin: the role of folding in intracellular transport. Cell *46*, 939–950.

Gibson, D.G., Young, L., Chuang, R.-Y., Venter, J.C., Hutchison, C.A., and Smith, H.O. (2009). Enzymatic assembly of DNA molecules up to several hundred kilobases. Nat. Methods *6*, 343–345.

Gil, G., Faust, J.R., Chin, D.J., Goldstein, J.L., and Brown, M.S. (1985). Membrane-bound domain of HMG CoA reductase is required for sterol-enhanced degradation of the enzyme. Cell *41*, 249–258.

Gillece, P., Luz, J.M., Lennarz, W.J., de La Cruz, F.J., and Römisch, K. (1999). Export of a cysteine-free misfolded secretory protein from the endoplasmic reticulum for degradation requires interaction with protein disulfide isomerase. J. Cell Biol. *147*, 1443–1456.

González, L., Bruix, M., Díaz-Mauriño, T., Feizi, T., Rico, M., Solís, D., and Jiménez-Barbero, J. (2000). Conformational studies of the Man8 oligosaccharide on native ribonuclease B and on the reduced and denatured protein. Arch. Biochem. Biophys. *383*, 17–27.

Grubb, S., Guo, L., Fisher, E.A., and Brodsky, J.L. (2012). A Highlights from MBoC Selection: Protein disulfide isomerases contribute differentially to the endoplasmic reticulum–associated degradation of apolipoprotein B and other substrates. Mol. Biol. Cell *23*, 520.

Guenzi, S., Fra, A.M., Sparvoli, A., Bet, P., Rocco, M., and Sitia, R. (1994). The efficiency of cysteine-mediated intracellular retention determines the differential fate of secretory IgA and IgM in B and plasma cells. Eur. J. Immunol. *24*, 2477–2482.

Haas, I.G., and Wabl, M. (1983). Immunoglobulin heavy chain binding protein. Nature *306*, 387–389.

Hagiwara, M., Maegawa, K., Suzuki, M., Ushioda, R., Araki, K., Matsumoto, Y., Hoseki, J., Nagata, K., and Inaba, K. (2011). Structural Basis of an ERAD Pathway Mediated by the ER-Resident Protein Disulfide Reductase ERdj5. Mol. Cell *41*, 432–444.

Hammond, C., Braakman, I., and Helenius, A. (1994). Role of N-linked oligosaccharide recognition, glucose trimming, and calnexin in glycoprotein folding and quality control. Proc. Natl. Acad. Sci. U. S. A. *91*, 913–917.

Hampton, R.Y., Gardner, R.G., and Rine, J. (1996). Role of 26S proteasome and HRD genes in the degradation of 3-hydroxy-3-methylglutaryl-CoA reductase, an integral endoplasmic reticulum membrane protein. Mol. Biol. Cell *7*, 2029–2044.

Hanson, S.R., Culyba, E.K., Hsu, T.-L., Wong, C.-H., Kelly, J.W., and Powers, E.T. (2009). The core trisaccharide of an N-linked glycoprotein intrinsically accelerates folding and enhances stability. Proc. Natl. Acad. Sci. *106*, 3131–3136.

Hartl, F.U., Bracher, A., and Hayer-Hartl, M. (2011). Molecular chaperones in protein folding and proteostasis. Nature *475*, 324–332.

Hatahet, F., and Ruddock, L.W. (2009). Protein disulfide isomerase: a critical evaluation of its function in disulfide bond formation. Antioxid. Redox Signal. *11*, 2807–2850.

Haynes, C.M., Titus, E.A., and Cooper, A.A. (2004). Degradation of misfolded proteins prevents ER-derived oxidative stress and cell death. Mol. Cell *15*, 767–776.

Hebert, D.N., Foellmer, B., and Helenius, A. (1995). Glucose trimming and reglucosylation determine glycoprotein association with calnexin in the endoplasmic reticulum. Cell *81*, 425–433.

Helenius, A. (1994). How N-linked oligosaccharides affect glycoprotein folding in the endoplasmic reticulum. Mol. Biol. Cell *5*, 253–265.

Helenius, A., and Aebi, M. (2004). Roles of N-linked glycans in the endoplasmic reticulum. Annu. Rev. Biochem. *73*, 1019–1049.

Henzler-Wildman, K., and Kern, D. (2007). Dynamic personalities of proteins. Nature *450*, 964–972.

Herscovics, A. (2001). Structure and function of Class I alpha 1,2-mannosidases involved in glycoprotein synthesis and endoplasmic reticulum quality control. Biochimie *83*, 757–762.

Hiller, M.M., Finger, A., Schweiger, M., and Wolf, D.H. (1996). ER Degradation of a Misfolded Luminal Protein by the Cytosolic Ubiquitin-Proteasome Pathway. Science *273*, 1725–1728.

Hopfield, J.J. (1974). Kinetic proofreading: a new mechanism for reducing errors in biosynthetic processes requiring high specificity. Proc. Natl. Acad. Sci. U. S. A. *71*, 4135–4139.

Hosokawa, N., Wada, I., Natsuka, Y., and Nagata, K. (2006). EDEM accelerates ERAD by preventing aberrant dimer formation of misfolded α1-antitrypsin. Genes Cells *11*, 465–476.

Hosokawa, N., Tremblay, L.O., Sleno, B., Kamiya, Y., Wada, I., Nagata, K., Kato, K., and Herscovics, A. (2010). EDEM1 accelerates the trimming of 1,2-linked mannose on the C branch of N-glycans. Glycobiology *20*, 567–575.

Hosomi, A., Tanabe, K., Hirayama, H., Kim, I., Rao, H., and Suzuki, T. (2010). Identification of an Htm1 (EDEM)-dependent, Mns1-independent Endoplasmic Reticulum-associated Degradation (ERAD) Pathway in Saccharomyces cerevisiae: APPLICATION OF A NOVEL ASSAY FOR GLYCOPROTEIN ERAD. J. Biol. Chem. *285*, 24324–24334.

Hughes, E.A., Hammond, C., and Cresswell, P. (1997). Misfolded major histocompatibility complex class I heavy chains are translocated into the cytoplasm and degraded by the proteasome. Proc. Natl. Acad. Sci. U. S. A. *94*, 1896–1901.

Hurtley, S.M., and Helenius, A. (1989). Protein oligomerization in the endoplasmic reticulum. Annu. Rev. Cell Biol. *5*, 277–307.

Huyer, G., Piluek, W.F., Fansler, Z., Kreft, S.G., Hochstrasser, M., Brodsky, J.L., and Michaelis, S. (2004). Distinct Machinery Is Required in Saccharomyces cerevisiae for the Endoplasmic Reticulum-associated Degradation of a Multispanning Membrane Protein and a Soluble Luminal Protein. J. Biol. Chem. *279*, 38369–38378.

Inoue, S., Bar-Nun, S., Roitelman, J., and Simoni, R.D. (1991). Inhibition of degradation of 3-hydroxy-3-methylglutaryl-coenzyme A reductase in vivo by cysteine protease inhibitors. J. Biol. Chem. *266*, 13311–13317.

Irvine, A.G., Wallis, A.K., Sanghera, N., Rowe, M.L., Ruddock, L.W., Howard, M.J., Williamson, R.A., Blindauer, C.A., and Freedman, R.B. (2014). Protein disulfide-isomerase interacts with a substrate protein at all stages along its folding pathway. PloS One *9*, e82511.

Ito, Y., Takeda, Y., Seko, A., Izumi, M., and Kajihara, Y. (2015). Functional analysis of endoplasmic reticulum glucosyltransferase (UGGT): Synthetic chemistry's initiative in glycobiology. Semin. Cell Dev. Biol. *41*, 90–98.

Izawa, T., Nagai, H., Endo, T., and Nishikawa, S. (2012). Yos9p and Hrd1p mediate ER retention of misfolded proteins for ER-associated degradation. Mol. Biol. Cell *23*, 1283–1293.

Izumi, M., Makimura, Y., Dedola, S., Seko, A., Kanamori, A., Sakono, M., Ito, Y., and Kajihara, Y. (2012). Chemical synthesis of intentionally misfolded homogeneous glycoprotein: a unique approach for the study of glycoprotein quality control. J. Am. Chem. Soc. *134*, 7238–7241.

Izumi, M., Oka, Y., Okamoto, R., Seko, A., Takeda, Y., Ito, Y., and Kajihara, Y. (2016). Synthesis of Glc1 Man9 -Glycoprotein Probes by a Misfolding/Enzymatic Glucosylation/Misfolding Sequence. Angew. Chem. Int. Ed Engl. *55*, 3968–3971.

Jakob, C.A., Burda, P., Roth, J., and Aebi, M. (1998). Degradation of misfolded endoplasmic reticulum glycoproteins in Saccharomyces cerevisiae is determined by a specific oligosaccharide structure. J. Cell Biol. *142*, 1223–1233.

Jakob, C.A., Bodmer, D., Spirig, U., Battig, P., Marcil, A., Dignard, D., Bergeron, J.J., Thomas, D.Y., and Aebi, M. (2001). Htm1p, a mannosidase-like protein, is involved in glycoprotein degradation in yeast. EMBO Rep. *2*, 423–430.

Jämsä, E., Simonen, M., and Makarow, M. (1994). Selective retention of secretory proteins in the yeast endoplasmic reticulum by treatment of cells with a reducing agent. Yeast Chichester Engl. *10*, 355–370.

Jarosch, E., Taxis, C., Volkwein, C., Bordallo, J., Finley, D., Wolf, D.H., and Sommer, T. (2002). Protein dislocation from the ER requires polyubiquitination and the AAA-ATPase Cdc48. Nat. Cell Biol. *4*, 134–139.

Jensen, T.J., Loo, M.A., Pind, S., Williams, D.B., Goldberg, A.L., and Riordan, J.R. (1995). Multiple proteolytic systems, including the proteasome, contribute to CFTR processing. Cell *83*, 129–135.

Jonikas, M.C., Collins, S.R., Denic, V., Oh, E., Quan, E.M., Schmid, V., Weibezahn, J., Schwappach, B., Walter, P., Weissman, J.S., et al. (2009). Comprehensive characterization of genes required for protein folding in the endoplasmic reticulum. Science *323*, 1693–1697.

Kearse, K.P., Williams, D.B., and Singer, A. (1994). Persistence of glucose residues on core oligosaccharides prevents association of TCR alpha and TCR beta proteins with calnexin and results specifically in accelerated degradation of nascent TCR alpha proteins within the endoplasmic reticulum. EMBO J. *13*, 3678–3686.

Kim, W., Spear, E.D., and Ng, D.T.W. (2005). Yos9p Detects and Targets Misfolded Glycoproteins for ER-Associated Degradation. Mol. Cell *19*, 753–764.

Klausner, R.D., and Sitia, R. (1990). Protein degradation in the endoplasmic reticulum. Cell *62*, 611–614.

Knop, M., Hauser, N., and Wolf, D.H. (1996). N-Glycosylation affects endoplasmic reticulum degradation of a mutated derivative of carboxypeptidase yscY in yeast. Yeast Chichester Engl. *12*, 1229–1238.

Kostova, Z. (2005). Importance of carbohydrate positioning in the recognition of mutated CPY for ER-associated degradation. J. Cell Sci. *118*, 1485–1492.

Kulak, N.A., Pichler, G., Paron, I., Nagaraj, N., and Mann, M. (2014). Minimal, encapsulated proteomic-sample processing applied to copy-number estimation in eukaryotic cells. Nat. Methods *11*, 319–324.

Labbadia, J., and Morimoto, R.I. (2015). The biology of proteostasis in aging and disease. Annu. Rev. Biochem. *84*, 435–464.

Lipari, F., and Herscovics, A. (1994). Production, purification and characterization of recombinant yeast processing alpha 1,2-mannosidase. Glycobiology *4*, 697–702.

Lippincott-Schwartz, J., Bonifacino, J.S., Yuan, L.C., and Klausner, R.D. (1988). Degradation from the endoplasmic reticulum: disposing of newly synthesized proteins. Cell *54*, 209–220.

Llambi, F., Wang, Y.-M., Victor, B., Yang, M., Schneider, D.M., Gingras, S., Parsons, M.J., Zheng, J.H., Brown, S.A., Pelletier, S., et al. (2016). BOK Is a Non-canonical BCL-2 Family Effector of Apoptosis Regulated by ER-Associated Degradation. Cell *165*, 421–433.

Mamathambika, B.S., and Bardwell, J.C. (2008). Disulfide-Linked Protein Folding Pathways. Annu. Rev. Cell Dev. Biol. *24*, 211–235.

Matsuo, I., Wada, M., Manabe, S., Yamaguchi, Y., Otake, K., Kato, K., and Ito, Y. (2003). Synthesis of Monoglucosylated High-Mannose-Type Dodecasaccharide, a Putative Ligand for Molecular Chaperone, Calnexin, and Calreticurin. J. Am. Chem. Soc. *125*, 3402–3403.

McCracken, A.A., and Brodsky, J.L. (1996). Assembly of ER-associated protein degradation in vitro: dependence on cytosol, calnexin, and ATP. J. Cell Biol. *132*, 291–298.

Minami, Y., Weissman, A.M., Samelson, L.E., and Klausner, R.D. (1987). Building a multichain receptor: synthesis, degradation, and assembly of the T-cell antigen receptor. Proc. Natl. Acad. Sci. U. S. A. *84*, 2688–2692.

Mittal, S., Chowhan, R.K., and Singh, L.R. (2015). Macromolecular crowding: Macromolecules friend or foe. Biochim. Biophys. Acta *1850*, 1822–1831.

Molinari, M. (2003). Role of EDEM in the Release of Misfolded Glycoproteins from the Calnexin Cycle. Science *299*, 1397–1400.

Moore, S.E., and Spiro, R.G. (1993). Inhibition of glucose trimming by castanospermine results in rapid degradation of unassembled major histocompatibility complex class I molecules. J. Biol. Chem. *268*, 3809–3812.

Morelle, W., and Michalski, J.-C. (2007). Analysis of protein glycosylation by mass spectrometry. Nat. Protoc. *2*, 1585–1602.

Mori, K., Ma, W., Gething, M.J., and Sambrook, J. (1993). A transmembrane protein with a cdc2+/CDC28-related kinase activity is required for signaling from the ER to the nucleus. Cell *74*, 743–756.

Nakasako, M., Maeno, A., Kurimoto, E., Harada, T., Yamaguchi, Y., Oka, T., Takayama, Y., Iwata, A., and Kato, K. (2010). Redox-dependent domain rearrangement of protein disulfide isomerase from a thermophilic fungus. Biochemistry (Mosc.) *49*, 6953–6962.

Nakatsukasa, K., Nishikawa, S. -i., Hosokawa, N., Nagata, K., and Endo, T. (2001). Mnl1p, an -Mannosidase-like Protein in YeastSaccharomyces cerevisiae, Is Required for Endoplasmic Reticulum-associated Degradation of Glycoproteins. J. Biol. Chem. *276*, 8635–8638.

Needham, P.G., and Brodsky, J.L. (2013). How early studies on secreted and membrane protein quality control gave rise to the ER associated degradation (ERAD) pathway: The early history of ERAD. Biochim. Biophys. Acta *1833*, 2447–2457.

Ninagawa, S., Okada, T., Sumitomo, Y., Kamiya, Y., Kato, K., Horimoto, S., Ishikawa, T., Takeda, S., Sakuma, T., Yamamoto, T., et al. (2014). EDEM2 initiates mammalian glycoprotein ERAD by catalyzing the first mannose trimming step. J. Cell Biol. *206*, 347–356.

Nishikawa, S.I., Fewell, S.W., Kato, Y., Brodsky, J.L., and Endo, T. (2001). Molecular chaperones in the yeast endoplasmic reticulum maintain the solubility of proteins for retrotranslocation and degradation. J. Cell Biol. *153*, 1061–1070.

Nørgaard, P., Westphal, V., Tachibana, C., Alsøe, L., Holst, B., and Winther, J.R. (2001). Functional differences in yeast protein disulfide isomerases. J. Cell Biol. *152*, 553–562.

Oda, Y. (2003). EDEM As an Acceptor of Terminally Misfolded Glycoproteins Released from Calnexin. Science *299*, 1394–1397.

Olivari, S., Cali, T., Salo, K.E.H., Paganetti, P., Ruddock, L.W., and Molinari, M. (2006). EDEM1 regulates ER-associated degradation by accelerating de-mannosylation of folding-defective polypeptides and by inhibiting their covalent aggregation. Biochem. Biophys. Res. Commun. *349*, 1278–1284.

Ou, W.J., Cameron, P.H., Thomas, D.Y., and Bergeron, J.J. (1993). Association of folding intermediates of glycoproteins with calnexin during protein maturation. Nature *364*, 771–776.

Packer, N.H., Lawson, M.A., Jardine, D.R., and Redmond, J.W. (1998). A general approach to desalting oligosaccharides released from glycoproteins. Glycoconj. J. *15*, 737–747.

Peterson, J.R., Ora, A., Van, P.N., and Helenius, A. (1995). Transient, lectin-like association of calreticulin with folding intermediates of cellular and viral glycoproteins. Mol. Biol. Cell *6*, 1173–1184.

Pfeiffer, A., Stephanowitz, H., Krause, E., Volkwein, C., Hirsch, C., Jarosch, E., and Sommer, T. (2016). A complex of Htm1 and the oxidoreductase Pdi1 accelerates degradation of misfolded glycoproteins. J. Biol. Chem. jbc.M115.703256.

Pollard, M.G., Travers, K.J., and Weissman, J.S. (1998). Ero1p: a novel and ubiquitous protein with an essential role in oxidative protein folding in the endoplasmic reticulum. Mol. Cell *1*, 171–182.

Price, J.L., Shental-Bechor, D., Dhar, A., Turner, M.J., Powers, E.T., Gruebele, M., Levy, Y., and Kelly, J.W. (2010). Context-Dependent Effects of Asparagine Glycosylation on Pin WW Folding Kinetics and Thermodynamics. J. Am. Chem. Soc. *132*, 15359–15367.

Puig, A., and Gilbert, H.F. (1994). Protein disulfide isomerase exhibits chaperone and anti-chaperone activity in the oxidative refolding of lysozyme. J. Biol. Chem. *269*, 7764–7771.

Puig, A., Lyles, M.M., Noiva, R., and Gilbert, H.F. (1994). The role of the thiol/disulfide centers and peptide binding site in the chaperone and anti-chaperone activities of protein disulfide isomerase. J. Biol. Chem. *269*, 19128–19135.

Quan, E.M., Kamiya, Y., Kamiya, D., Denic, V., Weibezahn, J., Kato, K., and Weissman, J.S. (2008). Defining the Glycan Destruction Signal for Endoplasmic Reticulum-Associated Degradation. Mol. Cell *32*, 870–877.

Rabinovich, E., Kerem, A., Fröhlich, K.-U., Diamant, N., and Bar-Nun, S. (2002). AAA-ATPase p97/Cdc48p, a Cytosolic Chaperone Required for Endoplasmic Reticulum-Associated Protein Degradation. Mol. Cell. Biol. *22*, 626–634.

Radhakrishnan, S.K., Lee, C.S., Young, P., Beskow, A., Chan, J.Y., and Deshaies, R.J. (2010). Transcription factor Nrf1 mediates the proteasome recovery pathway after proteasome inhibition in mammalian cells. Mol. Cell *38*, 17–28.

Raines, R.T. (1998). Ribonuclease A. Chem. Rev. *98*, 1045–1066.

Ritter, C., and Helenius, A. (2000). Recognition of local glycoprotein misfolding by the ER folding sensor UDP-glucose:glycoprotein glucosyltransferase. Nat. Struct. Biol. *7*, 278–280.

Ritter, C., Quirin, K., Kowarik, M., and Helenius, A. (2005). Minor folding defects trigger local modification of glycoproteins by the ER folding sensor GT. EMBO J. *24*, 1730–1738.

Rock, K.L., Gramm, C., Rothstein, L., Clark, K., Stein, R., Dick, L., Hwang, D., and Goldberg, A.L. (1994). Inhibitors of the proteasome block the degradation of most cell proteins and the generation of peptides presented on MHC class I molecules. Cell *78*, 761–771.

Ron, E., Shenkman, M., Groisman, B., Izenshtein, Y., Leitman, J., and Lederkremer, G.Z. (2011). Bypass of glycan-dependent glycoprotein delivery to ERAD by up-regulated EDEM1. Mol. Biol. Cell *22*, 3945–3954.

Ruggiano, A., Foresti, O., and Carvalho, P. (2014). Quality control: ER-associated degradation: Protein quality control and beyond. J. Cell Biol. *204*, 869–879.

Sakoh-Nakatogawa, M., Nishikawa, S. -i., and Endo, T. (2009a). Roles of Protein-disulfide Isomerase-mediated Disulfide Bond Formation of Yeast Mnl1p in Endoplasmic Reticulum-associated Degradation. J. Biol. Chem. *284*, 11815–11825.

Sakoh-Nakatogawa, M., Nishikawa, S.-I., and Endo, T. (2009b). Roles of protein-disulfide isomerase-mediated disulfide bond formation of yeast Mnl1p in endoplasmic reticulum-associated degradation. J. Biol. Chem. *284*, 11815–11825.

Satoh, T., Chen, Y., Hu, D., Hanashima, S., Yamamoto, K., and Yamaguchi, Y. (2010). Structural Basis for Oligosaccharide Recognition of Misfolded Glycoproteins by OS-9 in ER-Associated Degradation. Mol. Cell *40*, 905–916.

Sekijima, Y., Wiseman, R.L., Matteson, J., Hammarström, P., Miller, S.R., Sawkar, A.R., Balch, W.E., and Kelly, J.W. (2005). The biological and chemical basis for tissue-selective amyloid disease. Cell *121*, 73–85.

Serve, O., Kamiya, Y., Maeno, A., Nakano, M., Murakami, C., Sasakawa, H., Yamaguchi, Y., Harada, T., Kurimoto, E., Yagi-Utsumi, M., et al. (2010). Redox-dependent domain rearrangement of protein disulfide isomerase coupled with exposure of its substrate-binding hydrophobic surface. J. Mol. Biol. *396*, 361–374.

Shenkman, M., Groisman, B., Ron, E., Avezov, E., Hendershot, L.M., and Lederkremer, G.Z. (2013). A shared endoplasmic reticulum-associated degradation pathway involving the EDEM1 protein for glycosylated and nonglycosylated proteins. J. Biol. Chem. *288*, 2167–2178.

Shental-Bechor, D., and Levy, Y. (2008). Effect of glycosylation on protein folding: a close look at thermodynamic stabilization. Proc. Natl. Acad. Sci. *105*, 8256–8261.

Shortle, D. (2002). The expanded denatured state: an ensemble of conformations trapped in a locally encoded topological space. Adv. Protein Chem. *62*, 1–23.

Shoulders, M.D., Ryno, L.M., Genereux, J.C., Moresco, J.J., Tu, P.G., Wu, C., Yates, J.R., Su, A.I., Kelly, J.W., and Wiseman, R.L. (2013). Stress-independent activation of XBP1s and/or ATF6 reveals three functionally diverse ER proteostasis environments. Cell Rep. *3*, 1279–1292.

Smith, M.H., Ploegh, H.L., and Weissman, J.S. (2011). Road to ruin: targeting proteins for degradation in the endoplasmic reticulum. Science *334*, 1086–1090.

Smith, M.H., Rodriguez, E.H., and Weissman, J.S. (2014). Misfolded Proteins Induce Aggregation of the Lectin Yos9. J. Biol. Chem. *289*, 25670–25677.

Sommer, T., and Jentsch, S. (1993). A protein translocation defect linked to ubiquitin conjugation at the endoplasmic reticulum. Nature *365*, 176–179.

Sousa, M., and Parodi, A.J. (1995). The molecular basis for the recognition of misfolded glycoproteins by the UDP-Glc:glycoprotein glucosyltransferase. EMBO J. *14*, 4196–4203.

Sousa, M.C., Ferrero-Garcia, M.A., and Parodi, A.J. (1992). Recognition of the oligosaccharide and protein moieties of glycoproteins by the UDP-Glc:glycoprotein glucosyltransferase. Biochemistry (Mosc.) *31*, 97–105.

Spear, E.D., and Ng, D.T.W. (2005). Single, context-specific glycans can target misfolded glycoproteins for ER-associated degradation. J. Cell Biol. *169*, 73–82.

Steffen, J., Seeger, M., Koch, A., and Krüger, E. (2010). Proteasomal degradation is transcriptionally controlled by TCF11 via an ERAD-dependent feedback loop. Mol. Cell *40*, 147–158.

Stein, A., Ruggiano, A., Carvalho, P., and Rapoport, T.A. (2014). Key steps in ERAD of luminal ER proteins reconstituted with purified components. Cell *158*, 1375–1388.

Strohalm, M., Kavan, D., Novák, P., Volný, M., and Havlíček, V. (2010). mMass 3: A Cross-Platform Software Environment for Precise Analysis of Mass Spectrometric Data. Anal. Chem. *82*, 4648–4651.

Su, K., Stoller, T., Rocco, J., Zemsky, J., and Green, R. (1993). Pre-Golgi degradation of yeast prepro-alpha-factor expressed in a mammalian cell. Influence of cell type-specific oligosaccharide processing on intracellular fate. J. Biol. Chem. *268*, 14301–14309.

Swanson, R., Locher, M., and Hochstrasser, M. (2001). A conserved ubiquitin ligase of the nuclear envelope/endoplasmic reticulum that functions in both ER-associated and Matalpha2 repressor degradation. Genes Dev. *15*, 2660–2674.

Szathmary, R., Bielmann, R., Nita-Lazar, M., Burda, P., and Jakob, C.A. (2005). Yos9 Protein Is Essential for Degradation of Misfolded Glycoproteins and May Function as Lectin in ERAD. Mol. Cell *19*, 765–775.

Tang, Y.-C., Chang, H.-C., Roeben, A., Wischnewski, D., Wischnewski, N., Kerner, M.J., Hartl, F.U., and Hayer-Hartl, M. (2006). Structural features of the GroEL-GroES nano-cage required for rapid folding of encapsulated protein. Cell *125*, 903–914.

Thaysen-Andersen, M., Mysling, S., and Højrup, P. (2009). Site-specific glycoprofiling of N-linked glycopeptides using MALDI-TOF MS: strong correlation between signal strength and glycoform quantities. Anal. Chem. *81*, 3933–3943.

Theillet, F.-X., Binolfi, A., Frembgen-Kesner, T., Hingorani, K., Sarkar, M., Kyne, C., Li, C., Crowley, P.B., Gierasch, L., Pielak, G.J., et al. (2014). Physicochemical properties of cells and their effects on intrinsically disordered proteins (IDPs). Chem. Rev. *114*, 6661–6714.

Tian, G., Xiang, S., Noiva, R., Lennarz, W.J., and Schindelin, H. (2006). The Crystal Structure of Yeast Protein Disulfide Isomerase Suggests Cooperativity between Its Active Sites. Cell *124*, 61–73.

Timms, R.T., Menzies, S.A., Tchasovnikarova, I.A., Christensen, L.C., Williamson, J.C., Antrobus, R., Dougan, G., Ellgaard, L., and Lehner, P.J. (2016). Genetic dissection of mammalian ERAD through comparative haploid and CRISPR forward genetic screens. Nat. Commun. *7*, 11786.

Totani, K., Matsuo, I., Ihara, Y., and Ito, Y. (2006). High-mannose-type glycan modifications of dihydrofolate reductase using glycan–methotrexate conjugates. Bioorg. Med. Chem. *14*, 5220–5229.

Totani, K., Ihara, Y., Tsujimoto, T., Matsuo, I., and Ito, Y. (2009). The Recognition Motif of the Glycoprotein-Folding Sensor Enzyme UDP-Glc:Glycoprotein Glucosyltransferase †. Biochemistry (Mosc.) *48*, 2933–2940.

Travers, K.J., Patil, C.K., Wodicka, L., Lockhart, D.J., Weissman, J.S., and Walter, P. (2000). Functional and genomic analyses reveal an essential coordination between the unfolded protein response and ER-associated degradation. Cell *101*, 249–258.

Trombetta, E.S., and Helenius, A. (2000). Conformational requirements for glycoprotein reglucosylation in the endoplasmic reticulum. J. Cell Biol. *148*, 1123–1129.

Tsai, B., Rodighiero, C., Lencer, W.I., and Rapoport, T.A. (2001). Protein disulfide isomerase acts as a redox-dependent chaperone to unfold cholera toxin. Cell *104*, 937–948.

Tu, B.P. (2000). Biochemical Basis of Oxidative Protein Folding in the Endoplasmic Reticulum. Science *290*, 1571–1574.

Ushioda, R., Hoseki, J., Araki, K., Jansen, G., Thomas, D.Y., and Nagata, K. (2008). ERdj5 is required as a disulfide reductase for degradation of misfolded proteins in the ER. Science *321*, 569–572.

Vallee, F., Karaveg, K., Herscovics, A., Moremen, K.W., and Howell, P.L. (2000). Structural Basis for Catalysis and Inhibition ofN-Glycan Processing Class I 1,2-Mannosidases. J. Biol. Chem. *275*, 41287–41298.

Vallée, F., Lipari, F., Yip, P., Sleno, B., Herscovics, A., and Howell, P.L. (2000). Crystal structure of a class I alpha1,2-mannosidase involved in N-glycan processing and endoplasmic reticulum quality control. EMBO J. *19*, 581–588.

Vashist, S. (2001). Distinct retrieval and retention mechanisms are required for the quality control of endoplasmic reticulum protein folding. J. Cell Biol. *155*, 355–368.

Vashist, S., and Ng, D.T.W. (2004). Misfolded proteins are sorted by a sequential checkpoint mechanism of ER quality control. J. Cell Biol. *165*, 41–52.

V. Sideraki, and Gilbert, H.F. (2000). Mechanism of the antichaperone activity of protein disulfide isomerase: facilitated assembly of large, insoluble aggregates of denatured lysozyme and PDI. Biochemistry (Mosc.) *39*, 1180–1188.

Walter, P., and Ron, D. (2011). The Unfolded Protein Response: From Stress Pathway to Homeostatic Regulation. Science *334*, 1081–1086.

Wang, C., Yu, J., Huo, L., Wang, L., Feng, W., and Wang, C. -c. (2012). Human Protein-disulfide Isomerase Is a Redox-regulated Chaperone Activated by Oxidation of Domain a'. J. Biol. Chem. *287*, 1139–1149.

Ward, C.L., Omura, S., and Kopito, R.R. (1995). Degradation of CFTR by the ubiquitin-proteasome pathway. Cell *83*, 121–127.

Weissman, J.S., and Kim, P.S. (1991). Reexamination of the folding of BPTI: predominance of native intermediates. Science *253*, 1386–1393.

Weissman, J.S., and Kim, P.S. (1995). A kinetic explanation for the rearrangement pathway of BPTI folding. Nat. Struct. Biol. *2*, 1123–1130.

Wieland, F.T., Gleason, M.L., Serafini, T.A., and Rothman, J.E. (1987). The rate of bulk flow from the endoplasmic reticulum to the cell surface. Cell *50*, 289–300.

Wiertz, E.J., Jones, T.R., Sun, L., Bogyo, M., Geuze, H.J., and Ploegh, H.L. (1996). The human cytomegalovirus US11 gene product dislocates MHC class I heavy chains from the endoplasmic reticulum to the cytosol. Cell *84*, 769–779.

Wilhovsky, S., Gardner, R., and Hampton, R. (2000). HRD gene dependence of endoplasmic reticulum-associated degradation. Mol. Biol. Cell *11*, 1697–1708.

Winther, J.R., and Sørensen, P. (1991). Propeptide of carboxypeptidase Y provides a chaperone-like function as well as inhibition of the enzymatic activity. Proc. Natl. Acad. Sci. U. S. A. *88*, 9330–9334.

Wiseman, R.L., Powers, E.T., Buxbaum, J.N., Kelly, J.W., and Balch, W.E. (2007). An adaptable standard for protein export from the endoplasmic reticulum. Cell *131*, 809–821.

Woo, C.M., Iavarone, A.T., Spiciarich, D.R., Palaniappan, K.K., and Bertozzi, C.R. (2015). Isotope-targeted glycoproteomics (IsoTaG): a mass-independent platform for intact N- and O-glycopeptide discovery and analysis. Nat. Methods *12*, 561–567.

Xie, W., Kanehara, K., Sayeed, A., and Ng, D.T. (2009). Intrinsic conformational determinants signal protein misfolding to the Hrd1/Htm1 endoplasmic reticulum–associated degradation system. Mol. Biol. Cell *20*, 3317–3329.

Xu, C., Wang, S., Thibault, G., and Ng, D.T.W. (2013). Futile protein folding cycles in the ER are terminated by the unfolded protein O-mannosylation pathway. Science *340*, 978–981.

Yang, M., Omura, S., Bonifacino, J.S., and Weissman, A.M. (1998). Novel aspects of degradation of T cell receptor subunits from the endoplasmic reticulum (ER) in T cells: importance of oligosaccharide processing, ubiquitination, and proteasome-dependent removal from ER membranes. J. Exp. Med. *187*, 835–846.

Ye, Y., Meyer, H.H., and Rapoport, T.A. (2001). The AAA ATPase Cdc48/p97 and its partners transport proteins from the ER into the cytosol. Nature *414*, 652–656.

Zhu, T., Satoh, T., and Kato, K. (2014). Structural insight into substrate recognition by the endoplasmic reticulum folding-sensor enzyme: crystal structure of third thioredoxin-like domain of UDP-glucose:glycoprotein glucosyltransferase. Sci. Rep. *4*, 7322.

Publishing Agreement

It is the policy of the University to encourage the distribution of all theses, dissertations, and manuscripts. Copies of all UCSF theses, dissertations, and manuscripts will be routed to the library via the Graduate Division. The library will make all theses, dissertations, and manuscripts accessible to the public and will preserve these to the best of their abilities, in perpetuity.

Please sign the following statement:

I hereby grant permission to the Graduate Division of the University of California, San Francisco to release copies of my thesis, dissertation, or manuscript to the Campus Library to provide access and preservation, in whole or in part, in perpetuity.

Author Signature

6, 27, 2016

Date